

BENZYL FUNCTIONALIZED BENZOTRIAZOLE CONTAINING CONJUGATED  
POLYMERS: EFFECT OF SUBSTITUENT POSITION ON ELECTROCHROMIC  
PROPERTIES  
AND SYNTHESIS OF CROWN ETHER FUNCTIONALIZED  
ELECTROCHROMIC POLYMERS

A THESIS SUBMITTED TO  
THE GRADUATE SCHOOL OF NATURAL AND APPLIED SCIENCES  
OF  
MIDDLE EAST TECHNICAL UNIVERSITY

BY

BAŞAK YİĞİTŞOY

IN PARTIAL FULFILLMENT OF THE REQUIREMENTS  
FOR  
THE DEGREE OF DOCTOR OF PHILOSOPHY  
IN  
CHEMISTRY

JUNE 2011

Approval of the thesis:

**BENZYL FUNCTIONALIZED BENZOTRIAZOLE CONTAINING  
CONJUGATED POLYMERS: EFFECT OF SUBSTITUENT POSITION ON  
ELECTROCHROMIC PROPERTIES  
AND SYNTHESIS OF CROWN ETHER FUNCTIONALIZED  
ELECTROCHROMIC POLYMERS**

submitted by **BAŞAK YİĞİT**SOY in partial fulfillment of the requirements for the degree of **Doctor of Philosophy in Chemistry Department, Middle East Technical University** by,

Prof. Dr. Canan Özgen  
Dean, Graduate School of **Natural and Applied Sciences**

\_\_\_\_\_

Prof. Dr. İlker Özkan  
Head of Department, **Chemistry**

\_\_\_\_\_

Prof. Dr. Levent Toppare  
Supervisor, **Chemistry Dept., METU**

\_\_\_\_\_

**Examining Committee Members:**

Prof. Dr. Zuhâl Küçükyavuz  
Chemistry Dept., METU

\_\_\_\_\_

Prof. Dr. Levent Toppare  
Chemistry Dept., METU

\_\_\_\_\_

Prof. Dr. Teoman Tinçer  
Chemistry Dept., METU

\_\_\_\_\_

Assoc. Prof. Dr. Metin Ak  
Chemistry Dept., Pamukkale University

\_\_\_\_\_

Assist. Prof. Dr. Ali Çırpan  
Chemistry Dept., METU

\_\_\_\_\_

**Date:** 22.06.2011

**I hereby declare that all information in this document has been obtained and presented in accordance with academic rules and ethical conduct. I also declare that, as required by these rules and conduct, I have fully cited and referenced all material and results that are not original to this work.**

Name, Last name : BAŐAK YİĐİTSOY

Signature :

## ABSTRACT

### BENZYL FUNCTIONALIZED BENZOTRIAZOLE CONTAINING CONJUGATED POLYMERS: EFFECT OF SUBSTITUENT POSITION ON ELECTROCHROMIC PROPERTIES AND SYNTHESIS OF CROWN ETHER FUNCTIONALIZED ELECTROCHROMIC POLYMERS

Yiğitsoy, Başak

Ph.D., Department of Chemistry

Supervisor: Prof. Dr. Levent Toppare

June 2011, 141 pages

A new class of  $\pi$ -conjugated monomers was synthesized with combination of electron donating and electron-withdrawing heterocyclics to understand the effects of structural differences on electrochemical and optoelectronic properties of the resulting polymers. Electron deficient benzotriazole, substituted with benzyl from two available sites, coupled with stannylated electron donating groups, ethylenedioxythiophene (EDOT) and thiophene (Th), to yield four different monomers; 1-benzyl-4,7-di(thiophen-2-yl)-2H-benzo[d][1,2,3] triazole (BBTA), 2-benzyl-4,7-di(thiophen-2-yl)-2H-benzo[d][1,2,3] triazole (BBTS), 1-benzyl-4,7-bis(2,3-dihydrothieno[3,4-b]dioxin-5-yl)-2H-benzo [d][1,2,3]triazole (BBTEA), 2-benzyl-4,7-bis(2,3-dihydrothieno[3,4-b]dioxin-5-yl)-2H-benzo [d][1,2,3]triazole (BBTES).

Furthermore, EDOT and thiophene terminated naphthalene-2,3-crown ether containing monomers, 14,19-di(thiophen-2-yl)-naphtho[2,3-b][1,4,7,10,13]pentaoxacyclo pentadecane (TNCT), 14,19-bis(2,3-dihydrothieno[3,4-b][1,4]dioxin-5-yl)-naphtho[2,3-b][1,4,7,10,13]pentaoxacyclopenta decane (ENCE), were synthesized to observe the effect crown ether moiety on the final electrochemical and optoelectronic properties of resultant polymers.

Cyclic voltammetry, UV-Vis-NIR spectroscopy and colorimetry techniques were employed to examine electrochemical and optoelectronic properties of all monomers and polymers. Experimental results showed that alteration of substituent, substitution position and donor groups' strength lead to obtain polymers with different redox behaviors, optical band gaps and different number of achievable colored states.

**Keywords:** Electrochemical polymerization, Conducting polymer, Low band gap, Electrochromism, Benzotriazole bearing monomers, Naphthalene-2,3-crown ether containing monomers

## ÖZ

# BENZİLLE FONKSİYOLANDIRILMIŞ BENZOTRIAZOL İÇEREN KONJÜGE POLİMERLER: SÜBSTİTÜENT KONUMUNUN ELEKTROKROMİK ÖZELLİKLERE ETKİSİ VE NAFTO TAÇ ETER İÇEREN ELEKTROKROMİK POLİMERLERİN SENTEZİ

Yiğitsoy, Başak

Doktora, Kimya Bölümü

Tez Yöneticisi: Prof. Dr. Levent Toppare

Haziran 2011, 141 sayfa

Yapısal değişikliklerin elektrokimyasal ve opteelektronik özelliklere etkisini incelemek üzere elektron verici ve electron çekici heterosikliklerin birleştirilmesi ile yeni  $\pi$ -konjügasyonlu monomerler sentezlenmiştir. Triazol halkasının uygun yerlerinden benzil takılmış elektronca yetersiz benzotriazol grubu, elektron verici gruplar içeren etilendioksitiyofen ve tiyofen ile eşleştirilerek, dört farklı monomer ,1-benzil-4,7-di(tiyofen-2-il))-2H-benzo[d][1,2,3] triazol (BBTA), 2-benzil-4,7-di(tiyofen-2-il))-2H-benzo[d][1,2,3] triazol (BBTS), 1-benzil-4,7-bis(2,3-dihidrotyieno[3,4-b]dioksin-5-il)-2H-benzo [d][1,2,3] triazol (BBTEA), 2-benzil-4,7-bis(2,3-dihidrotyieno[3,4-b]dioksin-5-il)-2H-benzo[d][1,2,3]triazol (BBTES),elde edilmiştir.

Ayrıca, Taç eter grubunun polimerlerin elektrokimyasal ve optoelektronik özelliklere etkisini görmek amacıyla EDOT ve tiyofen ile sonlandırılan naftalin-2,3-taç eter içeren monomerler, 14,19-bis(2,3-dihidrotyieno[3,4-b][1,4]dioksin-5-yl)-nafto[2,3-b][1,4,7,10,13] pentaokzasiklopentadekan (ENCE), 14,19-di(tiyofen-2-il)-nafto[2,3-b][1,4,7,10,13] pentaokzasiklopentadekan (TNCT), sentezlenmiştir.

Dönüşümlü voltametri, UV-Vis-NIR spektroskopisi ve kolorimetre teknikleri kullanılarak monomerlerin ve polimerlerin elektrokimyasal ve optoelektronik özellikleri incelenmiştir. Elde edilen deneysel sonuçlara göre, monomerlere bağlanan her farklı grubun, bağlanma konumunun ve elektron verici grubun gücünün polimerlerin redoks davranışına, optik band aralıklarına, elde edilen renklere ve renk sayılarına etkisi olduğu belirlenmiştir.

**Anahtar Kelimeler:** Elektrokimyasal Polimerleşme, İletken Polimerler, Düşük Bant Aralığı, Elektrokromizm, Benzotriazol İçeren Monomerler, Naftalin-2,3-taç eter içeren polimerler

*To My Family*

## ACKNOWLEDGMENTS

I would like to thank my supervisor Prof. Dr. Levent Toppare for his invaluable guidance, assistance, support and motivation throughout the research. Apart from the subject of this thesis, I learnt a lot from him, which will affect my future career and life.

I would like to thank to all past and present Toppare Research Group members for their cooperation and kind friendship. Special thanks go to Grkem Gnbař, Asuman Gnbař, Abidin Balan and Derya Baran for their endless helps, valuable discussions and friendship. I would like to thank Dr. S.M. Abdul Karim for his assistance. Thanks also go to Serhat Varıř for friendship during long and enjoyable working hours before Ph.D. proficiency exam.

I also appreciate the colleagues at ROKETSAN for being helpful when I needed.

This thesis would not have been possible without the confidence, endurance and support of my family. My family has always been a source of inspiration and encouragement. I would like to thank my parents, Sakine and Abbas Yiđitsoy whose love, teachings and support have brought me this far. I wish to thank my sister, Gl Yiđitsoy, for her affection, understanding and patience.

Finally, I want to thank Fatih Kamıřlı for his patience, endless support and helps at every stage of this thesis. I also would like to express gratitude to him for his everlasting love and encouragement.

## TABLE OF CONTENTS

ABSTRACT .....	iv
ÖZ.....	vi
ACKNOWLEDGMENTS.....	ix
TABLE OF CONTENTS .....	x
LIST OF TABLES.....	xiv
LIST OF FIGURES .....	xv
LIST OF FIGURES .....	xv
LIST OF SCHEMES .....	xx
ABBREVIATIONS .....	xxi
CHAPTERS	
1 INTRODUCTION .....	1
1.1 Conducting Polymers .....	1
1.2 Band Theory and Conduction Mechanism in Conducting Polymers.....	3
1.2.1 Band Theory .....	3
1.2.2 Conduction Mechanism.....	6
1.2.2.1 Charge Carriers.....	6
1.2.2.2 Doping.....	10
1.3 Synthesis of Conducting Polymers: .....	14
1.3.1 Chemical Polymerization .....	14
1.3.2 Electrochemical Polymerization.....	16
1.3.2.1 Mechanism of Electrochemical Polymerization.....	18
1.3.2.2 Electrolytic Medium.....	20
1.3.2.3 Monomer Structure: .....	21
1.4 Band Gap .....	22
1.4.1 Low Band Gap Systems.....	22

1.4.2	Low Band Gap Polythiophene Dervatives .....	27
1.5	Applications of Conducting Polymers .....	33
1.6	Electrochromism .....	34
1.7	Benzotriazoles .....	38
1.8	Crown Ethers .....	41
1.9	Aim of This Work .....	45
<b>2</b>	<b>EXPERIMENTAL.....</b>	<b>46</b>
2.1	Materials .....	46
2.2	Instrumentation .....	47
2.2.1	Potentiostats .....	47
2.2.2	Nuclear Magnetic Resonance.....	47
2.2.3	UV-VIS-NIR Spectrophotometer.....	47
2.2.4	Mass Spectrometer .....	48
2.2.5	Colorimetry Measurements .....	48
2.3	Synthetic Procedures.....	48
2.3.1	Synthesis of Stannylated Thiophene and EDOT .....	48
2.3.1.1	Synthesis of Tributyl(2,3-dihydrothieno[3,4-b][1,4]dioxin-5-yl)stannane .....	48
2.3.1.2	Synthesis of Tributyl(thiophen-2-yl) stannane.....	49
2.3.2	Synthesis of Benzotriazole Functionalized Monomers .....	50
2.3.2.1	Synthesis of 4,7-Dibromo-2.1.3-benzothiadiazole.....	50
2.3.2.2	Synthesis of 3,6-Dibromo-1,2-phenylenediamine.....	51
2.3.2.3	Synthesis of 4,7-Dibromo-1,2,3-benzotriazole .....	52
2.3.2.4	Syntheses of 1-Benzyl-4,7-dibromo-1H-benzo[d][1,2,3]triazole (1-Bn-BTBr) and 2-Benzyl-4,7-dibromo-1H-benzo[d][1,2,3]triazole (2-Bn-BTBr)53	
2.3.2.5	Synthesis of 1-Benzyl-4,7-Di(thiophen-2-yl)-2H-benzo[d][1,2,3]triazole (BBTA) .....	54

2.3.2.6	Synthesis of 2-Benzyl-4,7-di(thiophen-2-yl)-2H-benzo[d][1,2,3]triazole (BBTS) .....	55
2.3.2.7	Synthesis of Benzyl-4,7-bis(2,3-dihydrothieno[3,4-b]dioxin-5-yl)-2H-benzo[d][1,2,3] triazole (BBTEA).....	56
2.3.2.8	Synthesis of Benzyl-4,7-bis(2,3-dihydrothieno[3,4-b]dioxin-5-yl)-2H-benzo[d][1,2,3] triazole (BBTES).....	57
2.3.3	Synthesis of Napthelene-2,3-Crown Ether Functionalized Monomers	58
2.3.3.1	Synthesis of 1,4-Dibromonaphthalene-2,3-diol (BrNPOH) .....	58
2.3.3.2	Synthesis of 14,19-Dibromo-naphtho[2,3-b][1,4,7,10,13]pentaoxacyclo pentadecane (BrNPCr) .....	59
2.3.3.3	Synthesis of 14,19-Bis(2,3-dihydrothieno[3,4-b][1,4]dioxin-5-yl)-2,3,5,6,8,9,11,12-octahydronaphtho [2,3-b] [1,4,7,10,13] pentaoxacyclopentadecane (ENCE) .....	60
2.3.3.4	Synthesis of 14,19-Di(thiophen-2-yl)-2,3,5,6,8,9,11,12,13a,19a-decahydronaphtho[2,3-b][1,4,7,10,13]pentaoxacyclopentadecane (TNCT) ....	61
2.4	Electrochemical Methods .....	62
2.4.1	Cyclic Voltammetry System.....	62
2.5	Optical Methods .....	66
2.5.1	Spectroelectrochemistry .....	66
2.5.2	Switching Studies .....	68
2.5.3	Colorimetry .....	70
<b>3</b>	<b>RESULTS AND DISCUSSION .....</b>	<b>71</b>
3.1	Synthesis and Characterization of Benzotriazole Functionalized Monomers .....	71
3.1.1	Perspective of the work .....	71
3.1.2	Synthesis of Donor Moieties .....	72
3.1.3	Syntheses and Characterizations of Acceptor Moieties .....	74
3.1.4	Syntheses of Donor-Acceptor-Donor Type Benzotriazole Derivatives	78

3.2	Synthesis Characterization of of Napthelene-2,3-Crown Ether Functionalized Monomers .....	84
3.2.1	Perspective of the work .....	84
3.2.2	Synthesis and Characterization of Napthelene-2,3-Crown Ether Moiety .....	84
3.3	Electrochemical Characterization of Benzotriazole Containing Polymers..	89
3.3.1	Cyclic Voltammetry .....	89
3.3.2	Spectroelectrochemistry of Benzotriazole Containing Polymers .....	98
3.3.3	Kinetic Studies .....	105
3.3.4	Colorimetry Studies .....	109
3.4	Electrochemical Characterization of Napthelene-2,3-Crown Ether Functionalized Monomers and Polymers .....	112
3.4.1	Cyclic Voltammetry .....	112
3.4.2	Spectroelectrochemical Properties of PENCE .....	116
3.4.3	Kinetic Studies .....	120
3.4.4	Colorimetry Studies .....	122
<b>4</b>	<b>CONCLUSION .....</b>	<b>123</b>
	<b>REFERENCES.....</b>	<b>126</b>
	<b>APPENDIX A: SELECTED NMR DATA .....</b>	<b>133</b>
	<b>CURRICULUM VITAE .....</b>	<b>140</b>

## LIST OF TABLES

### TABLES

Table 3.1 Optical contrast and switching times for PBBTES <sup>a</sup> .....	106
Table 3.2 Optical contrast and switching times for PBBTS <sup>a</sup> .....	107
Table 3.3 Optical contrast and switching times for PBBTA.....	108
Table 3.4 Colors of the PBBTES and PBBTEA at their neutral and oxidized states .	110
Table 3.5 Colors of p-type and n-type doped PBBTS .....	111
Table 3.6 Colors of the PBBTA at their neutral and oxidized states.....	111
Table 3.7 Spectroelectrochemical properties of PENCE.....	118
Table 3.8 Optical contrast and switching times for PENCE <sup>a</sup> .....	120
Table 3.9 Colors of PENCE at neutral, partially and fully doped states.....	122

## LIST OF FIGURES

### FIGURES

Figure 1.1 Structures of some common conducting polymers.....	2
Figure 1.2 Schematic representations of band structures .....	4
Figure 1.3 Generation of bands in polythiophene, (n=number of rings) .....	5
Figure 1.4 Soliton structures of polyacetylene .....	7
Figure 1.5 Formation of polaron and bipolaron for polyacetylene .....	8
Figure 1.6 The degenerate ground states of PA (a) and the nondegenerate ground states of the fully aromatic polymer .....	9
Figure 1.7 The charged states, charge carries and energy bands for poly(pyrrole)....	9
Figure 1.8 Band model of (a) n-type, (b) p-type doped.....	10
Figure 1.9 p-type doping of PTh. ....	11
Figure 1.10 Conductivities of some metals, semiconductors and insulators. ....	13
Figure 1.11 Synthesis of polythiophene via a) metal catalyzed coupling and b) chemical oxidation .....	15
Figure 1.12 McCullough method for the synthesis of regioregular poly(alkylthiophenes) [48] .....	16
Figure 1.13 Electrochemical synthetic routes to polyheterocycles. ....	17
Figure 1.14 Radical-cation/monomer.....	18
Figure 1.15 Electrochemical polymerization mechanism for a five membered heterocyclic compound, where X = N-H, S, O.....	19
Figure 1.16 Methods for modification of band gap .....	23
Figure 1.17 Illustration of methods for alteration of band gap .....	23
Figure 1.18 The emergence of band gap by Peierls distortion [55] .....	24
Figure 1.19 Aromatic and quinoid forms of polythiophene.....	25
Figure 1.20 Aromatic and quinoid forms of polyisothianaphthene (PITN).....	25

Figure 1.21 Interannular rotations in polythiophene chain.....	26
Figure 1.22 Band gap energies of PTh, P3MT and P3HT.....	28
Figure 1.23 Polythiophene derivatives substituted from 3- and 4- position.....	29
Figure 1.24 Structures of bithiophene and 2,2'-bis(EDOT).....	30
Figure 1.25 Structures of bithiophene and 2,2'-bis(EDOT).....	31
Figure 1.26 Donor (D) -Acceptor (A) Concept.....	31
Figure 1.27 VB and CB levels for cyanovinylene substituted with different donor groups. ....	32
Figure 1.28 Applications of conducting polymers [74]. ....	34
Figure 1.29 Examples of multicolor electrochromic polymers synthesized by structural modification. 0 = neutral; I= intermediate; + =oxidized; and.....	37
Figure 1.30 1H-Benzotriazole and 2R-BTz.....	39
Figure 1.31 DAD type monomer containing benzoazole groups.....	39
Figure 1.32 Benzotriazole functionalized low band gap polymers.....	41
Figure 1.33 Twisting mechanism of crown ether-appended polythiophene.....	42
Figure 1.34 Schematic representation of conducting-polymerbased.....	43
Figure 1.35 15-crown-5 substituted thiophenes.....	44
Figure 2.1 Typical (a) Potential-time excitation signal in CV (b) cyclic voltammogram of a reversible $O + ne \leftrightarrow R$ redox process.....	63
Figure 2.2 Cyclic Voltammogram of a representative type of electroactive monomer [113].....	65
Figure 2.3 Illustration of spectroelectrochemical data of a PEDOT derivative.....	67
Figure 2.4 A three electrode electrochemical cell set up.....	68
Figure 2.5 Switching studies of a representative electrochromic conducting polymer.....	69
Figure 2.6 CIE 1931 Lab color space.....	70
Figure 3.1 Donor-Acceptor-Donor Type Benzotriazole Derivatives.....	72
Figure 3.2 Synthetic route for synthesis of 1-Bn-BTBr and 2-Bn-BTBr.....	78

Figure 3.3 Comparative <sup>1</sup> H-NMR spectra of BBTEA and BBTES .....	82
Figure 3.4 Comparative <sup>13</sup> C-NMR spectra of BBTA and BBTS .....	83
Figure 3.5 <sup>1</sup> H-NMR spectrum of TNCT.....	88
Figure 3.6 The cyclic voltammogram of the BBTES between -0.5 to +1.0 V at 100 mVs <sup>-1</sup> in 0.1 M TBAPF <sub>6</sub> /CH <sub>2</sub> Cl <sub>2</sub> /ACN on an ITO electrode .....	90
Figure 3.7 The cyclic voltammogram of the BBTEA between 0.2 to +1.2 V at 100 mVs <sup>-1</sup> in 0.1 M TBAPF <sub>6</sub> /CH <sub>2</sub> Cl <sub>2</sub> /ACN on an ITO electrode. ....	90
Figure 3.8 The cyclic voltammogram of the BBTS between 0.0 to +1.5 V at 100 mVs <sup>-1</sup> in 0.1 M TBAPF <sub>6</sub> /CH <sub>2</sub> Cl <sub>2</sub> /ACN on an ITO electrode.....	93
Figure 3.9 Single scan cyclic voltammogram of PBBTS films between 1.2 V and -2.1 V using ACN as the solvent and TBAPF <sub>6</sub> as supporting electrolyte at a scan rate of 100 mV/s. ....	94
Figure 3.10 a) The cyclic voltammogram of the BBTA between -0.3 to +1.7 V at 100 mVs <sup>-1</sup> in 0.1 M TBAPF <sub>6</sub> /CH <sub>2</sub> Cl <sub>2</sub> /ACN on an ITO electrode b) Single scan cyclic voltammogram of PBBTA film between 0.5 V and 1.65 V at 100 mVs <sup>-1</sup> in 0.1 M TBAPF <sub>6</sub> /ACN on an ITO electrode.....	95
Figure 3.11 Scan rate dependencies of BBTES and BBTEA at a)50 b) 100 c) 150 d) 200 mV/s in 0.1 M TBAPF <sub>6</sub> /CH <sub>2</sub> Cl <sub>2</sub> /ACN on an ITO electrode. ....	97
Figure 3.12 Scan rate dependencies of BBTA and BBTS at a)50 b) 100 c) 150 d) 200 mV/s in 0.1 M TBAPF <sub>6</sub> /CH <sub>2</sub> Cl <sub>2</sub> /ACN on an ITO electrode. ....	97
Figure 3.13 Spectroelectrochemistry of PBBTES film on an ITO coated glass slide in monomer-free, 0.1 M TBAPF <sub>6</sub> /ACN electrolyte-solvent couple at applied potentials (V) a) -0.5 b)-0.4 c )-0.3 d)-0.2 e)-0.1 f)0.0 g)0.1 h)0.2 i)0.3 j)0.4 k)0.5 l)0.6 m)0.7 n)0.8.99	
Figure 3.14 Spectroelectrochemistry of PBBTEA film on an ITO coated glass slide in monomer-free, 0.1 M TBAPF <sub>6</sub> /ACN electrolyte-solvent couple at applied potentials (V) a) 0.0 b)0.1 c )0.2 d)0.3 e)0.4 f)0.5 g)0.6 h)0.7 i)0.8 j)0.9 k)1.0 l)1.1 m)1.2. ....	100

Figure 3.15 Spectroelectrochemistry of PBBTS film on an ITO coated glass slide in monomer-free, 0.1 M TBAPF <sub>6</sub> /ACN electrolyte-solvent couple at applied potentials (V) a) 0.0 b) 0.1 c) 0.2 d) 0.3 e)0.4 f)0.5 g) 0.6 h) 0.7 i) 0.8 j) 0.9 k) 1.0 l) 1.1 m) 1.2 ...	101
Figure 3.16 n-Doping spectroelectrochemistry of PBBTS at applied potentials (V) a) 0.0 b) -1.65 c) -1.7 d) -1.8 e) -2.02 .....	102
Figure 3.17 Spectroelectrochemistry of PBBTA film on an ITO coated glass slide in monomer-free, 0.1 M TBAPF <sub>6</sub> /ACN electrolyte-solvent couple at applied potentials and corresponding colors observed at neutral and doped states.....	104
Figure 3.18 Switching time and ΔT% change monitored at 625 and 1800 nm for PBBTES in 0.1 M TBAPF <sub>6</sub> /ACN. ....	106
Figure 3.19 ΔT% change monitored at a) 504 nm and b) 1225 nm for PBBTS in 0.1 M TBAPF <sub>6</sub> /ACN.....	108
Figure 3.20 ΔT% change monitored at 1225 nm and 1300 nm for PBBTS and PBBTA in 0.1 M TBAPF <sub>6</sub> /ACN, respectively. ....	109
Figure 3.21 Cyclic Voltammogram of PENCE in the presence of 0.1 M tetrabutyl ammonium hexafluorophosphate (TBAPF <sub>6</sub> ) as the supporting electrolyte in acetonitrile-dichloromethane (CH <sub>2</sub> Cl <sub>2</sub> :CH <sub>3</sub> CN) solvent couple in 5:95 volume % ratios with 100 mVs <sup>-1</sup> scan rate between -0.5 V and +1.0 V. ....	113
Figure 3.22 Cyclic Voltammogram of TNCT in the presence of 0.1 M tetrabutyl ammonium hexafluorophosphate (TBAPF <sub>6</sub> ) as the supporting electrolyte in acetonitrile-dichloromethane (CH <sub>2</sub> Cl <sub>2</sub> :CH <sub>3</sub> CN) solvent couple in 5:95 volume % ratios with 100 mVs <sup>-1</sup> scan rate between -0.3 V and +1.3 V. ....	114
Figure 3.23 Comparison of PENCE cyclic voltammogram in the presence of LiClO <sub>4</sub> and NaClO <sub>4</sub> .....	116
Figure 3.24 Spectroelectrochemical spectrum of PENCE at 0.1 M TBAPF <sub>6</sub> /ACN electrolyte-solvent couple with applied potentials between -0.5 V and +1.0 V.....	117
Figure 3.25 Spectroelectrochemical spectrum of PENCE at 0.1 M NaClO <sub>4</sub> /ACN electrolyte-solvent couple with applied potentials between -0.5 V and +0.6 V.....	119

Figure 3.26 Spectroelectrochemical spectrum of PENCE at 0.1 M LiClO <sub>4</sub> /ACN electrolyte-solvent couple with applied potentials between -0.8 V and +0.6 V .....	119
Figure 3.27 Electrochromic switching, optical absorbance change monitored at 567 nm and 1400 nm for PENCE between -0.5 V and +0.7 V .....	121
Figure A.1. <sup>1</sup> H-NMR spectra of 2-Benzyl-BTBr and 1-Benzyl-BTBr.....	133
Figure A.2 <sup>1</sup> H and <sup>13</sup> C NMR Spectra of BBTEA.....	134
Figure A.3 <sup>1</sup> H- and <sup>13</sup> C NMR Spectra of BBTES .....	135
Figure A.4 <sup>1</sup> H- and <sup>13</sup> C NMR Spectra of BBTA.....	136
Figure A. 5 <sup>1</sup> H- and <sup>13</sup> C-NMR Spectra of BBTS .....	137
Figure A.6 <sup>1</sup> H-NMR Spectrum of NPBrOH.....	138
Figure A.7 <sup>1</sup> H-NMR spectrum of NPBrCr .....	138
Figure A. 8 <sup>1</sup> H-NMR spectrum of ENCE.....	139
Figure A.9 <sup>1</sup> H-NMR spectrum of TNCT .....	139

## LIST OF SCHEMES

### SCHEMES

Scheme 3.1 Preparation of organotin compounds.....	73
Scheme 3.2 Reaction mechanism for stannilation of thiophene.....	73
Scheme 3.3 Synthetic route for functionalization of benzotriazole.....	74
Scheme 3.4 Synthetic route for synthesis of 3,6-dibromo-1,2-phenylenediamine.....	75
Scheme 3.5 Synthetic route for 4,7-dibromo-1,2,3-benzotriazole.....	76
Scheme 3.6 Mechanism of triazole ring formation.....	76
Scheme 3.7 Synthetic route for 1-Bn-BTBr and 2-Bn-BTBr.....	77
Scheme 3.8 Catalytic cycle of the Stille reaction.....	79
Scheme 3.9 Synthetic route for BBTES and BBTEA.....	80
Scheme 3.10 Synthetic route for BBTES and BBTEA.....	80
Scheme 3.11 Representative cycle of Stille coupling reaction for BBTS.....	81
Scheme 3.12 Synthetic route for 1,4-Dibromonaphthalene-2,3-diol.....	85
Scheme 3.13 General mechanism of Mitsunobu reaction.....	85
Scheme 3.14 Synthetic route for 1,4-Dibromonaphthalene-2,3-diol.....	86
Scheme 3.15 Synthetic routes for ENCE and TNCT.....	87
Scheme 3.16 p-doping of PBBTES.....	91
Scheme 3.17 p-doping of PBBTEA.....	92
Scheme 3.18 p-doping of PBBTS.....	93
Scheme 3.19 p-doping of PBBTA.....	95
Scheme 3.20 p-doping of PENCE.....	112

## ABBREVIATIONS

BBTA	1-Benzyl-4,7-di(thiophen-2-yl)-2H-benzo[d][1,2,3] triazole
BBTS	2-Benzyl-4,7-di(thiophen-2-yl)-2H-benzo[d][1,2,3] triazole
BBTEA	1-Benzyl-4,7-bis(2,3-dihydrothieno[3,4-b]dioxin-5-yl)-2H-benzo[d][1,2,3]triazole
BBTES	2-Benzyl-4,7-bis(2,3-dihydrothieno[3,4-b]dioxin-5-yl)-2H-benzo[d][1,2,3]triazole
P(BBTA)	Poly(1-Benzyl-4,7-di(thiophen-2-yl)-2H-benzo[d][1,2,3] triazole)
P(BBTS)	Poly(2-Benzyl-4,7-di(thiophen-2-yl)-2H-benzo[d][1,2,3]triazole)
P(BBTEA)	Poly(1-benzyl-4,7-bis(2,3-dihydrothieno[3,4-b] dioxin -5-yl)-2H-benzo[d][1,2,3]triazole)
P(BBTES)	Poly(2-benzyl-4,7-bis(2,3-dihydrothieno[3,4-b] dioxin -5-yl)-2H-benzo[d][1,2,3]triazole)
TNCT	14,19-di(thiophen-2-yl)-naphtho[2,3-b][1,4,7,10,13]pentaoxacyclo pentadecane
ENCE	14,19-bis(2,3-dihydrothieno[3,4-b][1,4]dioxin-5-yl)-naphtho[2,3-b][1,4,7,10,13]pentaoxacyclo penta decane
EDOT	3,4-Ethylenedioxythiophene
Th	Thiophene
Py	Pyrrole
PEDOT	Poly(3,4-ethylenedioxythiophene)
ACN	Acetonitrile
NMR	Nuclear Magnetic Resonance
CV	Cyclic Voltammetry
SEM	Scanning Electron Microscopy
GPC	Gel Permeation Chromatography

ECD	Electrochromic Device
HOMO	Highest Occupied Molecular Orbital
LUMO	Lowest Unoccupied Molecular Orbital
E <sub>g</sub>	Band Gap Energy
CIE	La Commission Internationale de l'Eclairage
L a b	Luminance, hue, saturation
CB	Conduction band
VB	Valence Band
DCM	Dichloromethane
ITO	Indium Tin Oxide
TBAPF <sub>6</sub>	Tetrabutylammonium hexafluorophosphate
PF	Polyfuran
PA	Polyacetylene
PANI	Polyaniline
PCz	Polycarbazole
P3HT	Poly(3-hexylthiophene)
P3MT	Poly(3-methylthiophene)

## CHAPTER 1

### INTRODUCTION

#### 1.1 Conducting Polymers

The most important innovation in the field of conducting polymers is the discovery of increase in conductivity of polyacetylene by many orders of magnitude when it is chemically doped with halogen vapors. Alan MacDiarmid, Hideki Shirakawa and Alan Heeger were awarded with the Nobel Prize in 2000 for their discovery, and the discovery initiated significant amount of academic research in this field and many industrial products have been developed.

The assumption that all polymers are inherently electrical insulator has been changed by the discovery of conducting polymers. This concept began to change in the beginning of 1970s when it was discovered that polysulfur nitride (SN)<sub>x</sub> has an intrinsic conductivity of  $10^3$  S/cm which is very close to the conductivity of copper metal with  $1 \times 10^6$  S/cm. [1]. In 1977 it was reported that intrinsic conductivity of (SN)<sub>x</sub> can be increased at room temperature when it is doped by halogen derivatives [2-4].

In 1977, Heeger, MacDiarmid and Shirakawa found that polyacetylene became conductive when it is doped with a strong electron acceptor; iodine by 12 orders of magnitude. [5].

Although polyacetylene (PA) is highly conductive in doped form, it is unprocessable due to its instability in air and insolubility in common solvents. [6]. These disadvantages directed scientist to synthesize processable functionalized PA derivatives. However, it was observed that derivatives of PA have lower conductivity values with respect to PA itself.

After the synthesis of a free standing film of polypyrrole in 1979, conducting polymers based on aromatic-heteroaromatic compounds such as aniline, pyrrole and thiophene, which have higher stability and provide more diversity of structures, have been studied extensively for several decades [7]. Polyaniline (PANI) [8], polypyrrole (PPy) [9], polythiophene (PTh) [10], poly(3,4-ethylenedioxythiophene) (PEDOT) [11] and polycarbazole (PCz) [12] are examples of these new class of conjugated polymers and they are shown in Figure 1.1.

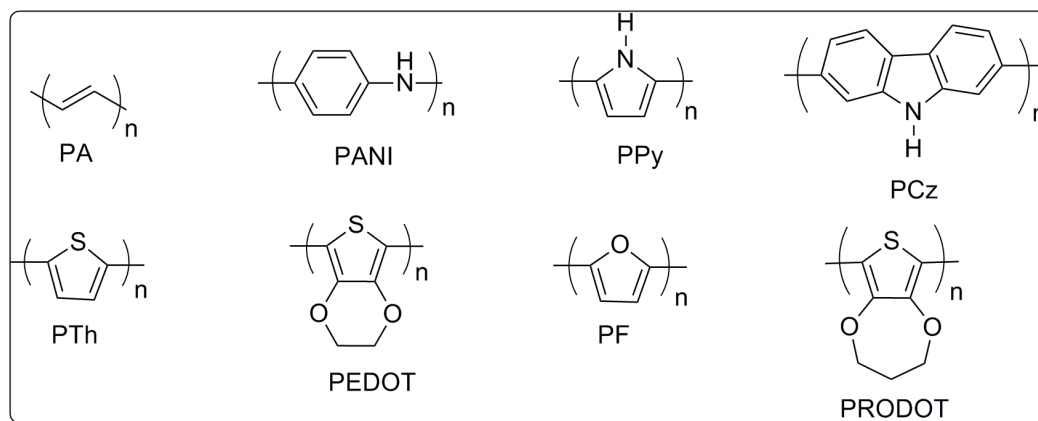


**Figure 1.1** Structures of some common conducting polymers

Conducting polymers are used in wide range of applications such as thin film transistors [13,14], sensors [15,16], polymer light emitting diodes [17,18], photovoltaics [19,20] and electrochromic devices [21,22].

## **1.2 Band Theory and Conduction Mechanism in Conducting Polymers**

### **1.2.1 Band Theory**

Differences between metals, insulators and semiconductors can be explained by the band theory. Two discrete energy levels exist for materials. The highest occupied electronic levels constitute the valence band and the lowest unoccupied levels constitute the conduction band. The energy difference between VB and CB is called band gap ( $E_g$ ) [23].

In order to occupy a given band, electrons must have a certain level of energy, and to move from the valence band to the conduction band they require extra energy. Neither empty nor full bands can carry electricity. Only partially full bands can carry electricity, and metals have high conductivity since their energy bands are partially filled.

For metals, valence and conduction bands are partially filled and they overlap to form a single band where charge carriers are free to move leading to conduction. Contrary to zero band gap for metals, insulators have a large band gap, higher than 3 eV, between valence and conduction bands. Therefore, transition of electrons between valence and conduction bands is impossible due to the large band gap (Figure 1.2). Most of the conventional polymers behave as insulators due to the large band gap between full valence and empty conduction bands.

The band gap of semiconductors is between those of metals and insulators. The conjugated organic polymers have narrower band gaps and exhibit semiconductor properties. Band structures of semiconductors can be changed by either taking electrons from the valence band (*p* doping) or adding electrons to the conduction band (*n* doping) to increase the conductivity [24].

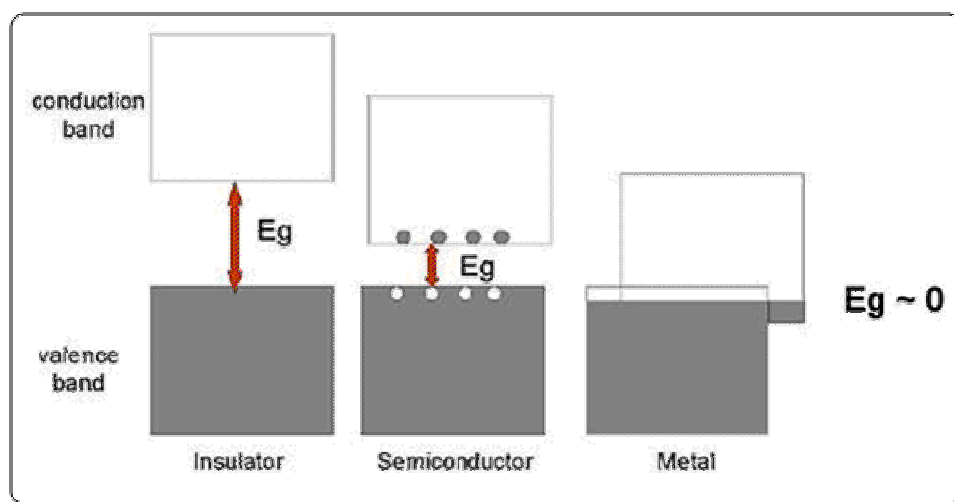


**Figure 1.2** Schematic representations of band structures

The intrinsic conductivity of organic conjugated polymers arises from an extended and delocalized framework originating from the overlap of  $\pi$  orbitals.  $\pi$  orbital interaction of the repeating units in the organic conjugated polymers yields band structures [25]. In Fig 1.3, it is shown that the energy levels differentiate between the oligothiophene and polythiophene. As more thiophene rings are added to oligothiophene ( $n = 1 - 4$ ) chain, new energy levels are formed due to increase of the number of  $\pi$  bonding and anti-bonding orbitals. After a certain chain length for the formation of polythiophene, energy bands are observed rather than discrete energy

levels. The valence band is formed by the filled  $\pi$  bonding orbitals and the conduction band is formed by empty  $\pi$  anti-bonding orbitals [26].

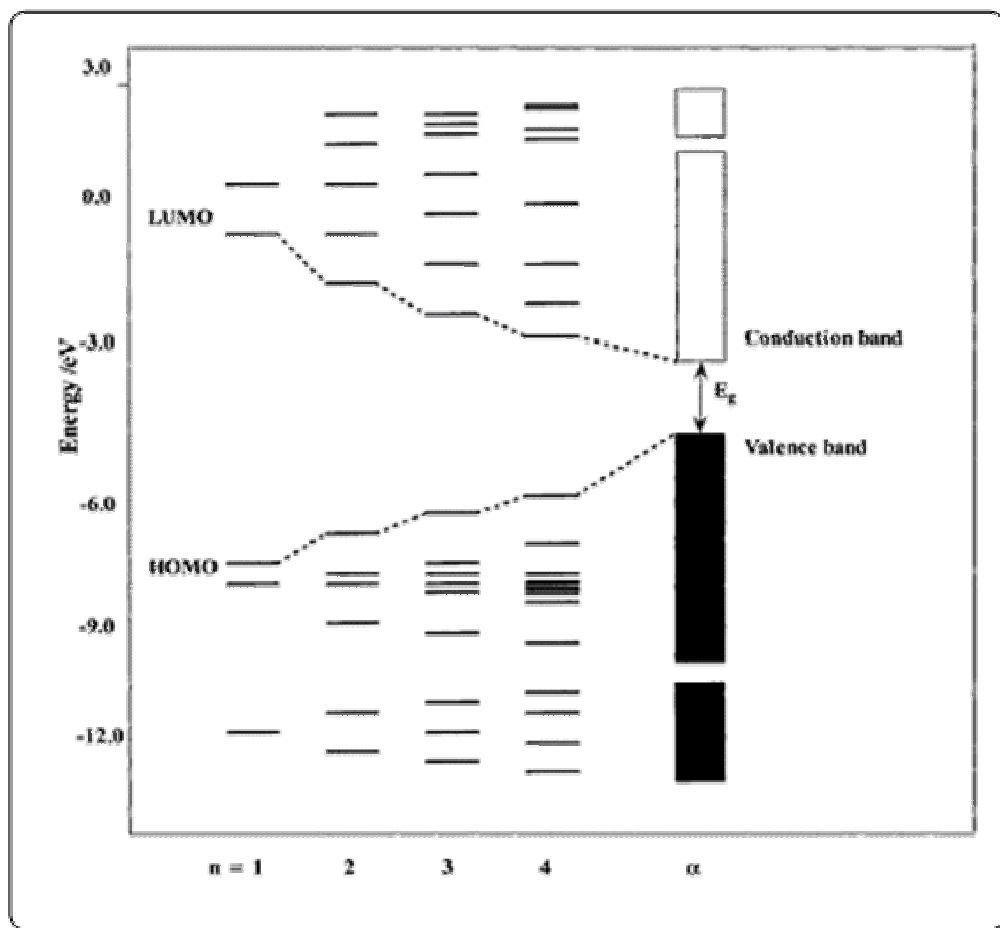


**Figure 1.3** Generation of bands in polythiophene, (n=number of rings) [26]

The band gap of the conjugated organic polymers is affected by different structural factors. Band gap value of an organic conjugated polymer can be calculated from the onset energy of the  $\pi$ - $\pi^*$  transition of neutral polymer in UV-Vis spectrum.

## 1.2.2 Conduction Mechanism

### 1.2.2.1 Charge Carriers

Band theory is not sufficient to explain the conduction behavior of CPs and a better understanding can be obtained using the concepts of solitons, polarons and bipolarons [27]. When polymers are doped in the polymer chain, conjugational defects, such as solitons, polarons or bipolarons, are formed. Polaron is a charge defect formed when oxidation of the polymer breaks one double bond and leaves a radical and a positive charge on the polymer chain. Another charge defect is soliton, which can be neutral, positive or negative. In neutral soliton, energy level is singly occupied and therefore, the spin has the value of  $\frac{1}{2}$ . Neutral solitons have spin but no charge. Insertion of acceptor band (p-type doping) or electrochemical oxidation, where an electron is removed, forms positive soliton. Negatively charged soliton can be obtained by the insertion of donor band, where an electron is added (Fig. 1.4).

Dications in the polymer are formed by further oxidation of the polymer. An electron can be removed either from the polaron or from the remaining neutral portion of the chain. If formation of a bipolaron is compared to the formation of two polarons, formation of bipolaron is preferable thermodynamically since it produces a larger decrease in ionization energy [28]. In addition, the new empty bipolaron states are located symmetrically within the band gap. Additional localized bipolaron states can be created by further doping, and at high enough doping levels, these states overlap and form continuous bipolaron bands.

The conjugated structure of trans-polyacetylene leads to formation of two resonance states which are degenerate and thermodynamically equivalent [29].

Therefore, an unpaired electron (a neutral soliton) exists in polyacetylene chains. Upon oxidation or reduction, a radical cation or soliton is generated which moves along the polymer chain and has zero spin. Double bonds get shorter and single bonds gets longer as the soliton moves over double and single bonds. This mechanism is shown in Figure 1.5. The localized electronic state of soliton is a nonbonding state and its energy level exist in the middle of bonding ( $\pi$ ) and antibonding( $\pi^*$ ) levels of perfect polyacetylene chain.

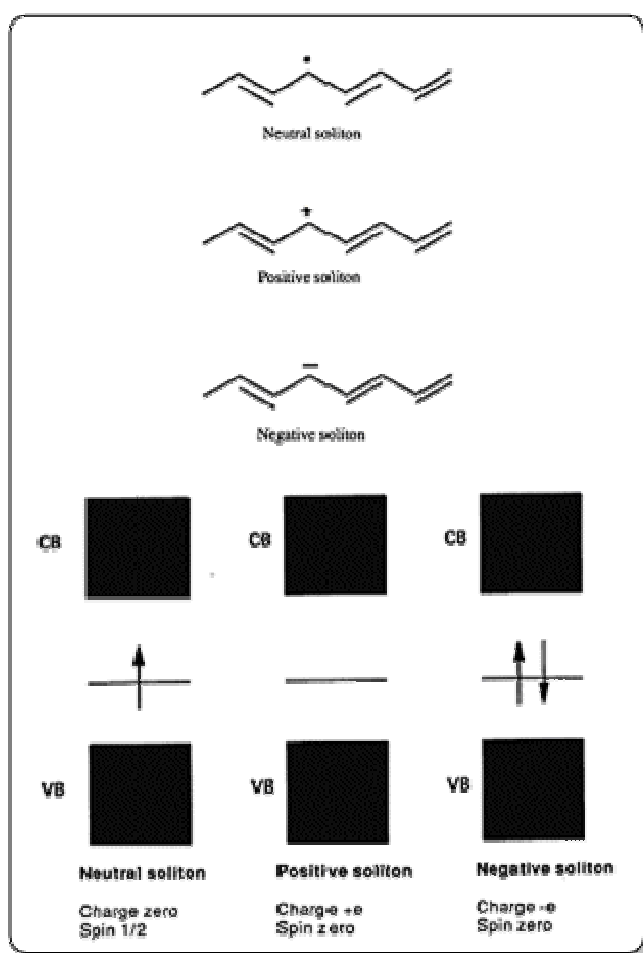
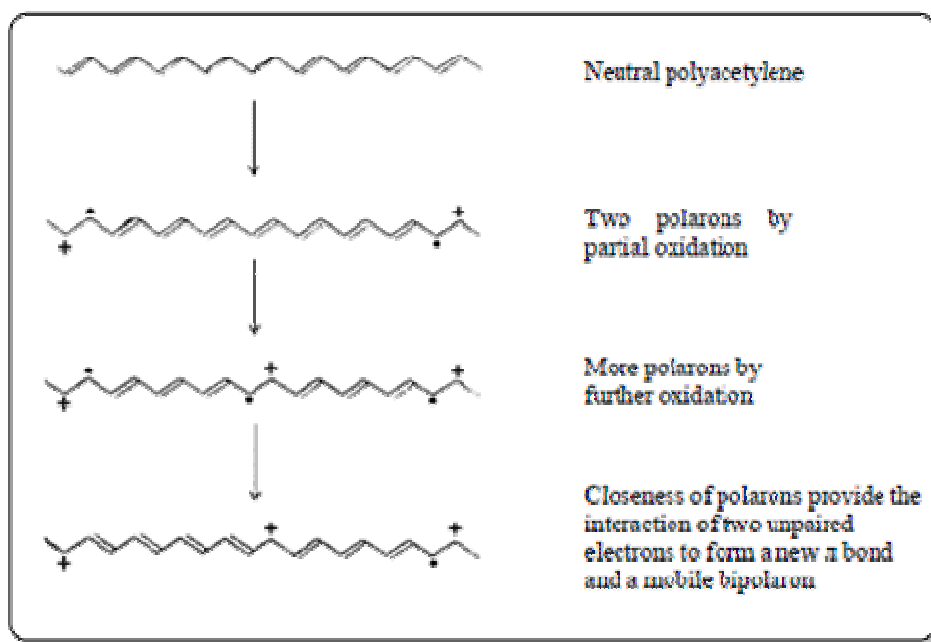


Figure 1.4 Soliton structures of polyacetylene



**Figure 1.5** Formation of polaron and bipolaron for polyacetylene

Unlike polyacetylene, other aromatic-heteroaromatic organic conducting polymers have non-degenerate ground states. For instance polypyrrole has both benzenoid and quinoid configurations and these configurations are shown in Figure 1.6. The quinoid structure generally has a slightly higher energy, and thus being less favorable with respect to the benzenoid structure [30].

In the case of polypyrrole (Fig. 1.7), chemical oxidation removes an electron from the  $\pi$ -system of its backbone creating an unpaired electron with spin  $\frac{1}{2}$  (a free radical) and a spinless positive charge (cation). Through a local bond rearrangement, the radical and the cation are coupled to each other creating a polaron which appears in the band structure as a single unpaired electron possessing charge and spin. This deformation results in the formation of two new electronic states, which appear within the valence and conduction band of the polymer.

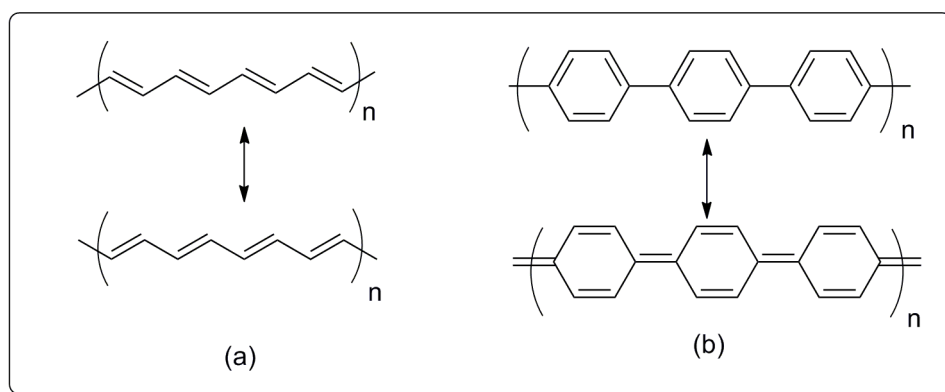


**Figure 1.6** The degenerate ground states of PA (a) and the nondegenerate ground states of the fully aromatic polymer

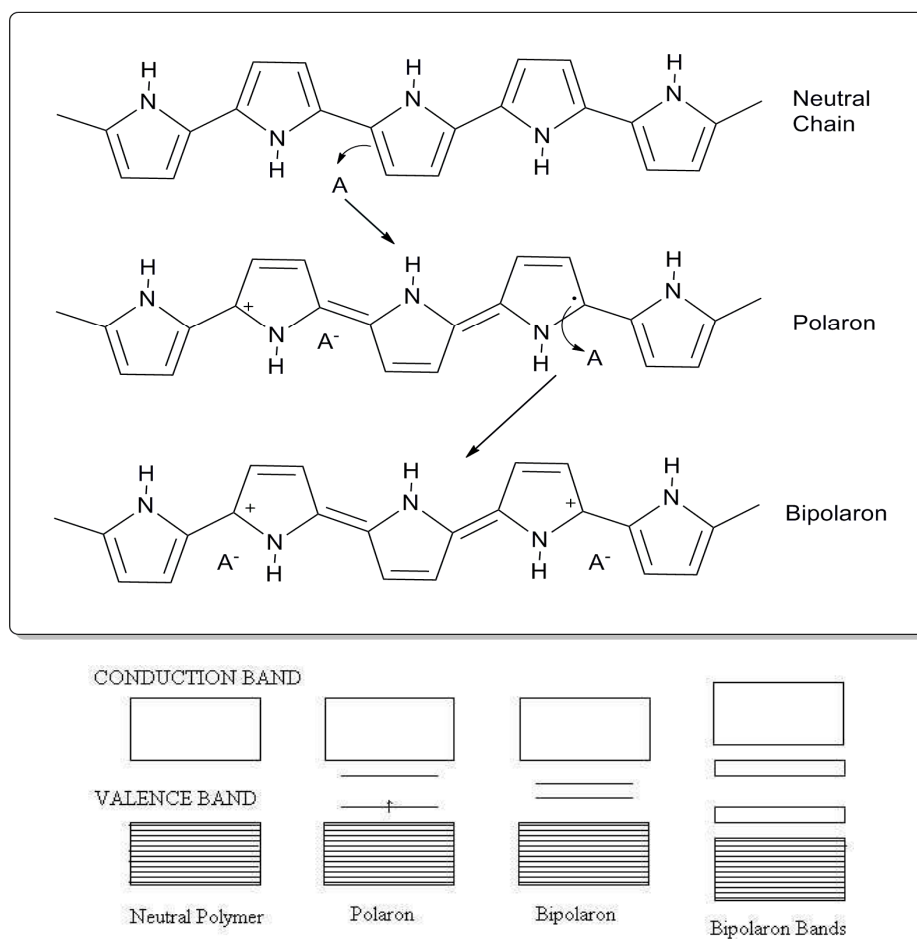


**Figure 1.7** The charged states, charge carriers and energy bands for poly(pyrrole)

### 1.2.2.2 Doping

The electrical conductivity of conjugated polymers can be altered by doping. Similar to semiconductors, organic conjugated polymers can be doped either by oxidizing (p-type) or reducing (n-type) polymer backbone. The conductivity of the polymer can be modified by changing the doping level [31]. Ejection of an electron from the valence band is defined as p-type doping and injection of an electron to its conduction band is called n-type doping [32]. n-Doping process requires dry and oxygen-free medium to avoid oxidation of negatively charged polymer [33]. Therefore, number of n-dopable conducting polymers is limited in the literature when it is compared to the p-dopable ones [34-36].

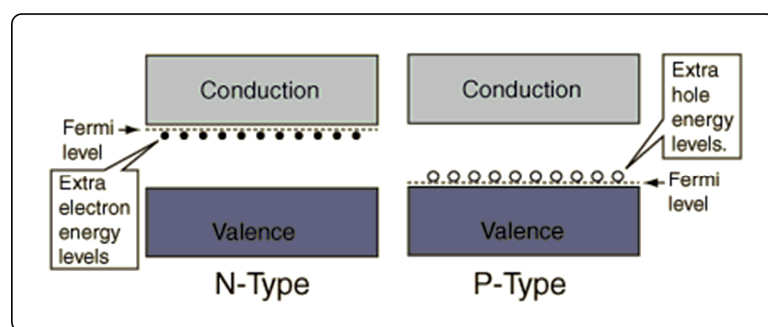


**Figure 1.8** Band model of (a) n-type, (b) p-type doped

When a charge is injected to the neutral polythiophene, the polymer is oxidized and an electron is added to the conduction band from the top of the valence band) of a conjugated polymer. It is converted into a radical ion which is delocalized over four rings. The charge is delocalized on the entire polymer chain causing a local distortion which confines the charge to a four ring section. This state is called as polaron in solid state physics.

The aromatic quinoid structure of the polaron enriches the  $\pi$  overlap and gives rise to formation of new intragap energy levels. When the polymer is saturated with polarons, further doping produce another structure with more quinoid character which is called bipolaron. The enhanced quinoid character of bipolaron with respect to that of polaron compresses the intragap energy levels.

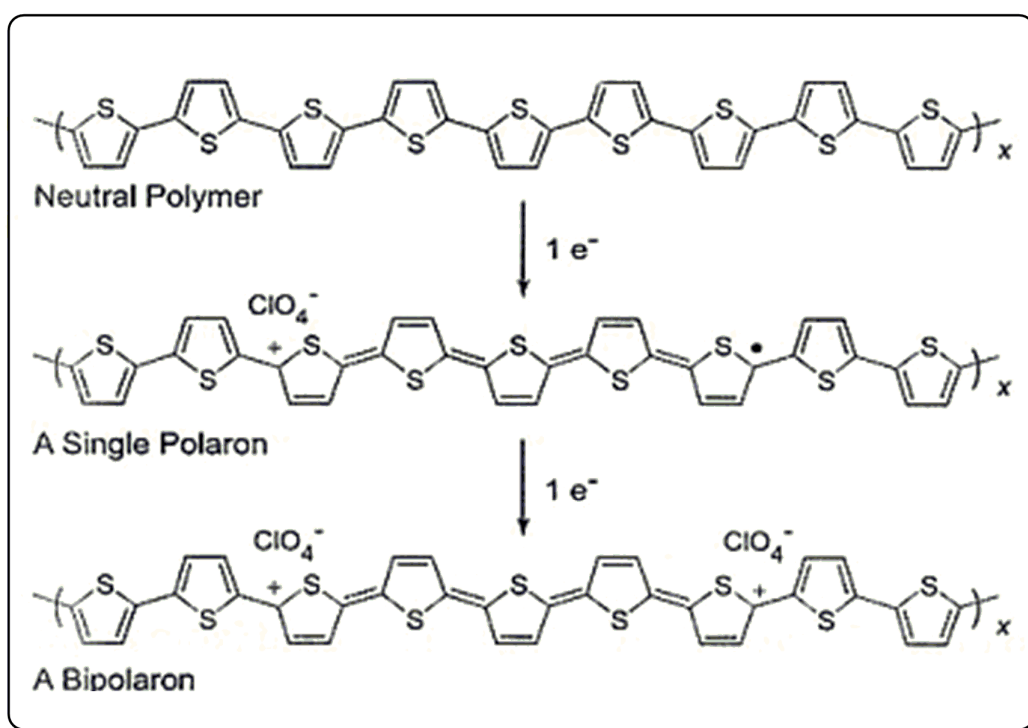


Figure 1.9 p-type doping of PTh.

Although the polymers can be doped by various methods such as chemical, photochemical, interfacial ways, doping by means of electrochemical methods is easy to control [31].

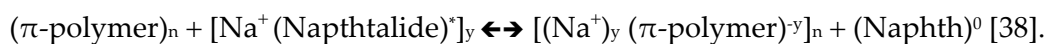
Chemical doping is a redox reaction between an oxidizing or reducing agent and the polymer. Despite efficient and straightforward process of chemical doping, disadvantages like difficulty of obtaining various doping levels makes electrochemical superior to chemical doping in term of controlling intermediate doping levels [37]. Chemical doping is favorable method when antistatic coating or transparent electrodes will be the application of final product.

Chemical doping involves charge-transfer redox chemistry:

(a) Oxidation (*p*-type doping)



(b) Reduction (*n*-type doping)

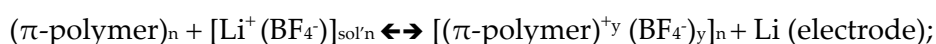


The oxidation or reduction of the polymer can be achieved electrochemically by subjecting the neutral polymer to appropriate oxidizing and reducing potential in an electrochemical cell.

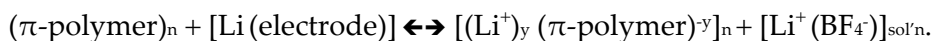
In the electrochemical doping, charge injection or doping level can be controlled by changing the applied potential. The conducting polymer coated on an electrode can be doped in the presence of electrolyte at desired degree of doping level by varying potential applied to the electrode. The charge formed on the polymer chain uptakes the counter ion from the electrolyte solution to neutralize itself [39].

Electrochemical doping is shown by the following examples [37, 40]:

(a) *p* type



(b) *n* type



The doping level is controlled with the potential applied between the conducting polymer and counter electrode and therefore doping at any level can be accomplished by setting the electrochemical cell at a fixed applied voltage and simply waiting for the system to come to electrochemical equilibrium [41].

An advantage of conducting polymers is that their conductivity can be tuned over eight or more orders of magnitude in the same material. The doping level of conducting polymers affects range of conductivity from insulator to metal. Figure 1.10 shows the typical conductivity ranges of the three most common conducting polymers (PA, PPy, PTh).

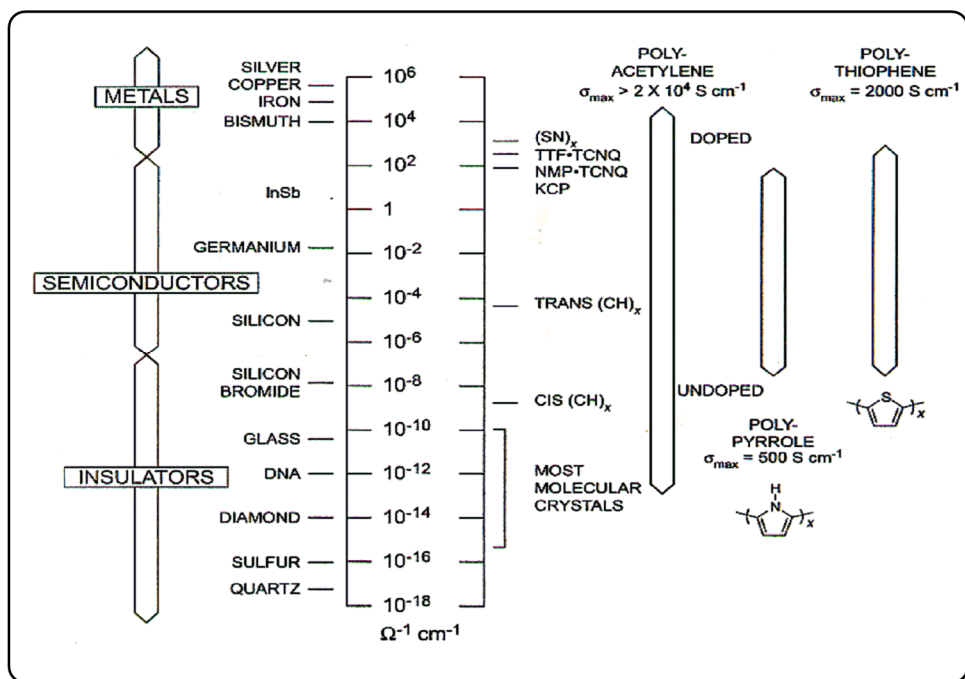


**Figure 1.10** Conductivities of some metals, semiconductors and insulators.

### 1.3 Synthesis of Conducting Polymers:

Organic conjugated polymers are synthesized commonly by chemical and electrochemical methods. There are also some other methods including photochemical polymerization, metathesis polymerization, Grignard reaction, and transition metal-catalyzed polymerization [42].

Not only the rapid polymerization time (a few seconds) and controllable polymerization degree but also the syntheses of polymer in its oxidized state are the advantages of electrochemical polymerization over chemical polymerization. After several hours and tedious work up of chemical polymerization; the resultant neutral polymer should be doped either chemically or electrochemically to its doped states. Chemical polymerization is a very useful technique when a large amount of polymer is needed.

#### 1.3.1 Chemical Polymerization

Chemical polymerization can be achieved successfully either by the least expensive oxidative polymerization technique in the presence of ferric chloride ( $\text{FeCl}_3$  or other Lewis acids) or metal catalyzed coupling reactions (Fig 1.11) [43].

The metal catalyzed coupling reactions include the condensation of the monomeric precursors in the presence of Ni catalyst. [44]. In Figure 1.12, polymerization of a heteroaromatic monomer by metal catalyzed coupling method is illustrated. Dibrominated heterocycle reacts with Mg metal to produce 2-magnesiobromo-5-bromo- heterocycle. This intermediate product reacts with the dibromo heterocycle to obtain polyheterocycle. [45]

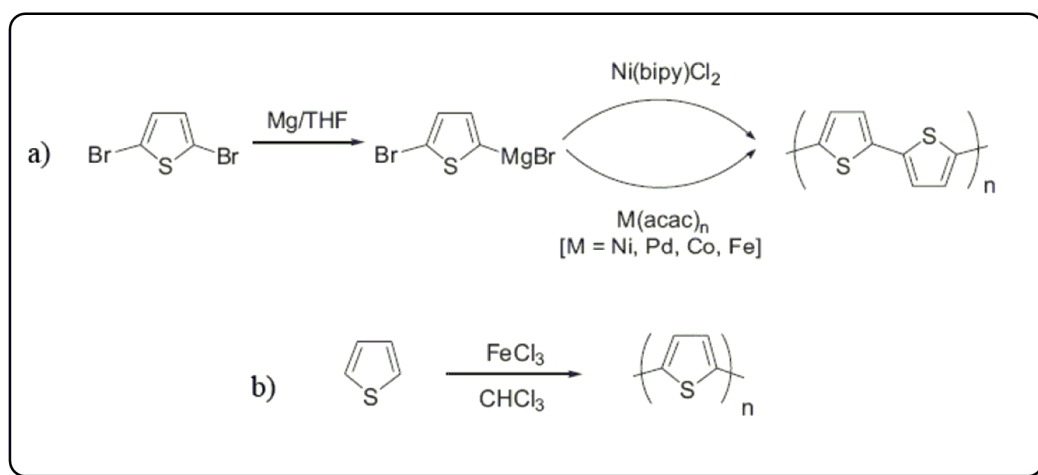


**Figure 1.11** Synthesis of polythiophene via a) metal catalyzed coupling and b) chemical oxidation

Polymerization under Friedel-Craft condition which is performed in the presence of  $\text{FeCl}_3$  or another Lewis acid is the oxidative polymerization taking place in bulk of the solution [46]. The chemically active cation radicals react with the monomer to yield oligomers and polymers. As the molecular weight of polymer increases, resultant polymer becomes insoluble. The oxidative chemical polymerization of thiophene yields an insoluble polymer with a polydispersity value ranging from 1.3 to 5 [47].

Insoluble polymers obtained by chemical polymerization are not processable thus being not practical to use for applications. Introduction of side chains into insoluble PTh enhances the solubility of the resulting polymer. Substitution from 3 and 4 positions of thiophene yields PTh with three different types of coupling along polymer chain. Coupling of 3 and 4 substituted thiophene can be head to tail (H-T), tail to tail (T-T) or head to head (H-H) type. H-H or T-T configuration of polymers results in the formation of irregular polymer chain and distorts the polymer

geometry with decrease in the conjugation length. Structural differences between different coupling types of polymers change the electronic structure with band gap.

Synthesis of regioregular H-T type polythiophene is achieved with McCullough method. This method is used to perform the regioselective polymerization by selective metalation at 5-position of 3-alkylthiophene derivatives (Fig. 1.12) [48].

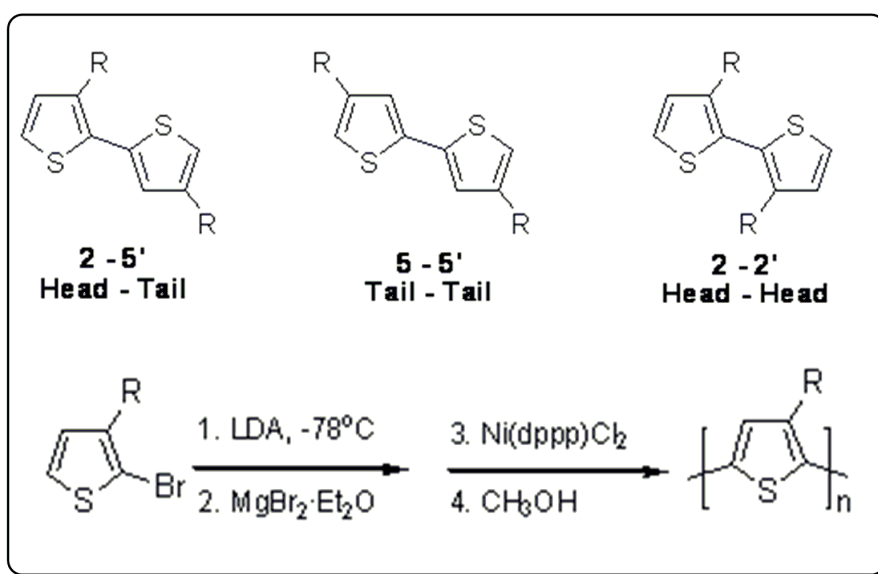


**Figure 1.12** McCullough method for the synthesis of regioregular poly(alkylthiophenes) [48]

### 1.3.2 Electrochemical Polymerization

Electrochemical polymerization is widely used for synthesis of conducting polymers because it is a simple and selective method. The polymers are produced on an electrode in the presence of electrolyte in an electrochemical cell.

The growing process and thickness of the film formed on the electrode can be controlled by applied potential or deposited charge. The advantage of electrochemical polymerization is possibility of performing further characterizations with electrochemical and spectroscopic methods. Furthermore, the resulting polymer is obtained in its doped state, whereas other conventional polymerization methods like chemical polymerization requires subsequently doping of neutral polymer and processing.

Electropolymerization is a standard oxidative method for preparing electrically conducting conjugated polymers. The electrochemical synthesis of polyheterocycles occurs through anodic and cathodic couplings (Fig. 1.13).

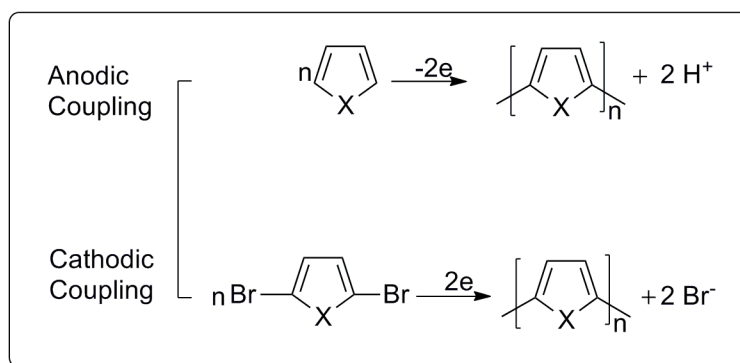


**Figure 1.13** Electrochemical synthetic routes to polyheterocycles.

Oxidative electrochemical polymerization is based on coupling of the oxidation of monomer to form a polymer chain accompanied with proton ( $H^+$ ) elimination. Anodic coupling is preferred because it uses the unmodified monomer and the resultant polymer, being more easily oxidized (doped), is produced in the

conductive state and therefore, allows the continuous deposition of the material up to considerable thickness.

### 1.3.2.1 Mechanism of Electrochemical Polymerization

The mechanism of electrochemical polymerization of a heterocycle is shown in Figure 1.14 and the process can be explained by the ECE mechanism comprising from electrochemical-chemical-electrochemical (ECE) reaction steps. [49].

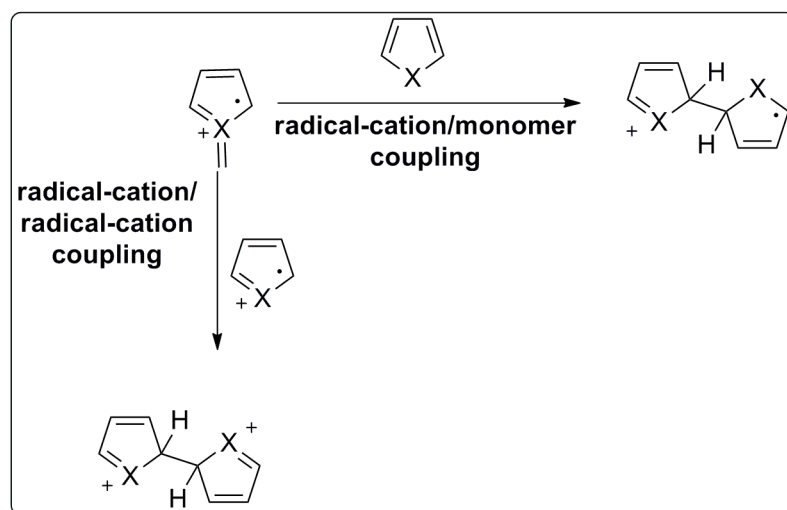


**Figure 1.14** Radical-cation/monomer

Firstly, a radical cation is formed when the heterocyclic monomer is oxidized. High concentrations of radical cations remain close to the electrode surface owing to faster transfer of electrons compared to diffusion of monomer to the bulk of solution. Second process is a chemical (C) reaction and this reaction happens either by the electrophilic addition of radical cation to heterocyclic monomer followed by oxidation to a dimeric dication or combination of two radical cations to yield a

dimeric dication (Fig 1.15). After the elimination of protons, the aromaticity of the molecule is regained. After dimers formed near the electrode surface, dimers oxidized by the help of applied potential which yields radical cations [50].

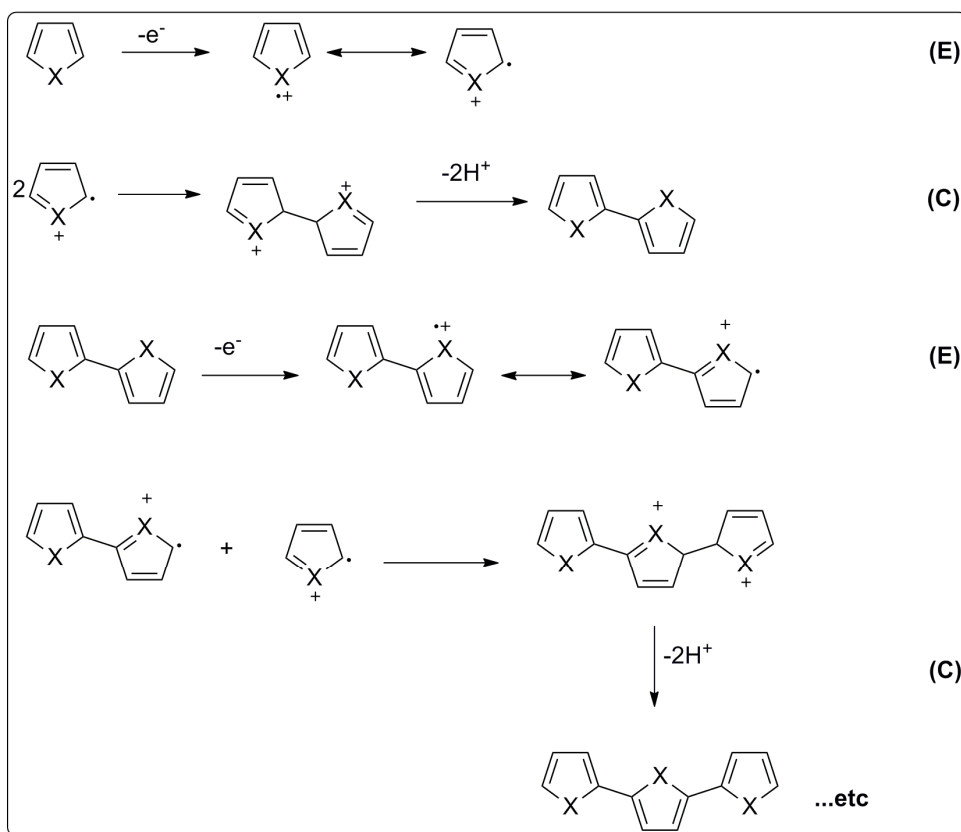


**Figure 1.15** Electrochemical polymerization mechanism for a five membered heterocyclic compound, where X = N-H, S, O

Final properties of conducting polymers are strongly affected by the electrolytic medium including, type of solvent, electrolyte systems, monomer concentration and the type of electrode. [51]

### 1.3.2.2 Electrolytic Medium

The choice of electrolytic medium consisting of solvent and electrolyte is very critical since radical cations are formed during the electrochemical polymerization. Assurance of the desired ionic conductivity of medium in electrochemical polymerization is provided by selecting a solvent with sufficiently high dielectric constant.

Supporting electrolyte should be soluble in solvent and solvent should possess adequate potential window range required to oxidize or reduce polymer. Nitrile solvents are commonly used in electrochemical polymerization studies of conducting polymers owing to its high dielectric constant with a wide range of redox potentials. [51].

Supporting electrolyte used in the electrochemical polymerization is used to make electrolytic bath solution conducting and dope the polymer by providing one of its ions to compensate charge created on the conjugated organic chain.

Selection of supporting electrolyte is done according to nucleophilicity, solubility and degree of dissociation of the supporting electrolyte. Tetraalkylammonium salts of perchlorates, tetrafluoroborates and hexafluorophosphate are used often as supporting electrolytes owing to high solubility and dissociation in the aprotic solvents. The morphology of the polymer films are strongly affected by the nature of the supporting electrolyte therefore the film quality is very low when the anion of electrolyte salts is halide due to its nucleophilic character and ease of oxidation [51,52].

The competitive reactions of the radical cations or the oxidized polymer with nucleophiles in the medium can be avoided by high concentration of monomer (0.1 M or more). As the oxidation potential of the monomer decreases, the number of competitive reactions decreases so that even millimolar concentrations may be used for efficient polymerization [51].

Three-electrode system consisting of working electrode, reference electrode and a separated counter electrode are used to perform electrochemical polymerization. Since the polymer films are produced with the oxidative polymerization the working electrode should be inert such as platinum, gold, carbon electrodes and indium-tin-oxide (ITO).

#### **1.3.2.3 Monomer Structure:**

Recent studies in the field of conducting polymers focused on the synthesis of monomer with new precursor structures to obtain better optical, electrical, processibility and environmental stability. [53]. Synthesis of monomer with desired properties requires basic knowledge of relation between the structural modification and material properties. Developing methodologies to attain such precise control over the electronic band structure of the polymer is a key aspect for the advancement of the conducting polymer field.

## 1.4 Band Gap

In today's technology, conjugated polymers take role in display technologies and other electronic. While ease of oxidation and emissive-absorptive colors of conducting polymers offers them to be used in electrochromic devices, their high match of entire or well defined portion of solar spectrum and high electron and hole mobility makes them promising material for use in photovoltaic devices, light emitting diodes. Variation of band gap energy allows changing the optical and electronic properties of polymers by adapting new strategies for design of new chemical structures.

### 1.4.1 Low Band Gap Systems

Color and the conductivity of a polymer is depend on band gap of polymer. Low band gap polymers are a popular research issue in recent investigations and have wide range of applications due their high conductivities without need of doping. Transparent color in oxidized form is a desired property for the electrochromic polymers for smart windows applications and this property can be obtained by band gap engineering on polymer. Band gap engineering enables researchers to synthesize different polymers with variable band gap values in order to be used in wide range of applications.

Band gap modifications are possible through the changes in the planarity of molecules ( $E^\ominus$ ), intrachain interactions ( $E^{\text{int}}$ ), resonance effects ( $E^{\text{res}}$ ), bond length variation ( $E^{\Delta r}$ ) and electron donor-acceptor (DA) type groups attached to polymer backbone ( $E^{\text{sub}}$ ) or present on polymer main chain (Fig 1.16-Fig 1.17). DA method has advantages over other methods since this method reduces solubility problems and also provides synthesis of diversity in synthesis of conducting polymers [54].

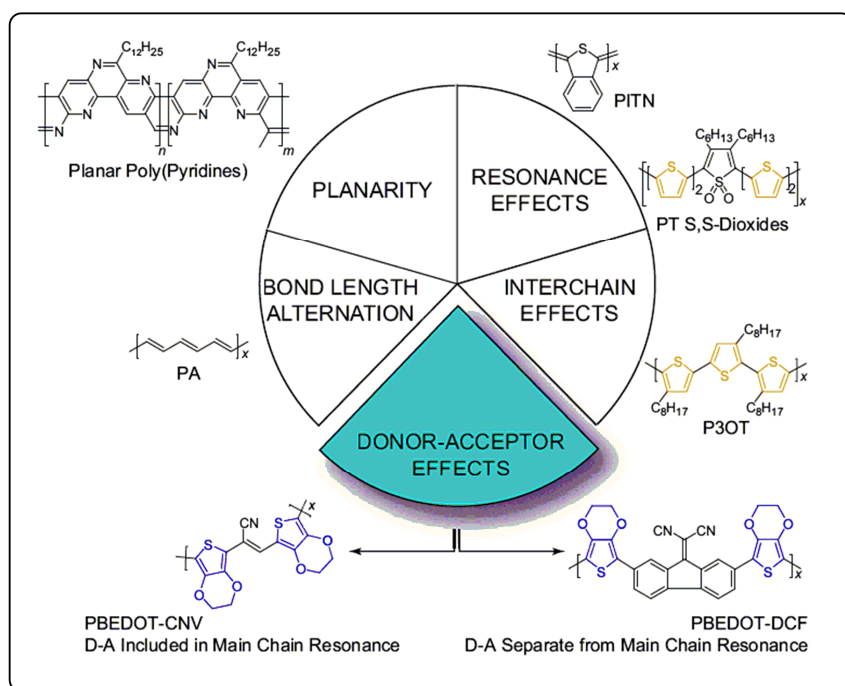


**Figure 1.16** Methods for modification of band gap

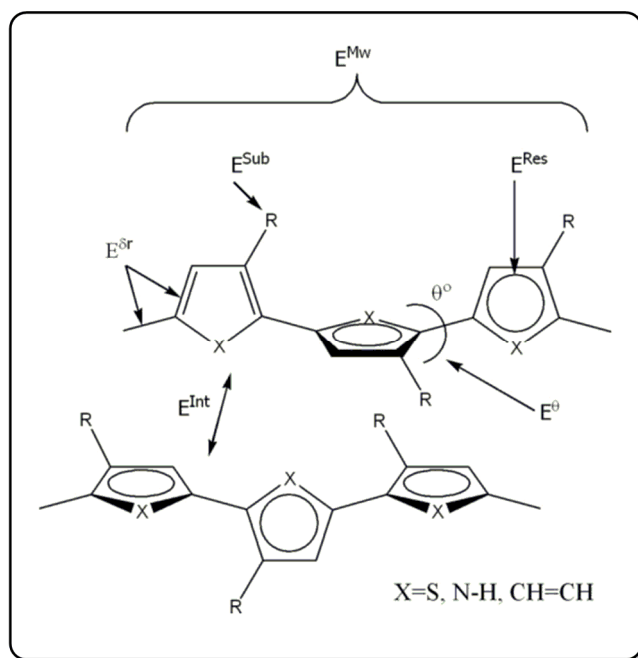


**Figure 1.17** Illustration of methods for alteration of band gap

One way of reducing band gap energy is to reduce the bond length alternation along the polymer chain. Bond length alternation is defined as the difference between single and double bond lengths for polyacetylene. Polyacetylene has a wide band gap and shows non-metallic behavior in neutral state due to bond length alternation on PA chain which is the result of Peierls effect (Fig. 1.18) [55].

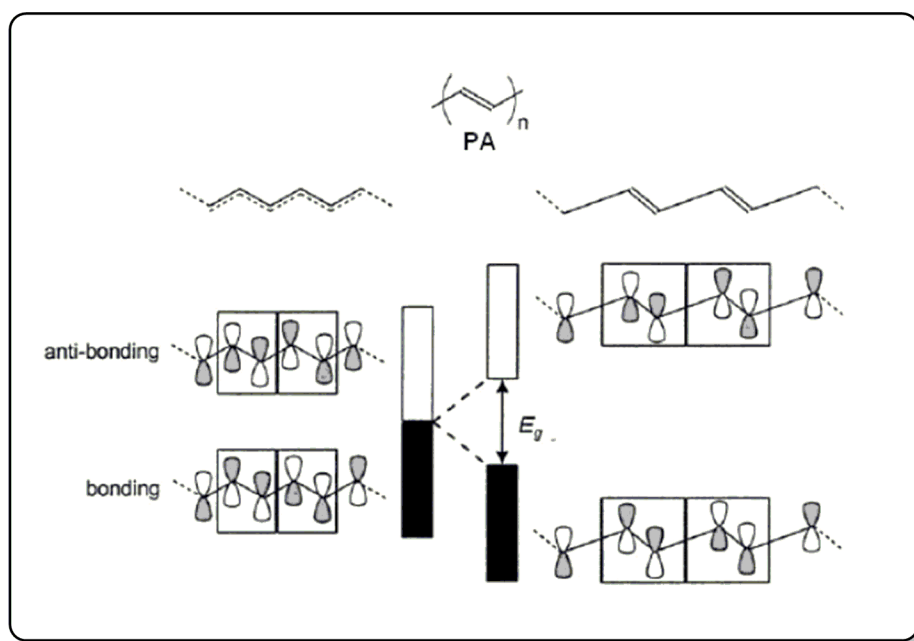


**Figure 1.18** The emergence of band gap by Peierls distortion [55]

The non-degenerate ground state of polyaromatics (PTh, PPy etc.) restrict the use of bond length alternation term due to unequal energy states of aromatic and quinoid forms (Fig 1.19). Therefore, the definition of bond length for polyaromatics differentiates from the one for polyacetylene which is defined as “the maximum difference between the length of C-C bond inclined relative to the chain axis and C-C bond parallel to the chain axis”. [56].

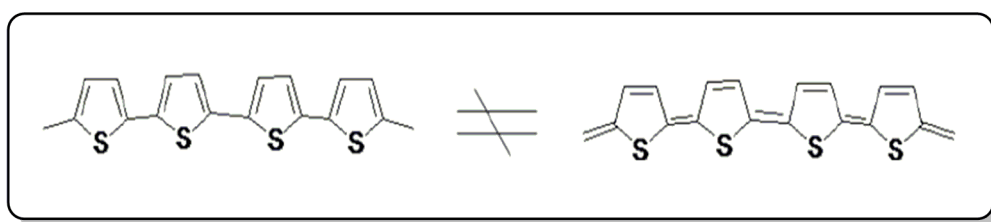


**Figure 1.19** Aromatic and quinoid forms of polythiophene

The band gap decreases as the contribution of the aromatic geometry decreases. Band gap of polythiophene is decreased by modification of the monomer structure in order to increase the quinoid character of  $\pi$ -conjugated system at the expense of its aromaticity [57-66]. Polyisothianaphthene (PITN) is an example of a low band gap polymer with increased quinoid character [67]. PITN ( $E_g=1.1$  eV) has low band gap value compared to polythiophene ( $E_g=2$ eV). The benzene ring fused to thiophene from 3- and 4- position leads to competition of aromaticity between the benzene and thiophene rings and by nature only one of them can be aromatic at the same time (Fig 1.20).

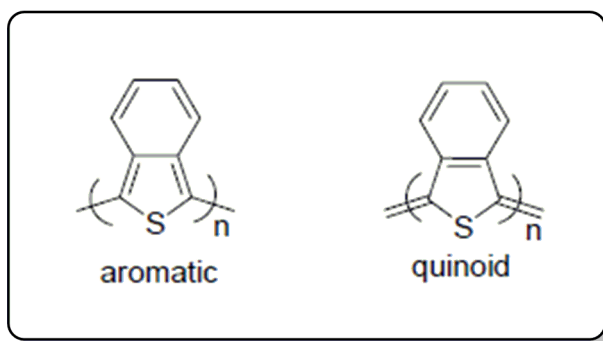


**Figure 1.20** Aromatic and quinoid forms of polyisothianaphthene (PITN)

As the structure of PITN concerned, thiophene loses the aromaticity when the structure changes from aromatic to quinoid form, and at the same time benzene ring gains aromaticity. The high energy of aromatization for benzene (1.56 eV) with respect to thiophene (1.26 eV) indicates that benzene has greater tendency to stay as aromatic. Therefore, PITN prefers to remain in the quinoidal state with a band gap of 1.1 eV and this shows that increase of quinoidal character decreases the band gap. Hence the entire loss of aromaticity decreases together with the increase in contribution of quinoid structure to the polymer chain in order to obtain low band gap polyisobenzofuran.

The presence of single bond between the aromatic rings leads to interannular rotations which cause decrease in the intermolecular and interchain interactions. These interactions reduce the  $\pi$ - $\pi$  interaction and orbital overlap due to deviation from planarity and increases band gap (Fig. 1.21) [68].

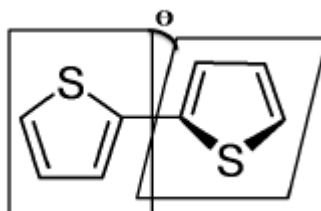


**Figure 1.21** Interannular rotations in polythiophene chain

Introduction of the substituent such as flexible side chains on main chain have an influence on the band gap. The side chain causes steric interactions between adjacent rings and cause twisting of the backbone. Twisting causes not only to deviation from planarity but also reduction in conjugation length to increase band gap. Replacing alkyl chain by alkoxy group causes the increase in electron density due to presence of the electron donating oxygen atoms.  $\pi$ -donation of the lone pairs

in to the main chain increases the HOMO level leading to decrease in band gap. Similarly, substitution of an electron withdrawing species in conjunction with the conjugated chain lowers the LUMO level to obtain low band gap.

#### **1.4.2 Low Band Gap Polythiophene Derivatives**

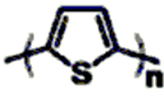
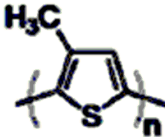
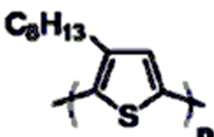
The band gap of the conducting polymers can be decreased by several different synthetic strategies. Attaching electron donating or withdrawing groups to conjugated polymer backbone, insertion of spacer groups to diminish steric interactions between adjacent rings, combining donor acceptor repeating units are only some of many routes to synthesize low band gap polymers.

The electrical and optoelectronic properties of conducting polymers are connected to chemical structure of the  $\pi$ -conjugated monomer building block.

Polythiophene has been known as strong candidate for using in optical and electronic applications due to their robust nature for decades. Pursuit of specific electronic and optical properties led to diverse structural modifications of polythiophene. Thiophene based conducting polymers are extensively studied on account of its environmental stability. In spite of robust nature of polythiophene, it has a wide band gap (approximately 2.1 eV) and a particular research has been devoted to decrease the band gap value by the methods described above.

Polythiophene chain is stiff and has limited flexibility and solubility due to delocalized  $\pi$ -conjugated system which provides novel electronic properties to this polymer. The inherent insolubility of the conducting polymer that limits the characterization and processing and this drawback of polythiophene have been overwhelmed by the introduction of flexible side chains.

Substituting thiophene with different length of alkyl chains not only increases the solubility of the resulting polymer but also decreases the oxidation potential since electron donating nature stabilizes the radical cation formed upon oxidation (Fig 1.22). Besides of these advantages of alkyl substitution, it causes a little change in the optoelectronic properties of the polymer [69]. The electronic band gap of pristine polythiophene is approximately 2.1 eV while poly(3-methylthiophene) (P3MT) has lower band gap (1.97 eV) as expected. When the length of alkyl chain increases, repulsive interactions between substituents of adjacent monomer units arise and extent of conjugation decreases to increase band gap energy. Therefore, poly(3-hexylthiophene) (P3HT) shows higher band gap of 2.10 eV with respect to polythiophene and poly(3-methylthiophene).

			
	PTh	P3MT	P3HT
$\lambda_{\text{max}}$	480 nm	500 nm	440 nm
$E_g$	2.00 eV	1.97 eV	2.10 eV

**Figure 1.22** Band gap energies of PTh, P3MT and P3HT

Synthesis of thiophene substituted from both 3- and 4- positions increases reactivity and selectivity of the monomer however similar to poly(3-hexylthiophene), steric interaction decreases the conjugation length to increase band gap.

Unlike substitution with alkyl groups, introduction of alkoxy groups both decreases band gap and hinders steric twist of the polymer. Introduction of electron rich substituent such as alkoxy groups raises the HOMO level of polythiophene. 3,4-Ethylene dioxothiophene (EDOT) is an example for this. The ethylenedioxy bridge blocks the 3- and 4- positions of thiophene to prevent coupling from these sites and polymerization proceeds through 2- and 5- positions thereby creating highly regular conjugated backbones (Fig. 1.23). Oxygen atoms present in the ethylene dioxy bridge donates electron to polymer main chain and not only electron density and but also HOMO level increases while the oxidation potential decreases in compare to thiophene itself. Cyclic substituent in the 3 and 4 positions of thiophene, eliminates the steric problems typically found with 3,4 disubstitution. Polymer of EDOT (PEDOT) has band gap (1.6 eV) of approximately 0.4 eV lower than that of PTh.

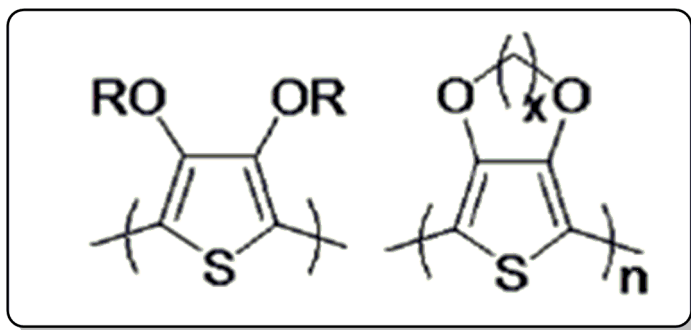


**Figure 1.23** Polythiophene derivatives substituted from 3- and 4- position

The high conjugation length in monomer increases the HOMO level energy to obtain low band gap polymer. During oxidation of the polymers, radical cations formed and the stability of these radical cations increases as the conjugation length of monomer increases. Therefore, synthesis of polythiophene from thiophene and

bithiophene differs from each other (Fig 1.24). Bithiophene has higher conjugation length than thiophene therefore, polybithiophene has ca. 0.4 V vs Ag/Ag<sup>+</sup> lower oxidation potential in comparison to polythiophene. Similarly, oxidation potential of 2,2'-bis(EDOT) (0.51 V) is lower than that of EDOT (1.1 V vs Ag/Ag<sup>+</sup>) [52].

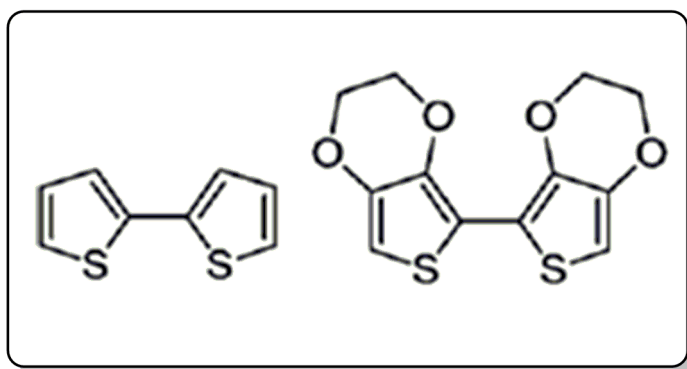


**Figure 1.24** Structures of bithiophene and 2,2'-bis(EDOT)

The twist in polymer chain can be reduced by inserting less sterically hindered groups between the rings to utilize low band gap polymers. Furthermore, insertion of vinylene bond restricts the rotation around bonds owing to certain configurations of double bond (cis or trans) (Fig 1.25). [51]. Therefore, the poly(thiophenevinylene) (PThV) has band gap energy of 1.7-1.8 eV which is approximately 0.4 eV lower than polythiophene. When the thiophene is replaced by the EDOT that contains electron donating substituents, the resulting monomer produces a polymer with a optical band gap of 1.4 eV.

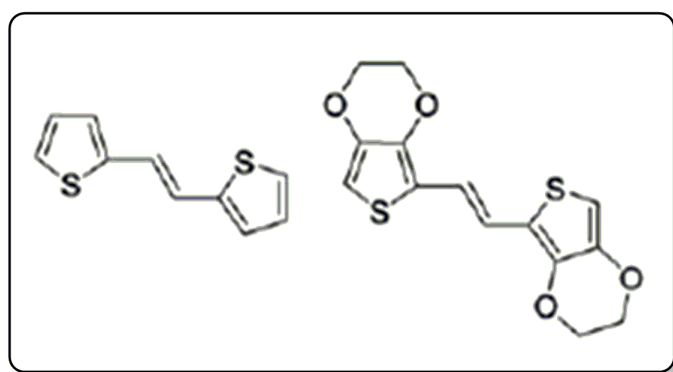


**Figure 1.25** Structures of bithiophene and 2,2'-bis(EDOT)

Incorporation of donor-acceptor units on main polymer chain is another strategy to obtain low band gap polymers with different optical and electrical properties. Donor-acceptor-donor (D-A-D) approach is based on integration of the donor and acceptor groups with high HOMO and low LUMO levels, respectively (Fig 1.26).

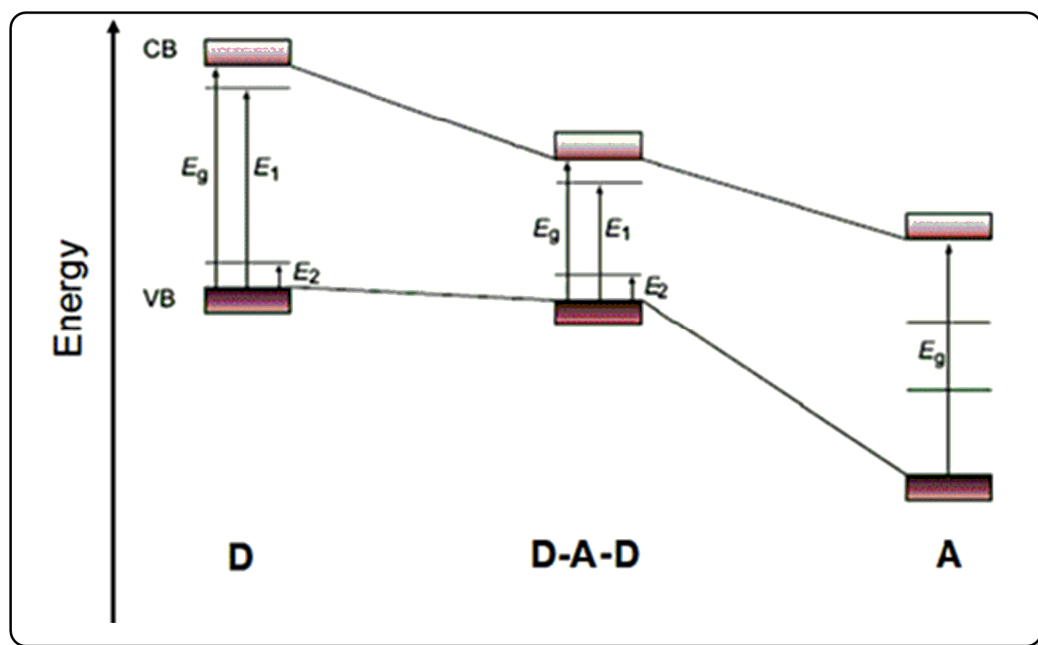


**Figure 1.26** Donor (D) - Acceptor (A) Concept

During the last decade, many researches have been devoted to syntheses of low band gap polymers with accessible oxidation and reduction potentials. Benzene fused aromatic rings with nitrogen such as pyrazine, quinoxaline, 2,1,3-benzothiadiazole and benzotriazole are used as electron accepting units while thiophene and substituted thiophene such as EDOT, 3-hexyl thiophene are used as electron donating moieties in  $\pi$ -conjugated donor-acceptor-donor (D-A-D) type. Intramolecular charge transfer (ICT) occurs between donor and acceptor units and an absorption band at lower energy is generated. The power of intramolecular charge transfer can be adjusted by the design and choice of donor-acceptor units.

The band gap of the polymer depends on the donor and acceptor ability of the units. Thomas et al showed this affect by changing the donor ability of electron donating group by keeping cyanovinylene group fixed as the acceptor unit on the polymer chain. Results given in Fig 1.27 show that as the donor ability of electron donating group increases band gap decreases. [70].

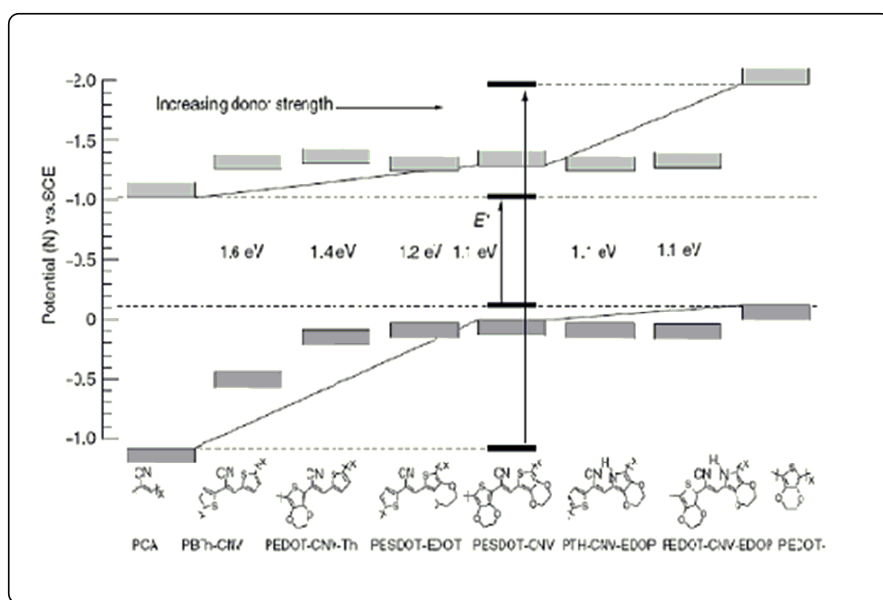


**Figure 1.27** VB and CB levels for cyanovinylene substituted with different donor groups.

Double bond character of the resultant polymers enriches relative to either of its parent components and the energy differences between HOMO and LUMO level decreases to lower band gap. [71]. The structure of D-A-D interaction in the polymer backbone resulted in much more red-shifted absorption spectra and low band gaps of ~1.0 eV have been obtained.

## **1.5 Applications of Conducting Polymers**

Conducting polymers are used in the development of electronic/optoelectronic devices like electrochromic devices (ECDs) [21,22], solar cells [19,20], light emitting diodes (LEDs) [17,18] and field effective transistors (FETs) [72].

Conducting polymers can be used in thin film technologies. Important fields where these technologies used are antistatic protection and electromagnetic interference shielding. Conducting polymers can be regarded as membranes due to their porosity and can be used for separation of gas and liquids. The use of conducting polymers in sensor technologies consists of use as an electrode modification to improve selectivity, to impart selectivity, to suppress interference and to support as a matrix for sensor molecules (Fig. 1.28) [73].

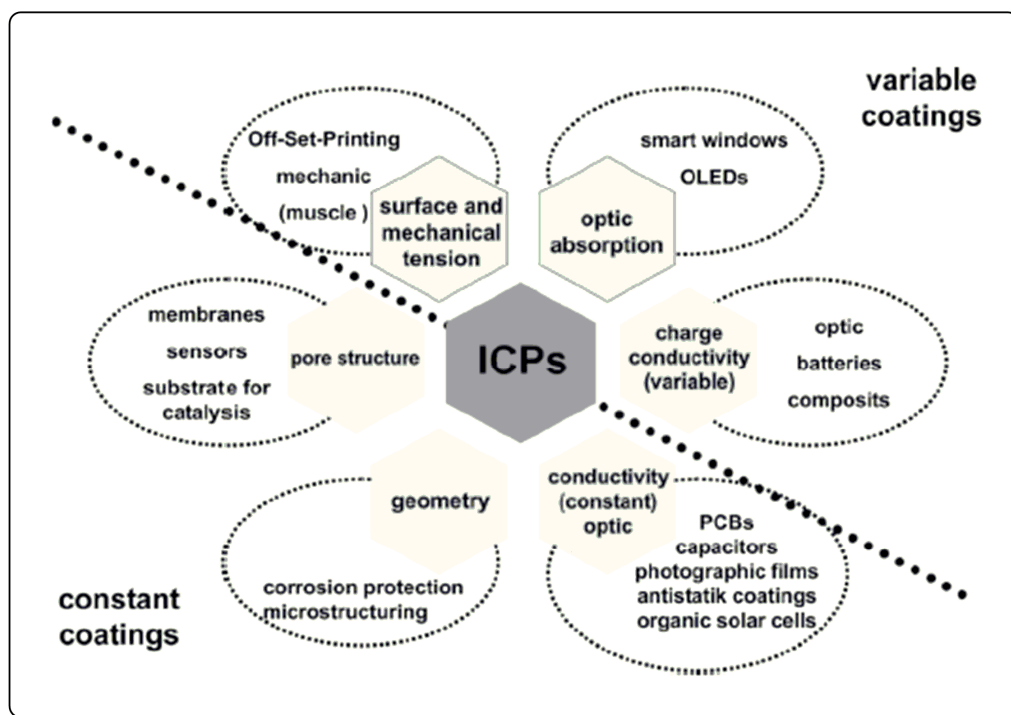


Figure 1.28 Applications of conducting polymers [74].

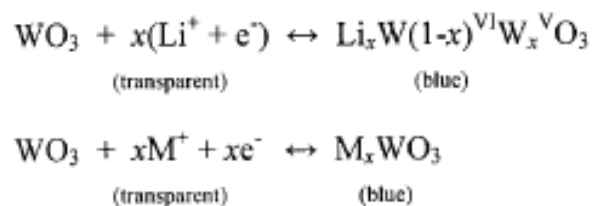
## 1.6 Electrochromism

Reversible change in the color of a material in response to external stimulus is called chromism. Such changes can be induced by temperature, electrical field, solvent, or absorption of light.

Reversible change in the absorption or transmission properties due to an external voltage is called electrochromism. Electrochromism has been shown in inorganic oxides, viologens, and metal complexes, in addition to conjugated polymers [75-77].

Inorganic electrochromic materials are oxide thin films of transition metals such as tungsten, iridium, rhodium, ruthenium [78-82]. The most widely known inorganic material is the tungsten oxide which alters color from yellow to green. Tungsten

oxide has a nearly cubic structure by  $\text{WO}_6$  octahedra that share corners. Guest ions enter to the free spaces between sites. As the tungsten sites are oxidized to  $\text{W}^{\text{VI}}$ , the film become transparent and reduction of tungsten to  $\text{W}^{\text{V}}$  generates blue coloration. The general mechanism of this process is shown by the equation [83]:



Conducting polymers have lots of advantages over inorganic electrochromic materials such as high coloration efficiency, fast switching capability and capability of fine tuning band gap and obtaining multicolored materials by structural modification in chemical structure [84].

Most chromic phenomena results from conjugation that breaks conformational changes in the polymer. Electrochromic materials can make transition between a colored and bleached state, between two color states, or between multiple color states, and can be grouped according to their color states. The electrochromic materials may exhibit several colors and termed as polyelectrochromic and the process is called to be multicolor electrochromism [85].

When the polymer is p- or n-type doped, structural modifications occur in the polymer backbone together with the electronic transition between high and low energy states. If these electronic transition takes place in visible region (400-800 nm), the neutral and doped states of polymer switches their colors between two colored states. On the other hand, if the transition takes place at lower energy levels

and higher wavelengths (near-IR region), this material reveals a transmissive state and a colored state. Band gap energy of the polymer controls these properties.

The electrochromic materials switch between two to four different colors upon applied potential is called multicolor electrochromic. Different colors can be obtained with creative design of monomers.

In the context of color tuning concept, donor-acceptor-donor (DAD) type monomers with electropolymerizable heterocyclics at both sides of the A unit symmetrically were studied quite extensively up to date and effects of different D and A groups were investigated.

Insertion of different aromatic spacers between two thiophene or alkylenedioxythiophene groups can yield multicolor electrochromic materials and some representative class of these materials is shown in Figure 1.29. Several examples of electron deficient groups coupled with electron donating groups such as ethylenedioxythiophene (EDOT) and thiophene (Th) revealed either better optical contrast, lower band gap and switching time or both p-type and n-type doping compared to pristine polymers polythiophene (PTh) and PEDOT. The presence of carbazole [86], alkoxybenzene [87] and biphenyl [88] increases band gap of neutral polymer and the polymer shows multichromic property due to transition of charge carriers in the visible region. When electron accepting groups are introduced such as a pyridine or a pyridopyrazine, resulting polymer exhibits other electrochromic colors through n-doping as well as p-doping [89].

The discrimination of colors is subjective, thus measurement and representation of colors are standardized to define three components to quantify color of electrochromic materials. Three components of color are defined as hue, saturation and brightness by "The Commission Internationale de l'Eclairage" (International

Commission on Illumination). Hue, also named as dominant wavelength or chromatic color, is defined as the “specific wavelength of light associated with an observed color” and designated as “a”. Saturation, also called chroma or tone, describes the level of white or black observed and designated as “b”. Lastly, brightness is also referred as luminance and represented by “L”. [91]

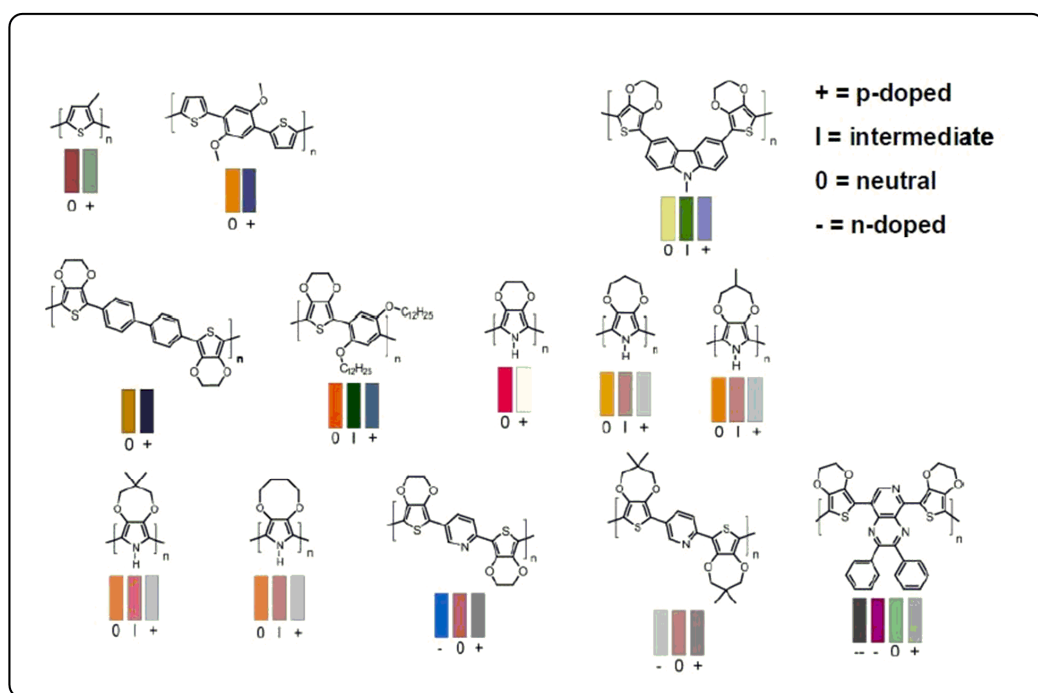


**Figure 1.29** Examples of multicolor electrochromic polymers synthesized by structural modification. 0 = neutral; I= intermediate; +=oxidized; and -- = reduced [90]

Several methods such as contrast, switching time and coloration efficiency are used to characterize the quality of electrochromic polymers. The contrast between neutral and doped states is usually defined by the change in percent transmittance at the wavelength of highest optical contrast. The time required to

pass between neutral and doped states is defined as switching time. Magnitude of the applied potential, ionic conductivity of electrolyte, thickness and morphology of thin films are the factor affecting switching time. Coloration efficiency, also called electrochromic efficiency, is determined by the change in optical density due to amount of charge transport through an electrochromic polymer [91]

Optical displays, smart windows for buildings, dimming rear view windows for automotive applications are the examples where electrochromic materials are used. Rear view windows get dimed and avoid dazzling from the headlights of a following car. Smart windows are very useful for the buildings in order to control the amount of light passing into a room.

The color exhibited by the polymer is closely related to the band gap. Tuning of color states is possible by suitable choice of monomer. This represents a major advantage of using conducting polymers for electrochromic applications. Subtle modifications to the monomer can significantly alter spectral properties [92].

## 1.7 Benzotriazoles

Benzotriazole is a heterocyclic compound and a benzazole derivative and commonly used to inhibit corrosion [93-95]. Benzotriazole consists of benzene and triazole ring (Figure 1.30) and considered to act as an electron transporting material owing to presence of electron-withdrawing  $-N=N-$  or  $-C=N-$  groups. The 2R-triazole unit in 2R-BTz is known as an electron-accepting unit.[96-97]

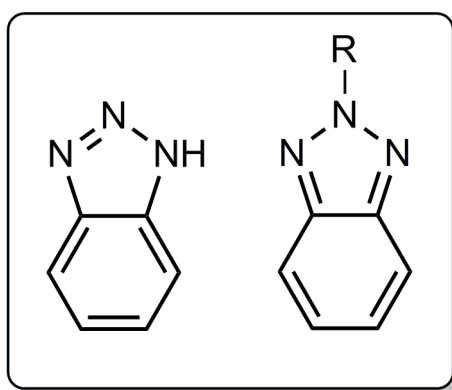


**Figure 1.30** 1H-Benzotriazole and 2R-BTz

Recently, benzoazole derivatives such as benzothiadiazole (BTd), benzotriazole (BTz), benzimidazole (BIm) and benzoselenadiazole (BSe) have been used for the design of new low band gap polymers with superior electrochromic properties (Figure 1.31) .

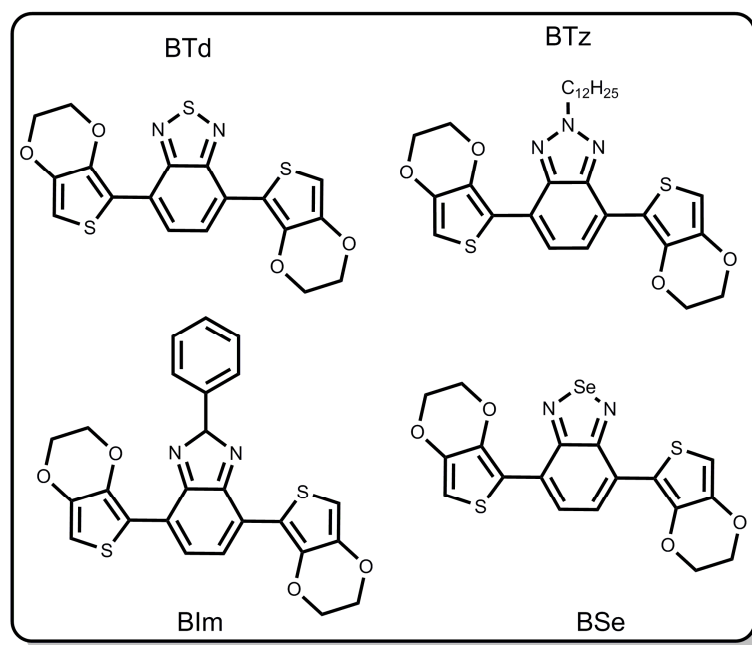


**Figure 1.31** DAD type monomer containing benzoazole groups

BTd derivative DAD polymer was synthesized [98] and later it was shown to be the first green to transmissive electrochromic polymer. BSe based polymer was also investigated as a green to transmissive polymer with red shifted absorptions compared to BTd derivative [99].

For the electrochromic materials, it is crucial to obtain all three primary color in order to obtain all visible spectrum. Color mixing theory enables us to obtain all colors by addition or subtraction of primary colors in their neutral state. For use in displays, polymers should switch between one of the three primary colors and their transmissive states.

Recently, synthesis and optoelectronic properties of new DAD type polymers bearing benzotriazole (BTz) as the A unit were reported. These BTz based DAD type polymers were seen to be ambipolar due to the electron accepting nature of imine containing triazole ring which also provides a possible alkylation position to improve solubility. BTz containing polymers were also studied by other research groups for solar cell and electrochromic applications recently [16-18].

Poly(2-dodecyl-4,7-di(thiophen-2-yl)-2H-benzo[d][1,2,3]triazole) (PTBT) as an example of BTz based polymers revealed multicolored electrochromism with the ability to switch between all RGB colors, black and transmissive states which make this polymer unique among numerous electrochromic conjugated polymers [15]. Furthermore, synthesis of a novel DAD type polymer bearing 2-dodecyl benzotriazole together with 3,4-ethylenedioxythiophene (EDOT) was reported (P(BEBT)). This polymer showed superior electrochromic properties than the pristine PEDOT and became great candidate to be used as a multipurpose material in display technologies (Figure 1.32)[100,101].

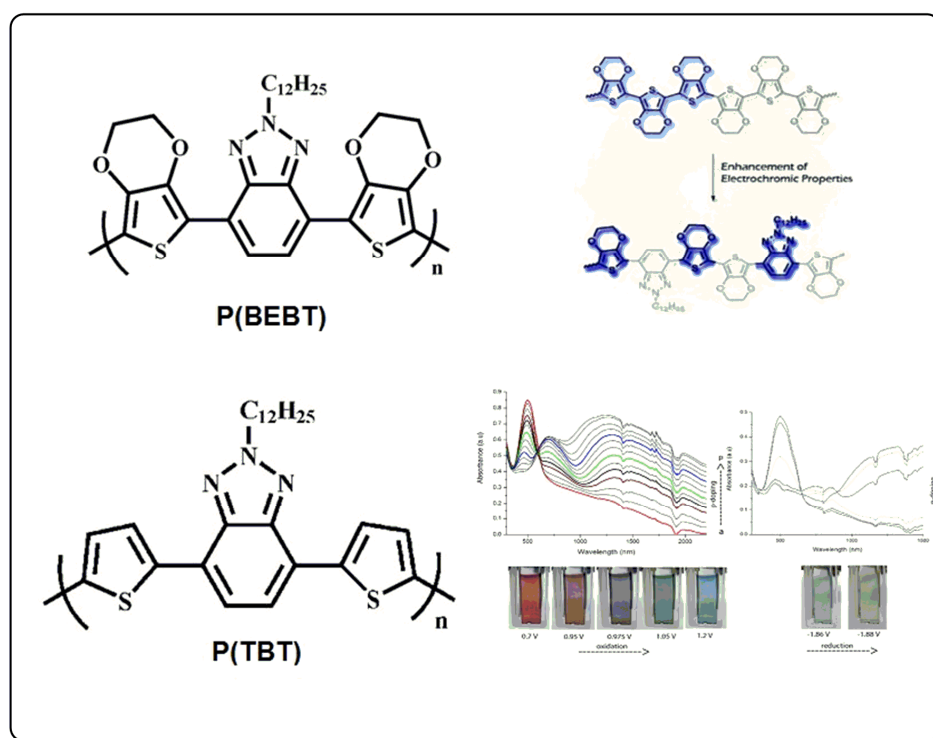


**Figure 1.32** Benzotriazole functionalized low band gap polymers

BTz can receive easy chemical modification with various side chains or groups from triazole ring. Although syntheses of conducting polymers possessing benzotriazole group functionalized from 1- position was reported, there is no  $\pi$  conjugated polymer containing benzotriazole unit functionalized from 2-position.

## 1.8 Crown Ethers

The unique electrical, electrochemical and optical properties of conjugated polymers can be employed to transform chemical information to electrical or optical signals in the solid state, thus conducting polymer can be used as chemical sensors. The synthetic strategy for sensory type conducting polymers based on

functionalization of the polymer backbone with selective molecular recognition groups [102].

Crown ethers are known as the receptor for detecting metal ions with cyclic structure containing several ether groups. Simple synthesis of crown ethers was discovered by Charles Pederson in 1967 and this discovery was awarded by the Nobel Prize in 1987. Cations with certain sizes bind to crown ethers with certain denticity to form complexes. The size of the cation should match denticity of crown ether [103].

Thiophene based polymers possessing crown ether moieties in the structures were studied previously in the literature. Binding of certain cations to crown ether bridges between thiophene groups changes the conformation of polymer backbone, therefore changes electrical and optical properties of polymer (Fig. 1.33) [104-105] .

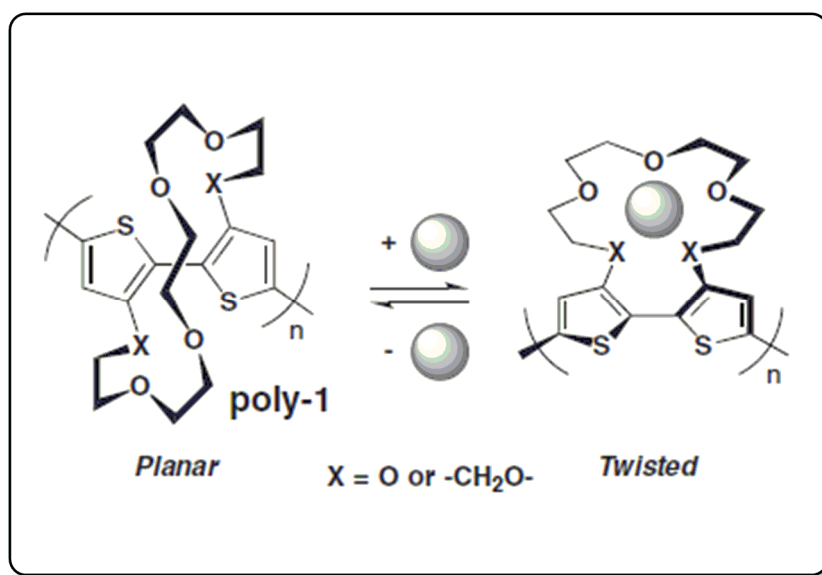


**Figure 1.33** Twisting mechanism of crown ether-appended polythiophene for the detection of alkali metal ions [105].

An advantage of polymeric materials is that sensory devices can easily be fabricated from these materials on electrodes either by spin coating and/or drop casting from solution (Method A in Fig. 1.34) or anodic electrochemical polymerization from an electrolyte solution (Method B in Figure 1.34). [105]

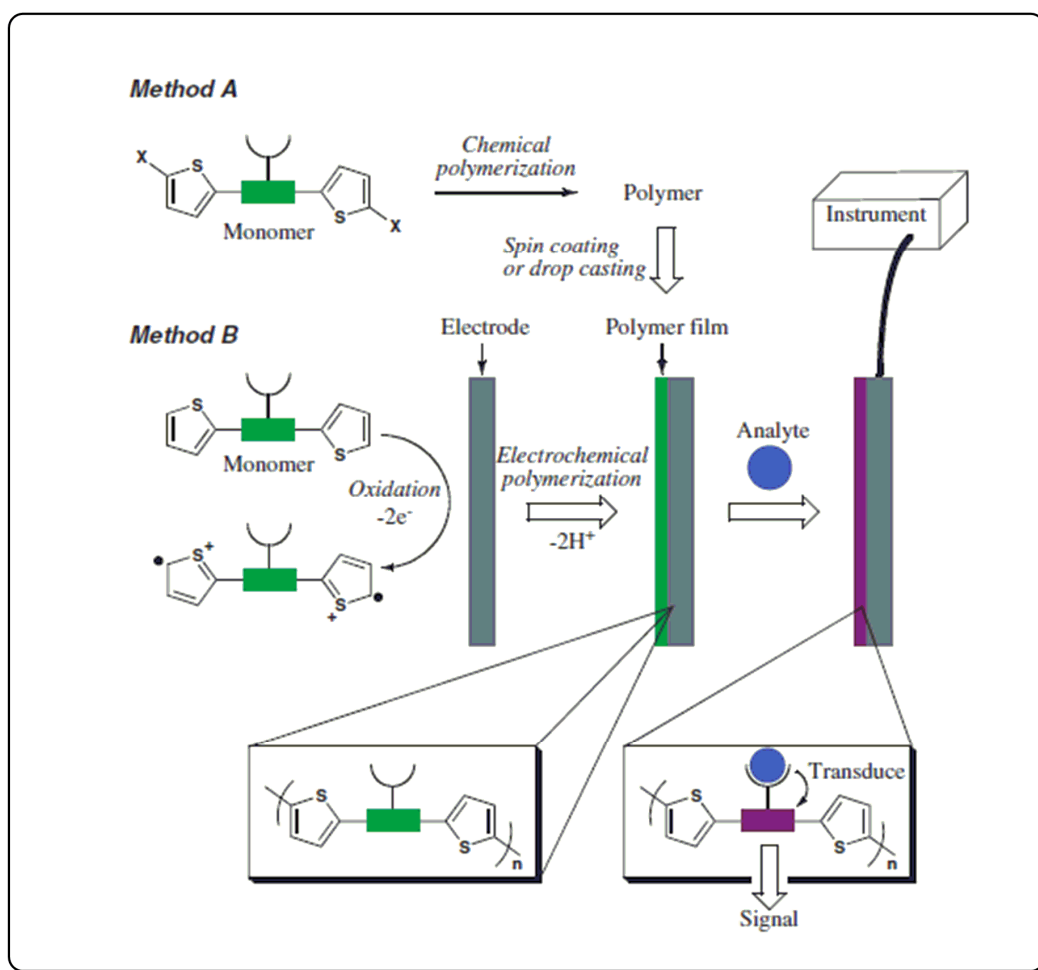


**Figure 1.34** Schematic representation of conducting-polymerbased chemical sensors

In 1995, Bauerle et al reported the syntheses of 15-crown-5 substituted thiophenes which the macrocycle is in direct  $\pi$ -conjugation. They characterized the polymers in the presence of different alkali metals with electrochemical and spectroscopic techniques. It was found that P4 and P5 (Fig. 1.35) have sensitivity to  $\text{Na}^+$  ion since  $\text{Na}^+$  ion size and 15-crown-5 cavity are similar [106].

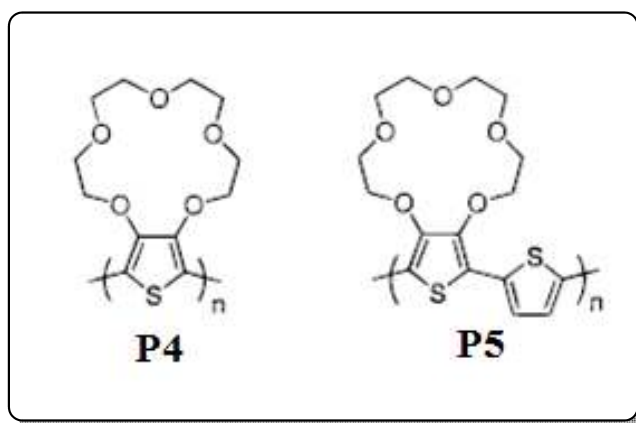


**Figure 1.35** 15-crown-5 substituted thiophenes

## 1.9 Aims of The Work

The aims of the work are

1. Syntheses of four different  $\pi$ -conjugated monomers; 1-Benzyl-4,7-bis(2,3-dihydrothieno[3,4-b]dioxin-5-yl)-2H-benzo[d][1,2,3]triazole (BBTEA), 2-benzyl-4,7-bis(2,3-dihydrothieno[3,4-b]dioxin-5-yl)-2H-benzo[d][1,2,3] triazole (BBTES), 1-benzyl-4,7-di(thiophen-2-yl)-2H-benzo[d][1,2,3]triazole (BBTA) and 2-benzyl-4,7-di(thiophen-2-yl)-2H-benzo[d][1,2,3]triazole (BBTS). Benzyl substituted benzotriazole unit is used as the electron acceptor and thiophene and EDOT units are used as the electron donor groups. The main purpose of synthesizing these monomers is investigating the effect of change in donor group and substitution site of benzotriazole group on electrochemical and electrochromic properties of resultant conducting polymers.
2. Syntheses of crown ether bearing  $\pi$ -conjugated monomers; 14,19-di(thiophen-2-yl)-naphtho[2,3-b][1,4,7,10,13]pentaoxacyclopentadecane (TNCT) and 14,19-bis(2,3-dihydrothieno[3,4-b][1,4]dioxin-5-yl)-naphtho[2,3-b][1,4,7,10,13] pentaoxacyclopentadecane (ENCE). The main purpose for syntheses of this monomer is examining the effect of different supporting electrolytes on the electrochemical and optical properties of conducting polymers functionalized via crown ethers with naphthalene subunits

## CHAPTER 2

### EXPERIMENTAL

#### 2.1 Materials

2,1,3-Benzothiadiazole (Aldrich), benzyl bromide (Aldrich), potassium *t*-butoxide (Aldrich), bromine (Br<sub>2</sub>) (Merck), hydrobromic acid (HBr, 47%) (Merck), sodium borohydride (NaBH<sub>4</sub>) (Merck), 3,4-ethylenedioxythiophene (EDOT) (Aldrich), *n*-butyllithium (*n*-BuLi, 2.5M in hexane) (Acros Organics), tributyltin chloride (Sn(Bu)<sub>3</sub>Cl, 96%) (Aldrich), naphthalene-2,3-diol (Aldrich), diisopropyl azodicarboxylate (DIAD) (Aldrich), tetraethyleneglycol (Merck) were used as received. Tetrahydrofuran (THF) (Acros), dichloromethane (DCM) (Sigma-Aldrich), acetic acid (Merck), acetonitrile (ACN) (Merck), methanol (Merck) were used without further purification. Thiophene (Aldrich) and 3,4-ethylenedioxythiophene (EDOT) (Aldrich) were used as received. Column chromatography of products was performed using Merck Silica Gel 60 (particle size: 0.040–0.063 mm, 230–400 mesh ASTM).

Reactions were monitored by thin layer chromatography with fluorescent coated aluminum sheets. Solvents used for spectroscopy experiments were spectrophotometric grade. Deuterated Chloroform (CDCl<sub>3</sub>) or DMSO solvents was used as received for the NMR characterization technique.

Supporting electrolytes; tetrabutylammonium hexafluorophosphate (TBAPF<sub>6</sub>), lithium perchlorate (LiClO<sub>4</sub>) and sodium perchlorate (NaClO<sub>4</sub>) were all purchased from Aldrich and used as received.

## **2.2 Instrumentation**

### **2.2.1 Potentiostats**

The cyclic voltammograms were recorded using VoltaLab PST050 in a three electrode one-compartment cell consisting of platinum wire or indium tin oxide (ITO) coated glass as the working electrode, platinum wire as the counter electrode, and an Ag wire as the pseudo reference electrode (0.3 V vs Fc/Fc<sup>+</sup>). Solartron 1285 potentiostat were used to provide a constant potential in the electrochemical polymerization. Experiments carried out at room temperature and open to air unless otherwise mentioned. This device is used to keep the voltage difference between the working and reference electrodes at a constant desired value during the electrolysis and compensates for the voltage drop in the electrolysis solution.

### **2.2.2 Nuclear Magnetic Resonance**

<sup>1</sup>H-NMR and <sup>13</sup>C-NMR spectra of monomers were recorded on a Bruker Spectrospin Avance (DPX-400) Spectrometer using CDCl<sub>3</sub> and DMSO as the solvent. Chemical shifts (δ) were given in ppm relative to tetramethylsilane as the internal Standard.

### **2.2.3 UV-VIS-NIR Spectrophotometer**

Varian Cary 5000 UV-Vis-NIR spectrophotometer was used in order to perform the spectroelectrochemical studies of the polymers.

## 2.2.4 Mass Spectrometer

Mass analysis was carried out on a Bruker timeofflight (TOF) mass spectrometer with an electron impact ionization source.

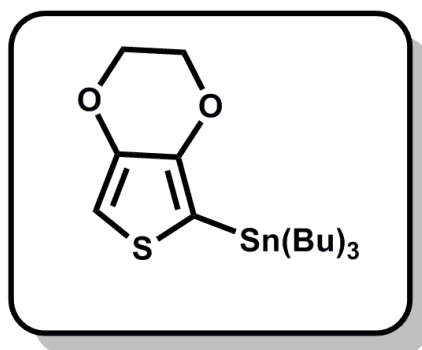
## 2.2.5 Colorimetry Measurements

Colorimetry measurements of the polymers were done via Minolta CS-100 spectrophotometer.

## 2.3 Synthetic Procedures

### 2.3.1 Synthesis of Stannylated Thiophene and EDOT

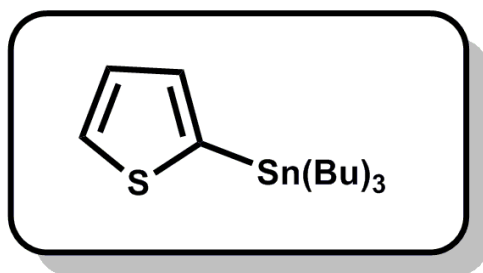
#### 2.3.1.1 Synthesis of Tributyl(2,3-dihydrothieno[3,4-b][1,4]dioxin-5-yl)stannane



Tributyl(2,3-dihydrothieno[3,4-b][1,4]dioxin-5-yl)stannane was synthesized according to a method described in the literature [107]. EDOT (2 g, 14 mmol) was dissolved in THF (40 mL) and the solution was cooled to -78°C. n-BuLi (8.7mL, 14 mmol) was added drop-wise and the mixture was stirred -78 °C for 1 h. Tributyltin

chloride (4.6 g, 14 mmol) was added at -78 °C and the mixture was allowed to warm to room temperature for 24 h. After that period, 50 ml of water (50 mL) was added to the mixture and mixture was extracted with DCM and water. Finally, DCM phase, subsequently dried over MgSO<sub>4</sub> and concentrated to get product as a brown viscous liquid. <sup>1</sup>H NMR (CDCl<sub>3</sub>) δ 6.56 (s, 1H), 4.16 (s, 4H), 1.61-1.49 (m, 6H), 1.39-1.22 (m, 6H), 1.09(m, 9H), 0.9 (m, 6H). <sup>13</sup>C NMR (CDCl<sub>3</sub>) δ 147.88, 142.65, 109.8, 105.99, 64.86, 64.80, 29.08, 27.40, 13.76, 10.72.

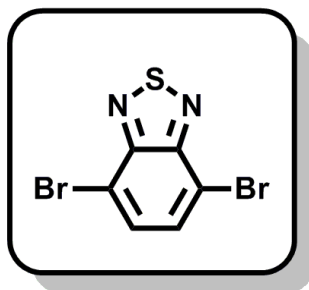
### 2.3.1.2 Synthesis of Tributyl(thiophen-2-yl) stannane



Tributyl(thiophen-2-yl)stannane was synthesized according to procedure described previously [108]. Thiophene (4.0 g, 47.1 mmol) was dissolved in THF and cooled to -30°C. n-Butyl lithium was added (29.5 mL, 47.1 mmol) and stirred for 30 min at -30°C. Then tributyl tinchloride (15.4 g, 47.1 mmol) was added dropwise at this temperature and mixture is allowed to warm to room temperature. The solution is stirred over night at room temperature and the solvent was evaporated to give crude compound as a brown oily residue (NMR).

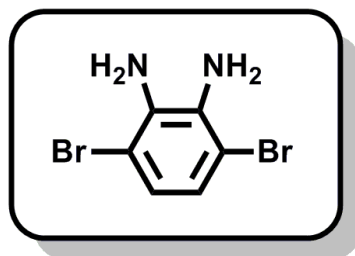
## 2.3.2 Synthesis of Benzotriazole Functionalized Monomers

### 2.3.2.1 Synthesis of 4,7-Dibromo-2,1,3-benzothiadiazole



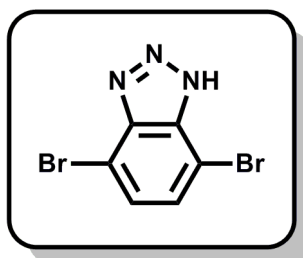
4,7-Dibromo-2,1,3-benzothiadiazole was synthesized according to previously described methods [109]. Benzothiadiazole (2.0 g, 14.69 mmol) and HBr (36 mL) were mixed in a 250 ml round bottom flask and 16 ml of HBr solution containing 1.6 ml Br<sub>2</sub> was added dropwise to the mixture at room temperature. When bromine solution addition was completed, the solution was refluxed for 6 h. During reflux precipitation of orange solids were observed. After cooling to room temperature, saturated solution of NaHSO<sub>3</sub> was added to mixture to remove excess Br<sub>2</sub>. Precipitate was dissolved in DCM and extracted with water several times. Organic layer was dried over MgSO<sub>4</sub> and solvent was removed under vacuum and the crude product was obtained as a yellow solid in yield 90% (3.9 g, 13.22 mmol). <sup>1</sup>H NMR (400 MHz, CDCl<sub>3</sub>, TMS) δ 7.66 (s, 2H). <sup>13</sup>C NMR (101 MHz, CDCl<sub>3</sub>) δ 152.9, 132.3, 113.9.

### 2.3.2.2 Synthesis of 3,6-Dibromo-1,2-phenylenediamine



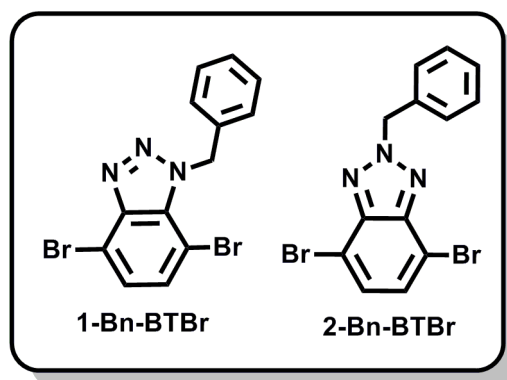
3,6-Dibromo-1,2-phenylenediamine was synthesized according to procedure described in the literature [110]. 4,7-Dibromo-2,1,3-benzothiadiazole (300 mg, 1.03 mmol) was dissolved in EtOH (25 mL) and the solution was cooled to 0 °C. Sodium borohydride (1.5 g, 0.04 mol) was added to this solution in small portions at 0 °C. After complete addition, the mixture was allowed to warm room temperature. After stirring for 24 h at room temperature, the Ethanol was evaporated completely with rotary evaporator under vacuum, and the crude product was extracted with first ether and water, secondly with ether and brine. The ether phase was collected and ether was removed to obtain 3,6-dibromo-1,2-phenylenediamine (234 mg, 0.88 mmol) as a pale yellow solid in 86% yield. <sup>1</sup>H NMR (400 MHz, CDCl<sub>3</sub>) δ 6.78 (s, 2H), 3.82 (s, 4H). <sup>13</sup>C NMR (101 MHz, CDCl<sub>3</sub>) δ 133.5, 123.2, 109.5.

### 2.3.2.3 Synthesis of 4,7-Dibromo-1,2,3-benzotriazole



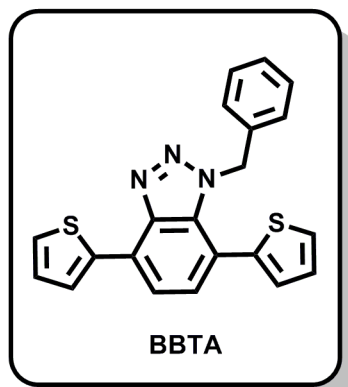
1,2-Diamino-3,6-dibromobenzene (0.80 g, 3.0 mmol) was dissolved in 12 mL of glacial acetic acid, and NaNO<sub>2</sub> (0.30 g, 3.3 mmol) in 6 mL of H<sub>2</sub>O was added to this solution. After 20 min stirring at room temperature, the precipitate was collected by filtration and washed with water to afford 4,7-dibromo-1,2,3-benzotriazole as a pink powder [97]; yield: 80%. <sup>1</sup>H NMR (400 MHz, CD<sub>3</sub>OD): δ 7.56 (s, 2H, aromatic).

### 2.3.2.4 Syntheses of 1-Benzyl-4,7-dibromo-1H-benzo[d][1,2,3]triazole (1-Bn-BTBr) and 2-Benzyl-4,7-dibromo-1H-benzo[d][1,2,3]triazole (2-Bn-BTBr)



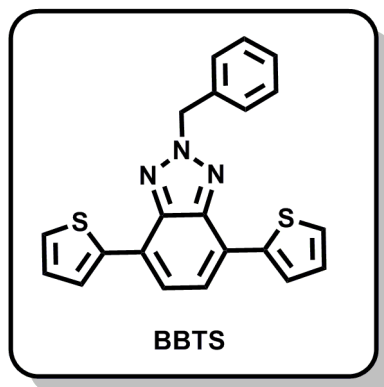
Benzyl bromide (575 mg, 3.4 mmol) was added to a solution of 4,6-dibromo-1,2,3-benzotriazole (500 mg, 1.8 mmol), potassium *t*-butoxide (224 mg, 2 mmol) in ethanol (20 mL) and the reaction mixture was stirred for 12 h at room temperature. The reaction was monitored by thin layer chromatography (TLC). After removal of the solvent by evaporation, the residue was dissolved in CH<sub>2</sub>Cl<sub>2</sub> and washed with water and then with brine. The organic layer was dried over MgSO<sub>4</sub> and the solvent was evaporated under reduced pressure. The residue was subjected to column chromatography (CH<sub>2</sub>Cl<sub>2</sub>:Hexane = 1:1) to obtain 1-Bn-BTBr (*R<sub>f</sub>*, 0.23) as a light pink solid in 47% yield (308 mg) and 2-Bn-BTBr (*R<sub>f</sub>*, 0.43) as a white solid in 28% yield (187 mg). Overall yield is 75%. 1-Bn-BTBr: <sup>1</sup>H NMR (400 MHz, CDCl<sub>3</sub>, TMS) δ 7.39 (d, 1H, *J* = 8 Hz), 7.33 (d, 1H, *J* = 8 Hz), 7.24 (m, 2H), 7.19 (s, 1H), 7.13 (m, 2H), 6.10 (s, 2H). <sup>13</sup>C NMR (100 MHz, CDCl<sub>3</sub>, TMS) δ 51.71, 100.76, 112.10, 126.00, 127.07, 127.23, 127.83, 130.99, 131.32, 134.75, 145.05. MS (*m/z*): 367 [M<sup>+</sup>]. 2-Bn-BTBr: <sup>1</sup>H NMR (400 MHz, CDCl<sub>3</sub>, TMS) δ 7.41 (s, 1H), 7.40 (s, 1H), 7.36 (s, 1H), 7.30 – 7.26 (m, 4H), 5.86 (s, 2H). <sup>13</sup>C NMR (100 MHz, CDCl<sub>3</sub>, TMS) δ 59.41, 108.61, 126.94, 127.34, 127.39, 128.23, 132.38, 142.57. MS (*m/z*): 367 [M<sup>+</sup>].

### 2.3.2.5 Synthesis of 1-Benzyl-4,7-Di(thiophen-2-yl)-2H-benzo[d][1,2,3]triazole (BBTA)



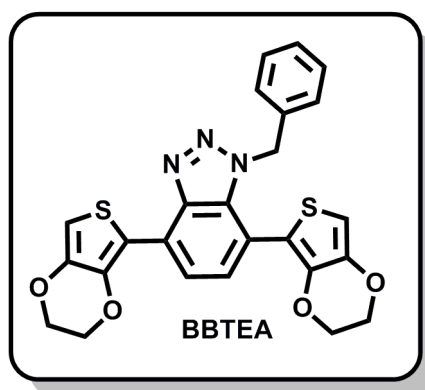
1-Benzyl-4,7-dibromo-1H-benzo[d][1,2,3]triazole (1-BTBr) (0.233 g, 0.635 mmol) and tributyl(thiophen-2-yl)stannane (1.185 g, 3.175 mmol) were dissolved in dry THF (50 mL). The solution was purged with argon for 30 min and dichlorobis(triphenylphosphine)-palladium(II) (60 mg, 0.085 mmol) was added at room temperature under an argon atmosphere. The mixture was refluxed for 48 h, cooled, and concentrated on the rotary evaporator. The residue was subjected to column chromatography (Hexane/CH<sub>2</sub>Cl<sub>2</sub>, 1:1, *R<sub>f</sub>*, 0.43) to afford a yellow solid (0.168 g, 71% yield). <sup>1</sup>H NMR (400 MHz, CDCl<sub>3</sub>, TMS) δ 8.27 (d, 1H, *J* = 3.7 Hz), 7.51 (d, 1H, *J* = 7.5 Hz), 7.36 (d, 1H, *J* = 5.1 Hz), 7.32 (d, 1H, *J* = 5.1 Hz), 7.27 (d, 1H, *J* = 7.5 Hz), 7.17-7.15 (m, 1H), 7.13-6.98 (m, 5H), 6.80 (d, 1H, *J* = 3.5 Hz), 6.55 (d, 1H, *J* = 6.6 Hz), 5.66 (s, 2H) <sup>13</sup>C NMR (100 MHz, CDCl<sub>3</sub>, TMS) δ 52.03, 115.93, 119.44, 125.61, 125.66, 125.71, 125.78, 126.08, 126.67, 127.22, 127.37, 127.44, 127.48, 129.91, 130.75, 134.63, 136.39, 137.77, 142.59. MS (*m/z*): 373.5 [M<sup>+</sup>].

### 2.3.2.6 Synthesis of 2-Benzyl-4,7-di(thiophen-2-yl)-2H-benzo[d][1,2,3]triazole (BBTS)



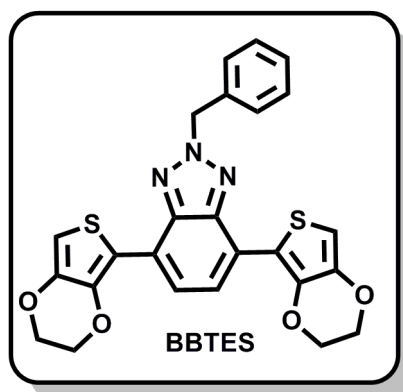
2-Benzyl-4,7-dibromo-1H-benzo[d][1,2,3]triazole (2-BTBr) (120 mg, 0.327 mmol) and tributyl(thiophen-2-yl)stannane (610 mg, 1.63 mmol) were dissolved in dry THF (40 mL). The solution was purged with argon for 30 min and dichlorobis(triphenylphosphine)-palladium(II) (60 mg, 0.085 mmol) was added at room temperature under an argon atmosphere. The mixture was refluxed for 15 h, cooled, and concentrated on the rotary evaporator. The residue was subjected to column chromatography (Hexane/CHCl<sub>3</sub>, 2:1, *R<sub>f</sub>*, 0.35) to afford a bright yellow solid (118 mg, 96%). <sup>1</sup>H NMR (400 MHz, CDCl<sub>3</sub>, TMS) δ 8.01 (s, 2H), 7.53 (s, 2H), 7.41 (d, 2H, *J* = 6.6 Hz), 7.28 (m, 4H), 7.17 (s, 1H), 7.09 (m, 2H), 5.89 (s, 2H). <sup>13</sup>C NMR (100 MHz, CDCl<sub>3</sub>, TMS) δ 60.55, 122.98, 123.74, 125.58, 127.13, 128.13, 128.34, 128.54, 128.82, 134.80, 139.88, 142.50 MS (*m/z*): 373.5 [*M*<sup>+</sup>].

### 2.3.2.7 Synthesis of Benzyl-4,7-bis(2,3-dihydrothieno[3,4-b]dioxin-5-yl)-2H-benzo[d][1,2,3] triazole (BBTEA)



1-Benzyl-4,7-dibromo-1H-benzo[d][1,2,3]triazole (135 mg, 0.37 mmol) and tributyl(2,3-dihydrothieno[3,4-b][1,4]dioxin-5-yl)stannane (820 mg, 1.90 mmol) were dissolved in dry THF (30 mL). The solution was purged with argon for 30 min and dichlorobis(triphenylphosphine)-palladium(II) (50 mg, 0.071 mmol) was added at room temperature under an argon atmosphere. The mixture was refluxed for 48 h, cooled, and concentrated on the rotary evaporator. The residue was subjected to column chromatography ( $\text{CHCl}_3$ ,  $R_f$ , 0.22) to afford an yellow solid (128.6 mg, 71% yield).  $^1\text{H}$  NMR (400 MHz,  $\text{DMSO-d}_6$ )  $\delta$  7.99 (d, 1H,  $J = 7.7$  Hz), 7.26 (d, 1H,  $J = 7.7$  Hz), 7.08 (m, 3H), 6.68 (m, 2H), 6.52 (s, 1H), 6.38 (s, 1H), 5.76 (s, 2H), 4.31 (s, 2H), 4.24 (s, 2H), 4.09 (s, 2H), 3.92 (s, 2H).  $^{13}\text{C}$  NMR (100 MHz,  $\text{DMSO-d}_6$ , TMS)  $\delta$  51.86, 64.00, 64.17, 64.58, 65.03, 100.52, 102.91, 110.06, 111.16, 112.92, 120.69, 124.68, 126.37, 127.54, 128.41, 131.11, 131.39, 136.07, 139.32, 141.01, 141.06. MS ( $m/z$ ): 489 [ $\text{M}^+$ ].

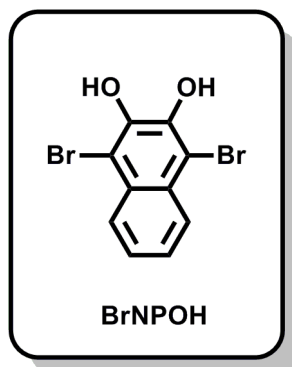
### 2.3.2.8 Synthesis of Benzyl-4,7-bis(2,3-dihydrothieno[3,4-b]dioxin-5-yl)-2H-benzo[d][1,2,3] triazole (BBTES)



2-Benzyl-4,7-dibromo-1H-benzo[d][1,2,3]triazole (125 mg, 0.34 mmol) and tributyl(2,3-dihydrothieno[3,4-b][1,4]dioxin-5-yl)stannane (732 mg, 1.70 mmol) were dissolved in dry THF (30 mL). The solution was purged with argon for 30 min and dichlorobis(triphenylphosphine)-palladium(II) (73 mg, 0.104 mmol) was added at room temperature under an argon atmosphere. The mixture was refluxed for 16 h, cooled, and concentrated on the rotary evaporator. The residue was subjected to column chromatography ( $\text{CHCl}_3$ ,  $R_f$ , 0.43) to afford a yellow solid (100.5 mg, 60%).  $^1\text{H}$  NMR (400 MHz,  $\text{CDCl}_3$ , TMS)  $\delta$  8.04 (s, 2H), 7.45 (s, 1H), 7.43 (s, 1H), 7.26 (m, 3H), 6.41 (s, 2H), 5.88 (s, 2H), 4.27 (s, 4H), 4.19 (s, 4H).  $^{13}\text{C}$  NMR (100 MHz,  $\text{CDCl}_3$ , TMS)  $\delta$  59.35, 63.41, 63.88, 99.69, 113.04, 120.34, 122.84, 127.36, 127.40, 127.67, 133.90, 138.47, 140.72, 141.12. MS (m/z): 489 [ $\text{M}^+$ ].

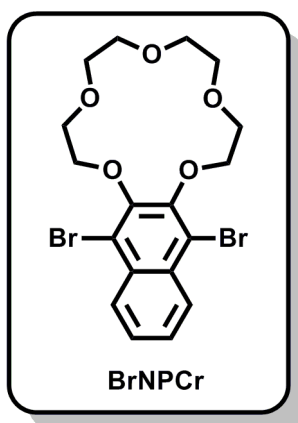
### 2.3.3 Synthesis of Naphthalene-2,3-Crown Ether Functionalized Monomers

#### 2.3.3.1 Synthesis of 1,4-Dibromonaphthalene-2,3-diol (BrNPOH)



1,4-Dibromonaphthalene-2,3-diol was synthesized according to previously reported method [111]. 1 g naphthalene-2,3-diol was dissolved in 2 mL glacial acetic acid, and 1 g bromine dissolved in 1.6 mL glacial acetic acid was added to this solution drop by drop. After a certain time, the white precipitate is formed in the mixture, the precipitate was filtered and crystallized in chloroform.  $^1\text{H}$  NMR (400 MHz,  $\text{CDCl}_3$ , TMS)  $\delta$  8.00-7.90 (m, 2H), 7.5-7.4 (m, 2H). 6.1 (s, 2H).  $^{13}\text{C}$  NMR (101 MHz, DMSO)  $\delta$  144.9, 127.2, 125.5, 125.4, 105.8.

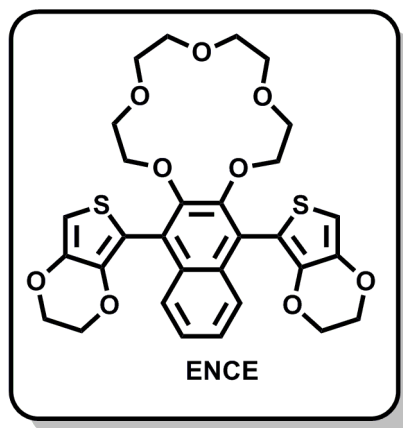
### 2.3.3.2 Synthesis of 14,19-Dibromo-naphtho[2,3-b][1,4,7,10,13]pentaoxacyclo pentadecane (BrNPCr)



1 g 1,4-dibromonaphthalene-2,3-diol (1 equiv.), 0.6 g tetraethyleneglycole (1 equiv.) and 1.6 g diisopropylazodicarboxylate (DIAD) were dissolved in distilled THF at room temperature. After complete solvation, the reaction mixture was cooled to 0°C and 1.6 g of tributylphosphine (PBU<sub>3</sub>) was added gradually in 1 hour. The reaction mixture was refluxed for 3 days when all PBU<sub>3</sub> addition is completed. The THF was removed under vacuum by rotary evaporator and the residue was diluted with 10 mL of ether and placed in refrigerator.

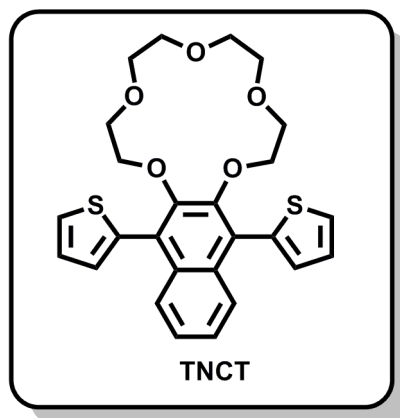
Precipitated triphenylphosphine oxide was filtered off and the residue was further concentrated and purified by column chromatography in 1:1 dichloromethane:chloroform. After removal of the solvent, the residue was crystallized in ethanol. <sup>1</sup>H NMR (400 MHz, CDCl<sub>3</sub>, TMS) δ 8.16 (dd, J = 6.44, 2H), 7.49 (dd, J = 6.46, 2H), 4.25 (t, J = 5.11 Hz, 4H), 4.01 (t, J = 5.11 Hz, 4H), 3.74-3.65 (m, 8H). <sup>13</sup>C NMR (101 MHz, CDCl<sub>3</sub>) δ 159.1, 130.22, 127.28, 123.52, 112.4, 73.28, 71.26, 70, 47, 70, 38.

2.3.3.3 Synthesis of 14,19-Bis(2,3-dihydrothieno[3,4-b][1,4]dioxin-5-yl)-2,3,5,6,8,9,11,12-octahydronaphtho[2,3-b][1,4,7,10,13]pentaoxacyclo pentadecane (ENCE)



14,19-Dibromo-naphtho[2,3-b][1,4,7,10,13]pentaoxacyclopentadecane (162 mg, 0.34 mmol) and tributyl(2,3-dihydrothieno[3,4-b][1,4]dioxin-5-yl)stannane (732 mg, 1.70 mmol) were dissolved in dry THF (30 mL). The solution was purged with argon for 30 min and dichlorobis(triphenylphosphine)-palladium(II) (73 mg, 0.104 mmol) was added at room temperature under an argon atmosphere. The mixture was refluxed for 16 h, cooled, and concentrated on the rotary evaporator. The residue was subjected to column chromatography with chloroform to afford a yellow solid (128.3 mg, 65%).  $^1\text{H}$  NMR (400 MHz,  $\text{CDCl}_3$ , TMS)  $\delta$  8.20 (dd,  $J = 6.44$ , 2H), 7.60 (dd,  $J = 6.46$ , 2H), 6.55 (s, 2H), 4.35 (t,  $J = 5.11$  Hz, 4H), 4.25 (t,  $J = 5.11$  Hz, 4H), 4.15 (t,  $J = 5.11$  Hz, 4H), 4.10 (t,  $J = 5.11$  Hz, 4H), 3.65-3.80 (m, 8H).

2.3.3.4 Synthesis of 14,19-Di(thiophen-2-yl)-2,3,5,6,8,9,11,12,13a,19a-decahydronaphtho[2,3-b][1,4,7,10,13]pentaoxacyclopentadecane (TNCT)



14,19-Dibromo-naphtho[2,3-b][1,4,7,10,13]pentaoxacyclopentadecane (162 mg, 0.34 mmol) and tributyl(thiophen-2-yl)stannane (610 mg, 1.63 mmol) were dissolved in dry THF (30 mL). The solution was purged with argon for 30 min and dichlorobis(triphenylphosphine)-palladium(II) (60 mg, 0.085 mmol) was added at room temperature under an argon atmosphere. The mixture was refluxed for 16 h, cooled, and concentrated on the rotary evaporator. The residue was subjected to column chromatography with chloroform to afford a yellow solid (109.9 mg, 67%).  $^1\text{H}$  NMR (400 MHz,  $\text{CDCl}_3$ , TMS)  $\delta$  7.29 (dd,  $J = 6.52$  Hz, 2H), 7.44 (dd,  $J = 5.11$  Hz, 2H), 7.72 (dd, 2H), 7.13 (dd,  $J = 5.09$  Hz, 2H), 7.09 (dd,  $J = 3.46$  Hz, 2H), 4.03 (t,  $J = 5.19$  Hz, 4H), 3.69-3.58 (m, 12H).  $^{13}\text{C}$  NMR (101 MHz,  $\text{CDCl}_3$ ) 150.19, 135.7, 131.2, 129.1, 126.8, 126.4, 125.7, 125.6, 125.5, 73.3, 70.9, 70.4, 70.3.

## 2.4 Electrochemical Methods

Conducting polymers were characterized using potentiostatic (controlled potential) and galvanostatic (controlled current) electroanalytical tools. Electroactivity of the monomers and red-ox properties of polymers were investigated by cyclic voltammetry and square wave potential (chronocoulometry) techniques.

This section will detail fundamentals of cyclic voltammetry and opto-electrochemical techniques: spectroelectrochemistry, switching and colorimetry studies of polymer films obtained by electrochemical polymerization technique.

### 2.4.1 Cyclic Voltammetry System

The basic electrochemical properties of a conducting polymer film can be determined by cyclic voltammetry which involves measurement of the current ( $I$ ) resulting from application of a cyclic potential ( $V$ ) scan to the polymer with a constant scan rate.

Cyclic voltammetry measurements were carried out by scanning the potential of the working electrode using triangular waveform and measuring the resulting current at the working electrode (Figure 2.1a). In cyclic voltammetry (CV) the current response is measured while the potential is linearly increases from an initial potential to a peak potential and back to initial potential again.

Expected response of a reversible redox couple during a single potential cycle is given in Figure 2.1b.

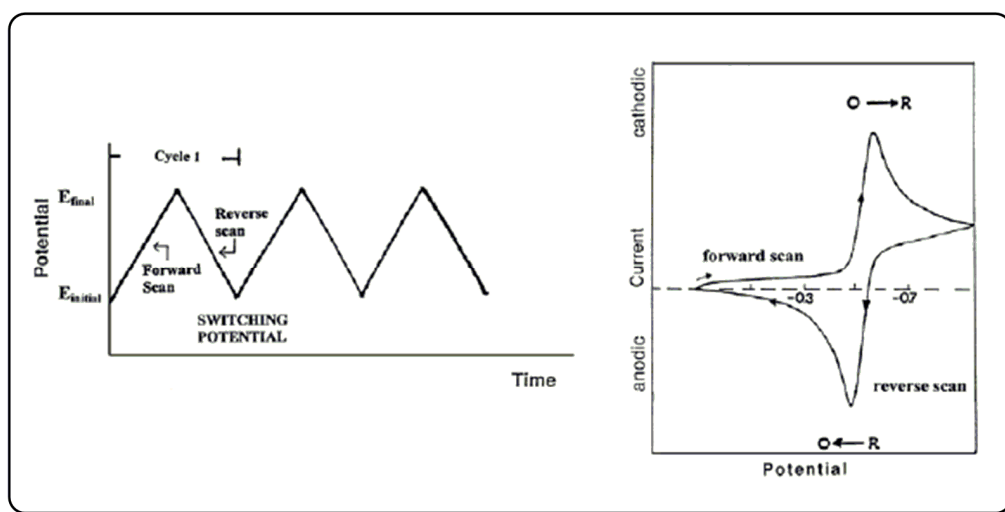


**Figure 2.1** Typical (a) Potential–time excitation signal in CV (b) cyclic voltammogram of a reversible  $O + ne \rightleftharpoons R$  redox process

Typical peaks in the CV are formed due redox reactions occurred at the diffusion layer near the electrode surface. The magnitude of the current peak indicates the change of concentration with time. The resulting current peak reflects the continuous change of concentration gradient with time. Hence, the increase in the current corresponds to the achievement of diffusion control, while current drop (beyond the peak) is independent of the applied potential.

The peak current ( $i_p$ ) of a reversible couple is described by the Randles-Sevcik equation:

$$i_p = (2.69 \times 10^5) n^{3/2} A D^{1/2} C V^{1/2}$$

where  $n$  is the number of electrons,  $A$  is the surface area of the electrode ( $\text{cm}^2$ ),  $D$  is the diffusion constant ( $\text{cm}^2/\text{s}$ ),  $C$  is the bulk concentration of electroactive species

(mol/cm<sup>3</sup>), and  $V$  is the scan rate (V/s). Therefore, for a diffusion-controlled system, the peak current is proportional to the square root of the scan rate.

The scenario of electrochemical process for electroactive polymers is different because polymerization of the electroactive monomers is irreversible. As the monomer gets irreversibly oxidized, polymer film begins to form on the electrode surface. Thus, in this situation there are two electroactive species in the system, one of which being the monomer and the other is polymer deposited on the electrode.

A typical CV experiment generally starts at low potentials where no redox reactions occur in anodic direction. When sufficient potentials are applied to oxidize monomer to its radical cation, anodic current starts to increase in the vicinity of the potential. A peak is observed when the concentration of monomer at working electrode surface approaches zero. The intensity of the current starts to decay since the solution in the vicinity of the electrode has almost zero monomer concentration. Monomer oxidation is immediately followed by chemical coupling which results in the formation of firstly the dimer and the oligomers. As the number of cycles increases there is an increase in the intensity of the current. This is due to increase in the active area of the working electrode owing to coating of already electroactive polymer on the metal electrode (Figure 2.3) [112].

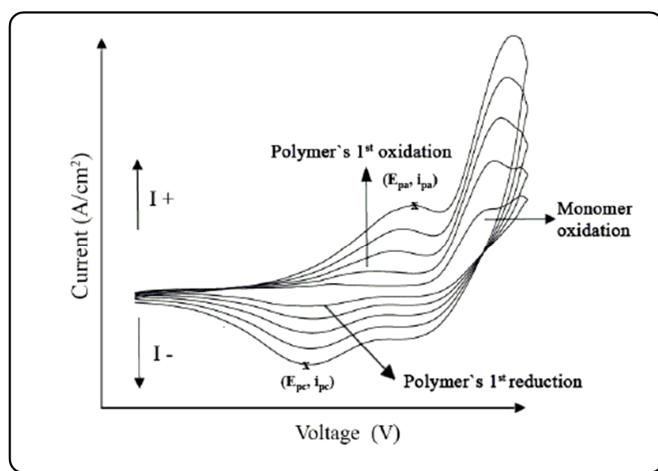


**Figure 2.2** Cyclic Voltammogram of a representative type of electroactive monomer [113]

Electrochemical properties of a polymer should be studied in a monomer free environment. The redox process of the polymer is quasi-reversible and the redox process is not diffusion controlled since the polymer is immobilized at the electrode surface and under these circumstances Randles & Sevcik equation is no longer valid. Instead, according to the theory of immobilized redox centers, the peak current is given by ;

$$i_p = n^2 F^2 \Gamma v / 4RT$$

where  $\Gamma$  is the total amount of reactant initially present at the electrode surface. According to this equation the current peak depends linearly on scan rate. Thus investigation of peak current intensity with respect to scan rate will indicate the nature of electrochemical process being diffusion controlled or the polymer is well adhered to the electrode surface [114].

## 2.5 Optical Methods

The electrochromic properties of neutral and doped polymer can be investigated by spectroelectrochemistry, electrochromic switching and colorimetry measurements. These experiments provide information about band gap energy, contrast and color, respectively.

### 2.5.1 Spectroelectrochemistry

One of the methods which are used to characterize the electrochromic polymers is spectroelectrochemistry. The optical changes due to electronic transitions arising during redox switching can be examined by UV-Vis-Near Infrared (NIR) spectroscopy. Spectroelectrochemistry experiments give information about the material's band gap and intraband states (polaron and bipolaron bands) that are created upon doping as well as give some insight into a polymer color through the location of the absorption maxima. Relation between the spectroelectrochemical data and intraband states of a PEDOT derivative is shown in Figure 2.3 [113].

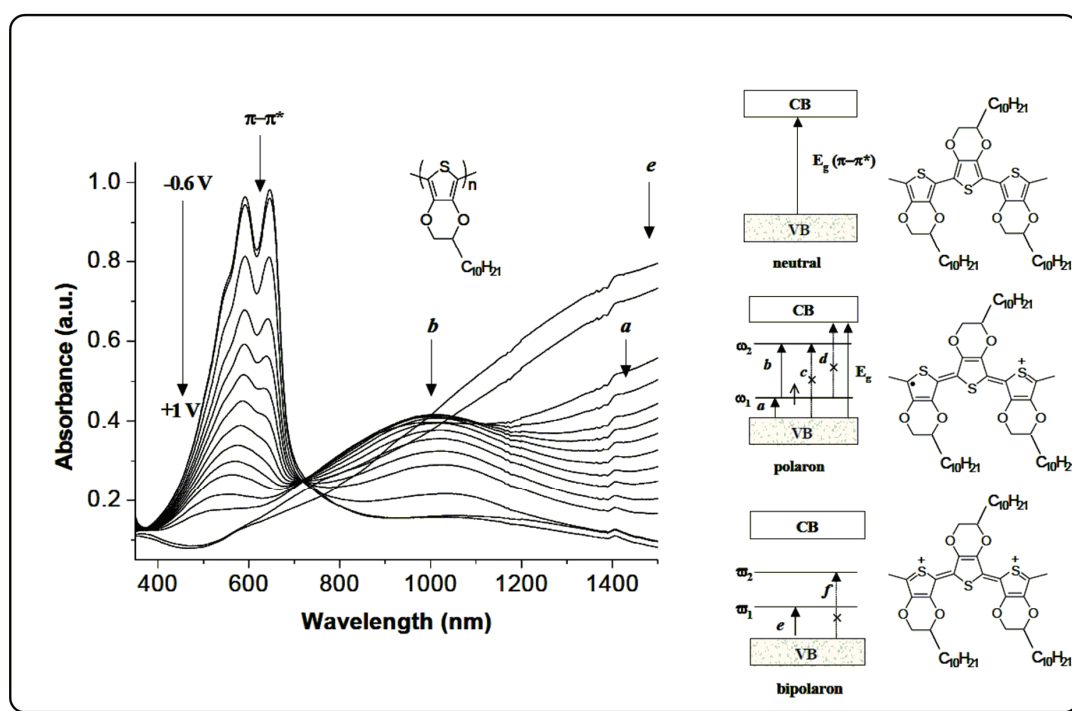


**Figure 2.3** Illustration of spectroelectrochemical data of a PEDOT derivative [113]

A three electrode cell was employed with ITO as the working electrode in a UV cuvette. Polymer films were deposited potentiostatically with  $25 \text{ mC/cm}^2$  (ca. 0.5 microns). UV-Vis-Near IR spectral data were collected while stepping the potential with 50 or 100 mV potential increments to oxidize polymers.

ITO working electrode was placed in a standard 1 cm path length cuvette fitted with a Teflon cap to hold the working electrode in place along with the reference and counter electrodes (Figure. 2.4). The cuvette was filled with the suitable electrolyte solution. After that, the counter and reference electrodes were placed on either side of the cuvette to avoid blocking of source beam and contact with the working electrode. The baseline is taken as an identical cell to the one to be measured minus the polymer film with the UV-Vis-NIR spectrophotometer. The ITO working electrode was replaced with the polymer coated one and three electrodes were

connected to a potentiostat to apply desired potential to the working electrode. The wavelength region of interest was being scanned while the potential applied was held constant.

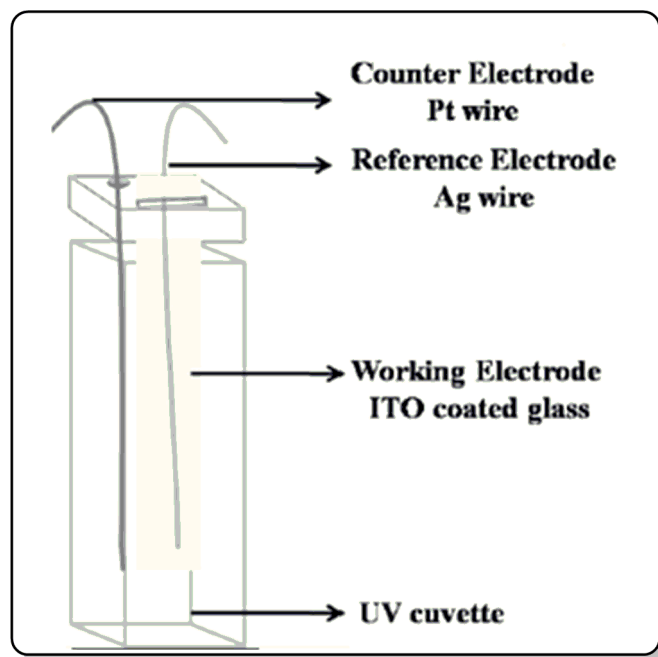


**Figure 2.4** A three electrode electrochemical cell set up

### 2.5.2 Switching Studies

Electrochromic switching studies are critical electrochromic applications of conducting polymers. A square potential sweep method (chronoabsorptometry) is applied to polymer to observe switching times and contrast for the polymers. Switching time ( $\Delta t$ ) is defined as the time required for the coloring/bleaching process of an electrochromic material. %T in the reduced ( $T_{red}$ ) and oxidized ( $T_{ox}$ ) forms and is defined as contrast and noted as %  $\Delta T$  (Figure 2.5).

The polymer coated on ITO electrode was switched in monomer free there electrode system between its fully reduced and fully oxidized states with a residence time of 5 seconds, while simultaneously the percent transmittance change during doping and dedoping process was monitored at the maximum absorption or other wavelengths.

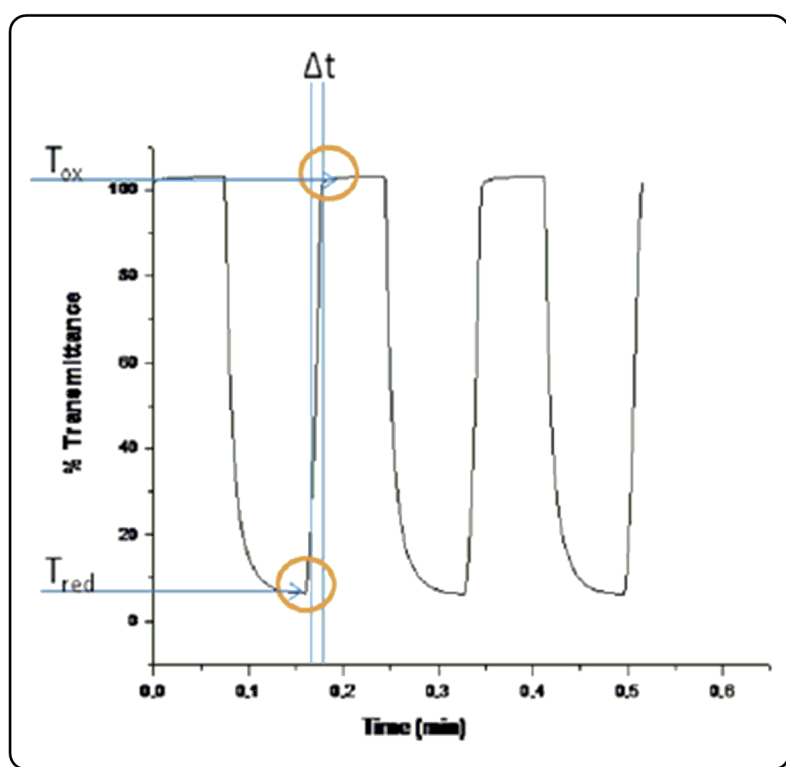


**Figure 2.5** Switching studies of a representative electrochromic conducting polymer

### 2.5.3 Colorimetry

Colorimetry measurements give precise color information for electrochromic polymers. It measures sensitivity of human eye to light across the visible region and defines the color with a mathematical function. This technique measures three values of color; the hue (dominant wavelength), which is the wavelength where maximum contrast occurs, saturation (purity), which is the color's intensity, and brightness (luminance). CIE L,a,b coordinates were shown in Figure 2.6.

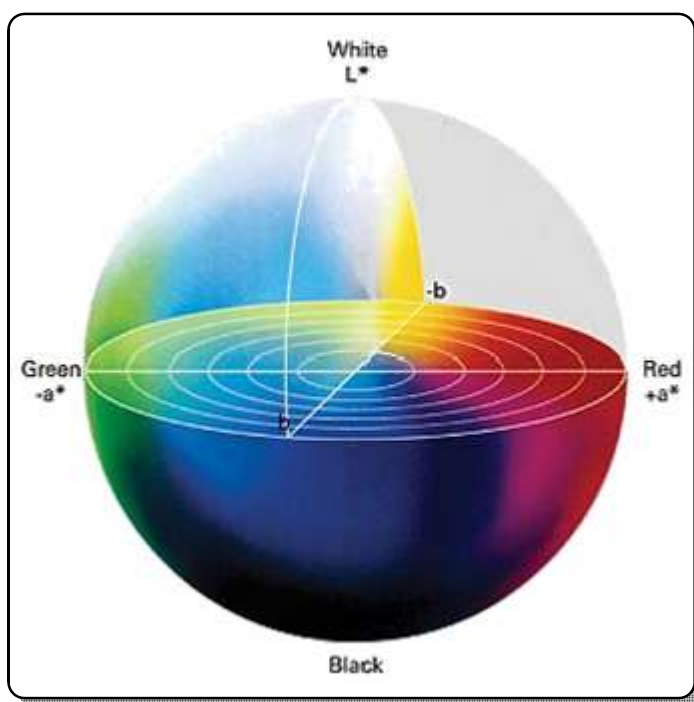


Figure 2.6 CIE 1931 Lab color space

## CHAPTER 3

### RESULTS AND DISCUSSION

#### 3.1 Synthesis and Characterization of Benzotriazole Functionalized Monomers

##### 3.1.1 Perspective of the work

Design of new electroactive monomers is a key tool to determine the electrochemical and optical properties of the final conducting polymers. Donor-acceptor (DA) approach, which is a useful method to synthesize low band gap polymers, was used to design for the benzotriazole unfunctionalized  $\pi$ -conjugated monomers.

Previously reported benzotriazole containing monomers were all symmetrical structures since benzotriazole was substituted only from 2- position of triazole ring. Therefore, syntheses of monomers and polymers containing benzotriazole groups functionalized from 1-position have not been reported yet. Furthermore, effect of position of the substitution on final properties of monomer and polymers has not been probed up to date.

Herein, electron-acceptor unit benzotriazole was terminated with electron rich/donor units; either ethylenedioxythiophene (EDOT) or thiophene. Functionalization of benzotriazole with benzyl group was done from either 1- or 2- positions in order to obtain four different monomers. The structures of these monomers are shown in Figure 3.1 The aim here was to investigate effect of substituent, substitution position and donor group.

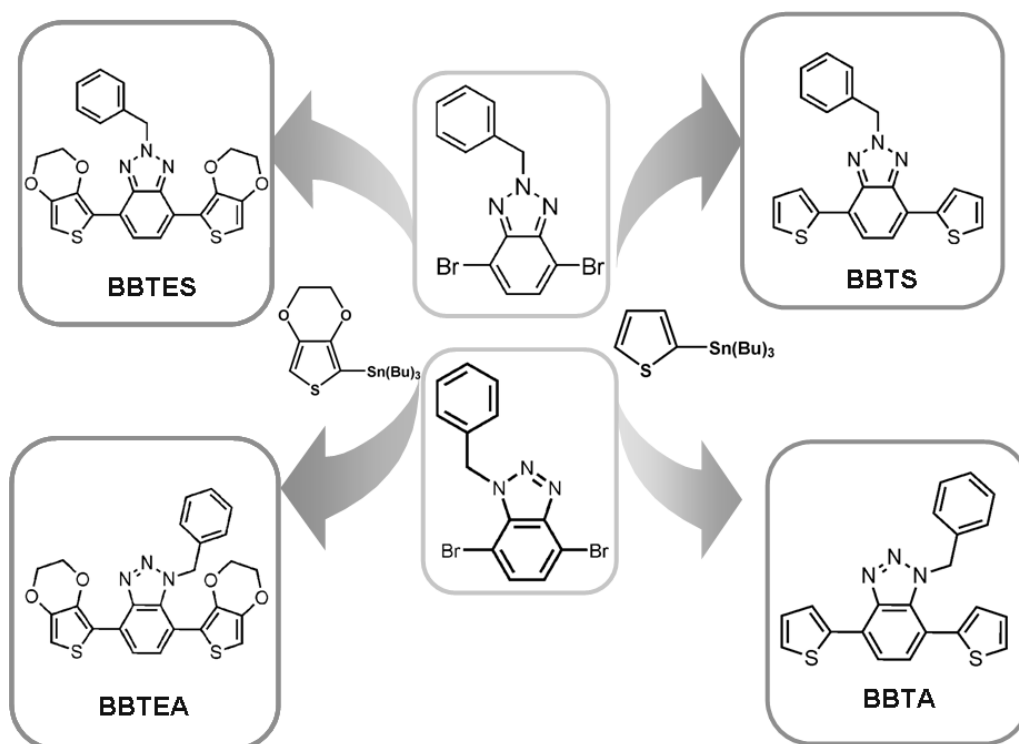
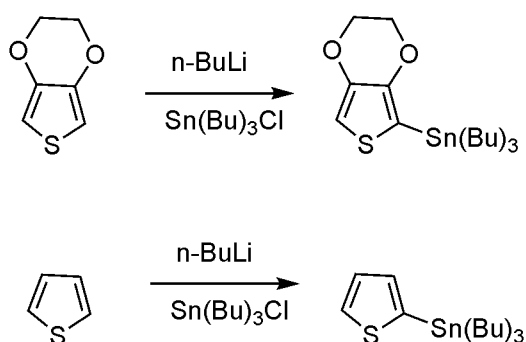


**Figure 3.1** Donor-Acceptor-Donor Type Benzotriazole Derivatives

### 3.1.2 Synthesis of Donor Moieties

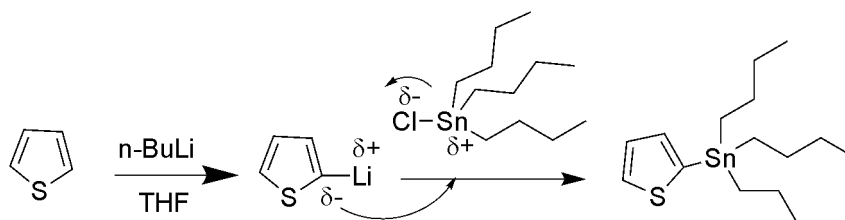
Modification of the donor or acceptor groups in a  $\pi$ -conjugated monomer changes the electrochemical and optoelectronic properties of resulting polymer. Thiophene and its electron rich derivatives were used as donor units in DAD type monomer in order to decrease band gap energy by increasing HOMO level energy. Electron-rich thiophene derivative, EDOT has higher donor strength than thiophene due to ethylenedioxy bridges thus; oxidation potentials and band gap energies of EDOT containing monomers/polymers are lower compared to thiophene containing ones.

Donor units, EDOT and thiophene, were converted to stannylated intermediate in order to be used in the Stille coupling reaction (Scheme 3.1). Stannylated EDOT or thiophene were coupled with the dibrominated acceptor moieties by Stille coupling route in the presence of palladium catalyst.



**Scheme 3.1** Preparation of organotin compounds

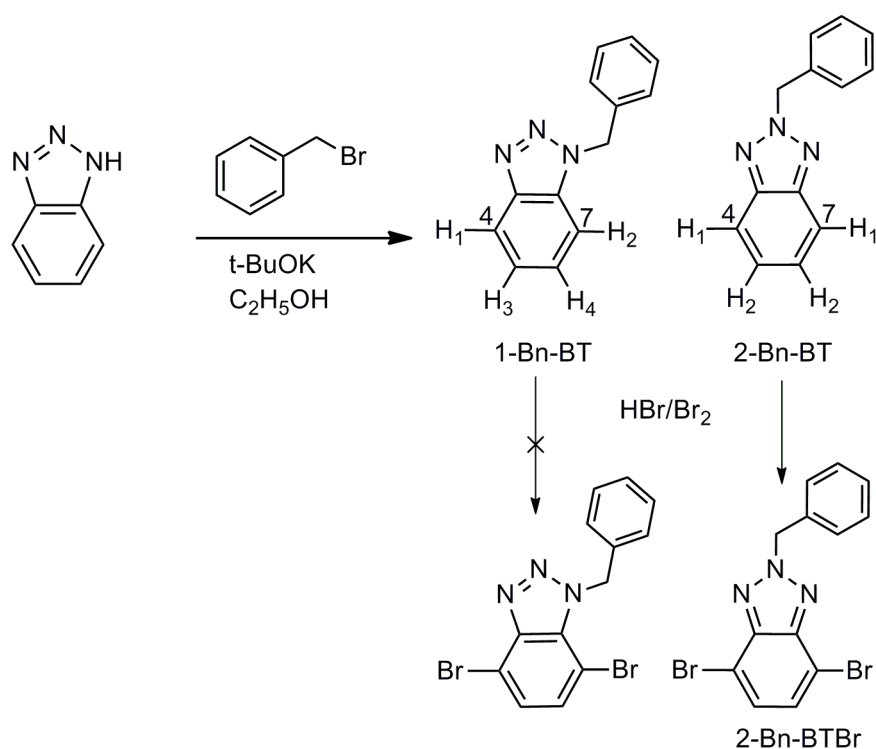
Stannylation of thiophene and EDOT were performed by lithiation with *n*-butyl lithium followed by the subsequent quenching with tributyltin chloride to obtain desired products. Stannylation mechanism for thiophene was demonstrated in Scheme 3.2.



**Scheme 3.2** Reaction mechanism for stannylation of thiophene

### 3.1.3 Syntheses and Characterizations of Acceptor Moieties

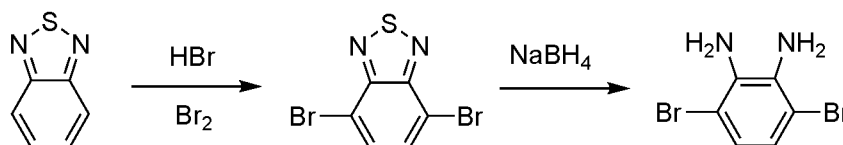
Synthetic strategy of central unit of monomer which has electron acceptor character was determined by investigating the recent literature on benzotriazole bearing DAD type monomers. BBTS and BBTES monomers could be obtained using previously reported synthetic routes [115]. However, this method has limitations to synthesize monomers containing 1-Bn-BTBr, BBTA and BBTEA. If the synthetic route of previous works had been followed (Scheme 3.3), it would be possible to obtain both 1-benzylbenzotriazole and 2-benzylbenzotriazole in a single step reaction. However, 1-benzylbenzotriazole would not be brominated from the desired 4,7 positions since the molecule was not symmetrical and electron densities of the 4,7 positions were not equal.



**Scheme 3.3** Synthetic route for functionalization of benzotriazole

Therefore, a different synthetic route was designed to obtain target monomers. This new synthetic route was able to synthesize 1-benzylbenzotriazole and 2-benzylbenzotriazole brominated from 4,7 positions.

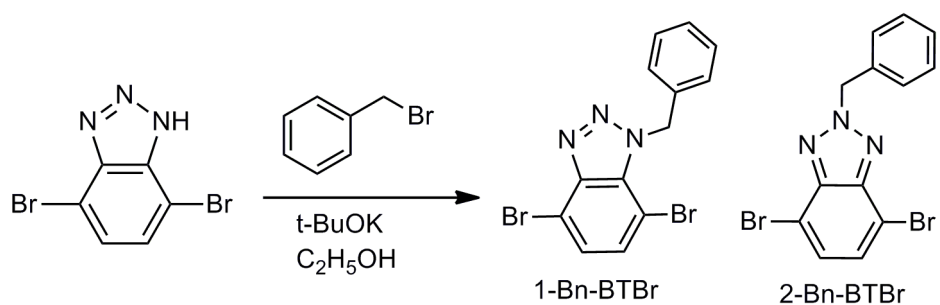
Benzo[*c*][1,2,5]thiadiazole was brominated with the HBr/Br<sub>2</sub> mixture to obtain 4,7-dibromo-2,1,3-benzothiadiazole. Slow addition of HBr/Br<sub>2</sub> solution was essential to control bromination. This step eliminated the obstacles for bromination of 1-substituted benzotriazole since bromination of benzyl groups was completed in this step. 4,7-Dibromo-2,1,3-benzothiadiazole then reduced by excess amount of NaBH<sub>4</sub> to give 3,6-dibromo-1,2-phenylenediamine as a pale yellow solid (Scheme 3.4). The structure of this material was confirmed by the observation of the broad peak belongs to amine groups at 3.8 ppm, in addition to resonance of aromatic protons on the benzene ring at 6.83 ppm as a singlet.



**Scheme 3.4** Synthetic route for synthesis of 3,6-dibromo-1,2-phenylenediamine

The diamine group was converted to triazole ring in the presence of NaNO<sub>2</sub> to obtain 4,7-dibromo-1,2,3-benzotriazole (Scheme 3.5).





**Scheme 3.7** Synthetic route for 1-Bn-BTBr and 2-Bn-BTBr

After purification of the mixture, the positions of the benzyl group in 1-Bn-BTBr and 2-Bn-BTBr was confirmed by comparing their  $^1\text{H-NMR}$  spectra. Examination of number of peaks belong to different hydrogens was the key information to differentiate the products. Hydrogen atoms in the 5- and 6- position of the molecules were equivalent for 2-Bn-BTBr while they differed from each other when in the case of 1-Bn-BTBr.

Furthermore, benzylic protons of 1-Bn-BTBr and 2-Bn-BTBr differed from each other owing to the difference in electron density and electronegativity of neighboring groups. Existence of two nitrogen atoms at both  $\alpha$ - $\beta$  positions of 2-Bn-BTBr and occupied carbon and nitrogen atoms at  $\alpha$  and  $\beta$  position of 1-Bn-BTBr induced the difference on benzylic protons. The triazole unit in 2-substituted benzotriazoles were reported as electron-accepting unit according to photoelectron spectroscopy studies and molecular orbital calculations [97, 116]. Therefore, the benzylic proton on 2-Bn-BTBr resonated at high field of the spectrum compare to benzylic proton of 1-Bn-BTBr due to connection with an electron-acceptor unit.  $^1\text{H-NMR}$  spectrum revealed that benzylic protons of 2-Bn-BTBr resonated at 5.8 ppm as a singlet while benzylic protons of 1-Bn-BTBr resonated at 6.1 ppm as shown in Figure 3.2.

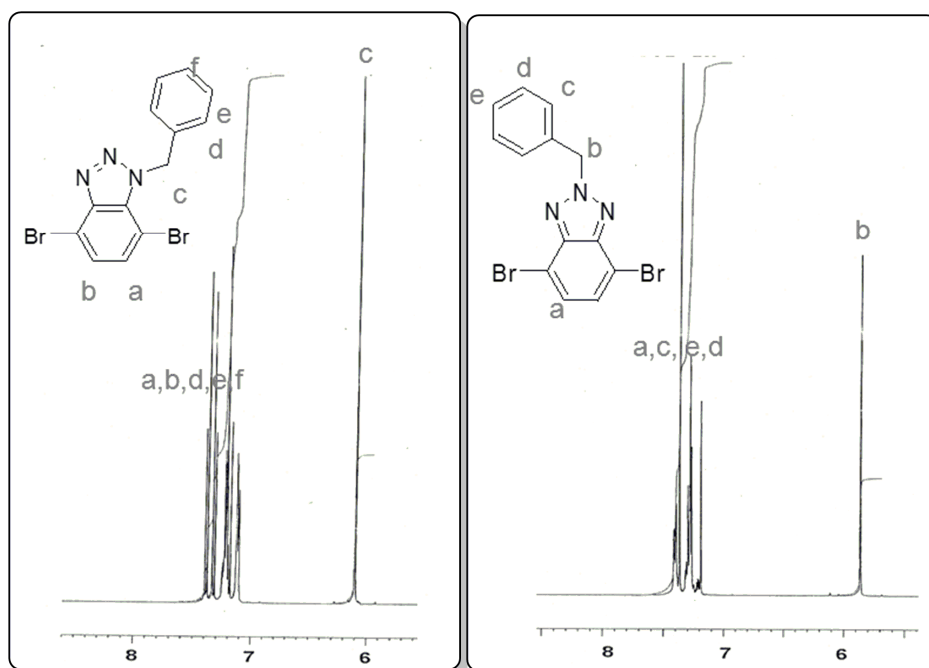


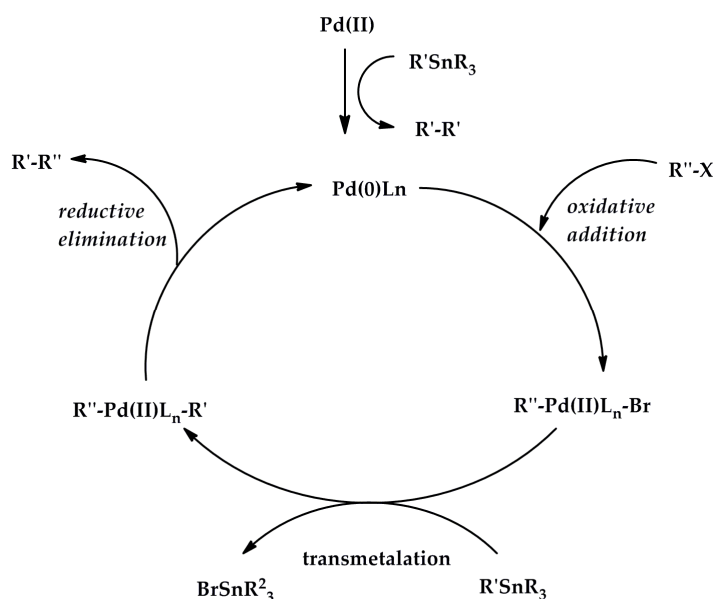
**Figure 3.2** Synthetic route for synthesis of 1-Bn-BTBr and 2-Bn-BTBr

### 3.1.4 Syntheses of Donor-Acceptor-Donor Type Benzotriazole Derivatives

Transition metal-catalyzed cross-coupling reaction which is called “Stille coupling reaction” was used to synthesize DAD type  $\pi$ -conjugated monomers.

Although there are many other types of coupling reaction used to synthesize donor-acceptor-donor type monomers, Stille coupling has some advantages over other methods. The organotin reagents used in Stille coupling or reaction itself are not air or moisture sensitive unlike Suzuki reaction conditions. Furthermore, synthesis, purification and storage are more practical. A general process of Stille coupling reaction was shown in Scheme 3.8. When the catalyst is introduced as Pd(II), fast reduction by the stannane to a Pd(0) species enters the cycle. Alternatively, the catalyst can be introduced directly as Pd(0). The first step of the catalytic cycle is

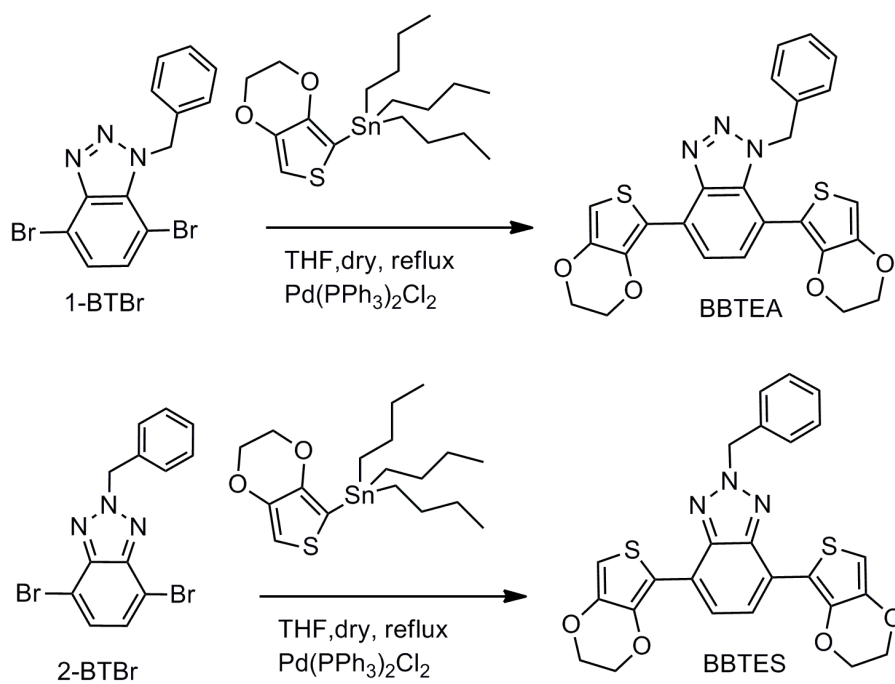
oxidative addition of  $R''-X$  to the active catalyst to give  $R''-Pd(II)L_n-X$ , followed by transmetalation to give  $R''-Pd(II)L_n-R'$  and finally reductive elimination to give  $R'-R''$  [117].



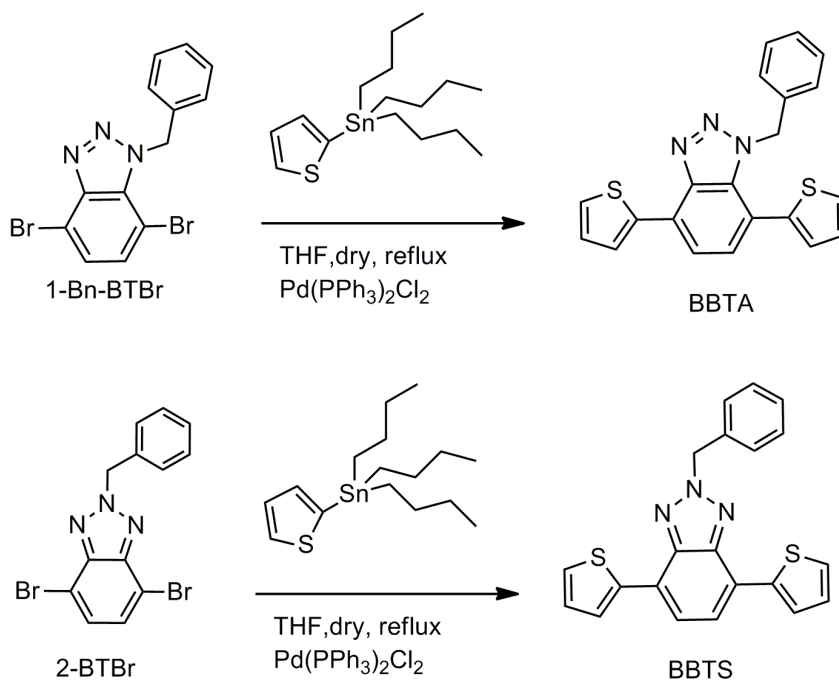
**Scheme 3.8** Catalytic cycle of the Stille reaction

Herein, intermediate dibrominated products 1-Bn-BTBr and 2-Bn-BTBr were coupled separately with the stannylated EDOT (tributyl(2,3-dihydrothieno[3,4-b][1,4]dioxin-5-yl)stannane) in the presence of  $Pd(PPh_3)_2Cl_2$  to obtain final products 1-benzyl-4,7-bis(2,3-dihydrothieno[3,4-b]dioxin-5-yl)-2H-benzo[d][1,2,3]triazole (BBTES) and 2-benzyl-4,7-bis(2,3-dihydrothieno[3,4-b]dioxin-5-yl)-2H-benzo[d][1,2,3]triazole (BBTEA) in satisfactorily good yields (Figure 3.9).

BBTS and BBTA were also synthesized by Stille reaction of intermediate dibrominated products 1-Bn-BTBr and 2-Bn-BTBr with stannylated thiophene (tributyl(thiophen-2-yl)stannane) in the presence of same Pd catalyst (Scheme 3.10).

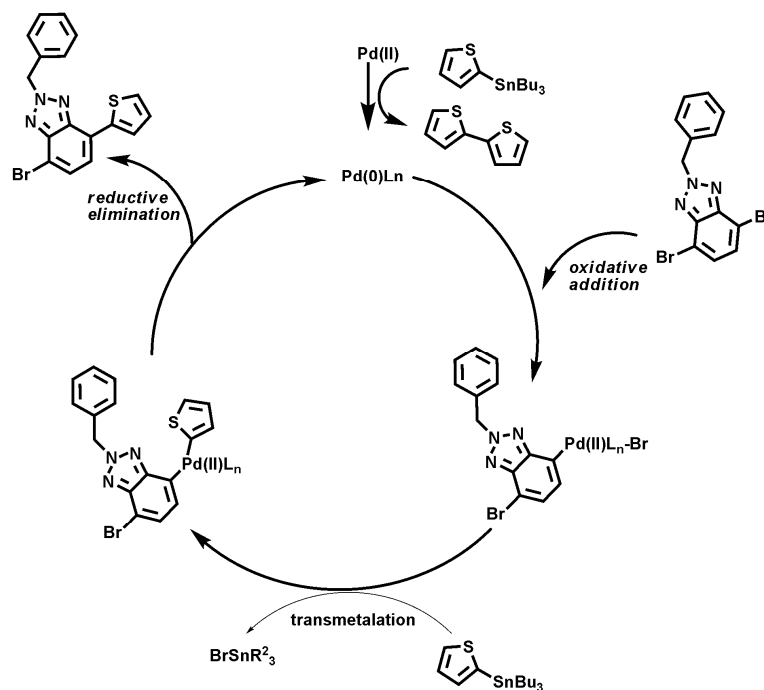


**Scheme 3.9** Synthetic route for BBTES and BBTEA



**Scheme 3.10** Synthetic route for BBTES and BBTEA

The mechanism of the Stille coupling reaction is illustrated in Scheme 3.11 for BBTS.



**Scheme 3.11** Representative cycle of Stille coupling reaction for BBTS

The structural confirmations of monomers were done by <sup>1</sup>H and <sup>13</sup>C NMR techniques. The change in the substitution position distorted the symmetry of the monomers therefore; NMR spectra of the BBTEA and BBTA differed from BBTES and BBTS, respectively.

The hydrogen atoms in ethylenedioxy bridges in BBTEA became different and behaved as four different hydrogen pairs due to asymmetry and thus; resonated at 4 different fields. On the other hand, the hydrogen on same position of BBTES resonated with two pairs of hydrogen which were equivalent on terminal EDOT groups owing to symmetry in molecule. Furthermore, the aromatic protons on

benzene ring of the benzotriazole heterocycle differed from each other due to loss of symmetry in structure. The only aromatic proton on benzene ring resonated at 8.04 ppm whereas the a and k aromatic protons resonated at 7.99 and 7.86ppm, respectively (Figure 3.3).

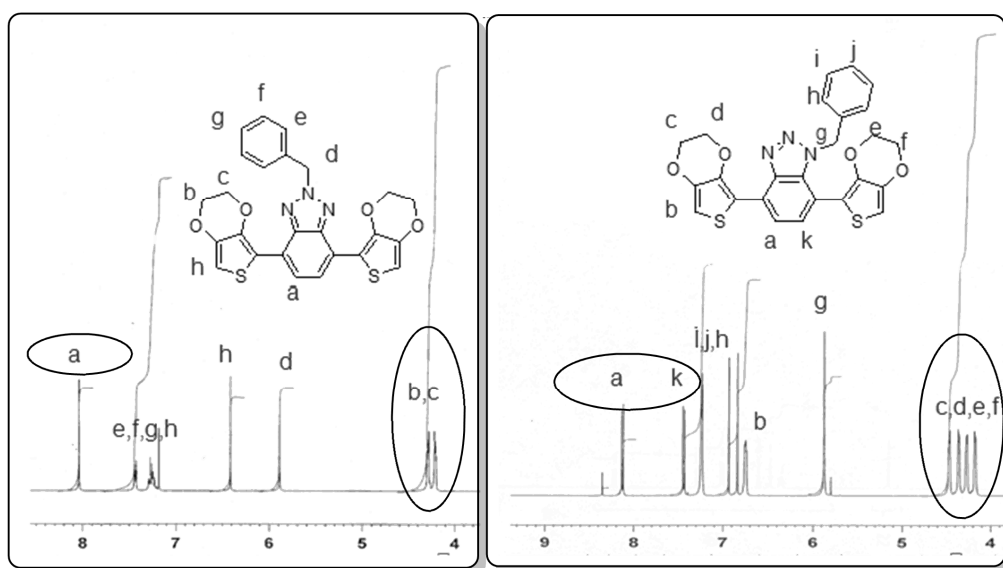


**Figure 3.3** Comparative  $^1\text{H}$ -NMR spectra of BBTEA and BBTES

Not only the hydrogen but also carbon atoms in the monomers differentiated from each other due to loss of symmetry and different carbons resonate at different frequencies. BBTA showed higher number of resonance of carbon atoms with respect to BBTS owing to presence of higher number of different carbon. 19 carbon atoms resonated for BBTA while only 12 carbon atoms resonated for BBTS. The  $^{13}\text{C}$ -NMR spectra of BBTS and BBTA were given in Figure 3.4..

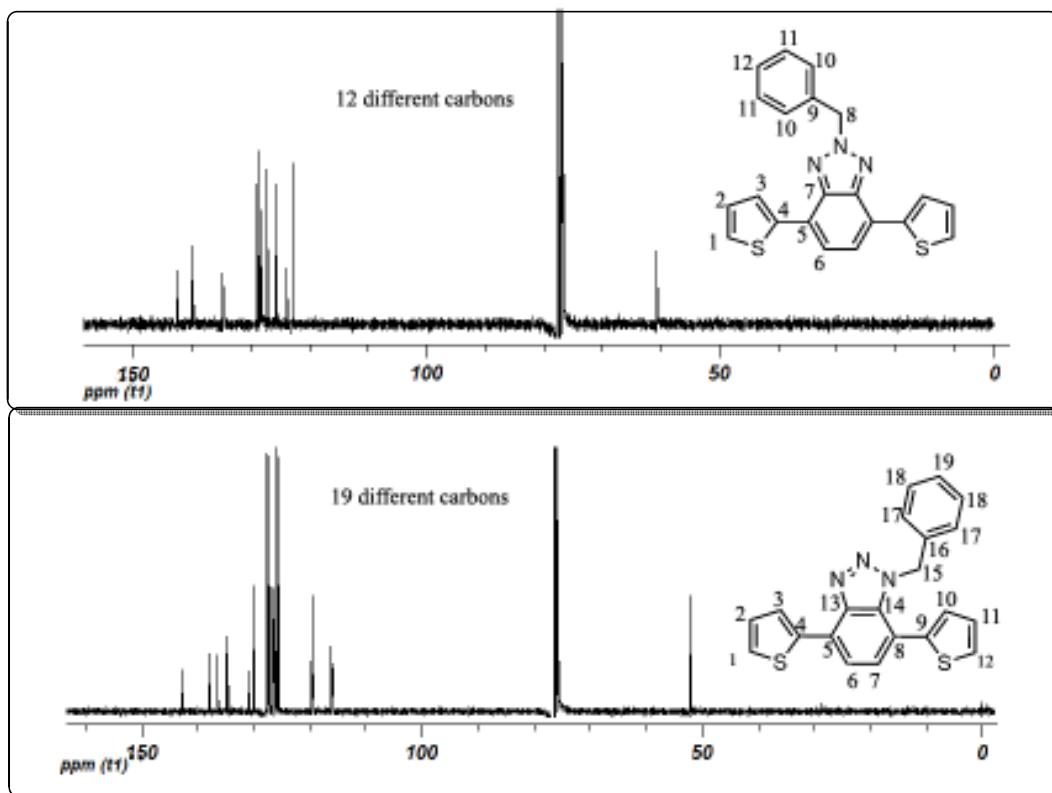


**Figure 3.4** Comparative <sup>13</sup>C-NMR spectra of BBTA and BBTS

Benzyl substituted benzotriazole functionalized monomers BBTA, BBTS, BBTEA and BBTES were also characterized by mass spectroscopy. MS results were in accordance with the calculated ones for BBTS and BBTA ( $C_{21}H_{15}N_3S_2$ ) as 373.07 [M<sup>+</sup>] and measured as 373.5 [M<sup>+</sup>]. Similarly, for BBTES and BBTEA ( $C_{25}H_{19}N_3O_4S_2$ ), MS results agreed with the expected MS value 489.08 [M<sup>+</sup>] which was found as 489.0 [M<sup>+</sup>].

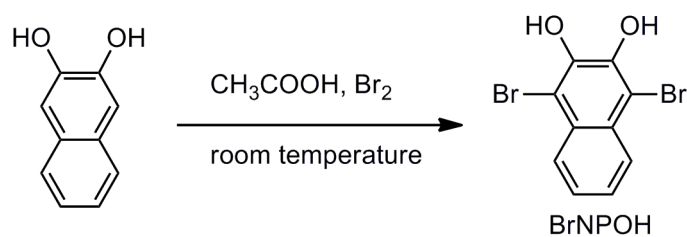
## **3.2 Synthesis Characterization of of Napthelene-2,3-Crown Ether Functionalized Monomers**

### **3.2.1 Perspective of the work**

EDOT and thiophene terminated monomers are designed mostly in order to synthesize low band gap polymers. The idea behind this work was other than synthesis low band gap polymer; it was the syntheses of electroactive monomers containing naphthelene-2,3-crown ethers terminated with EDOT and thiophene to observe effect of crown ether moiety on electrochemical and optoelectronic properties of resultant polymers.

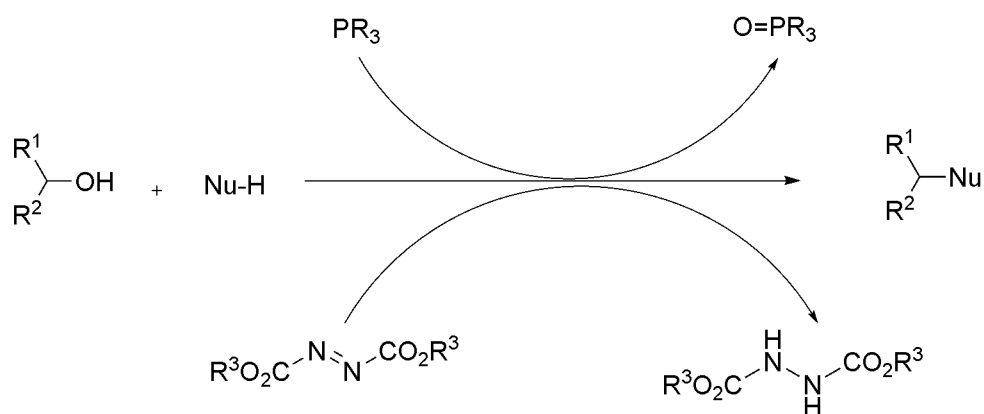
### **3.2.2 Synthesis and Characterization of Napthelene-2,3-Crown Ether Moiety**

Napthelene-2,3-crown ether moiety was synthesized in two main steps and started with bromination of naphthalene-2,3-diol to yield BrNPOH as shown in Scheme 3.12. Bromination was performed in the presence of acetic acid at room temperature since OH groups attached to naphthalene is electron releasing hence, activates the ring and speeds up the electrophilic substitution of halogen from desired positions. The bromination step was practical since reaction was performed at room temperature and purification was done only filtration followed by crystallization in chloroform with high yield. Aromatic proton on naphthalene groups resonated at around 8.00-7.9 and 7.5-7.4 ppm while OH group resonated with a broad singlet at 6.1 ppm in  $^1\text{H-NMR}$ .



**Scheme 3.12** Synthetic route for 1,4-Dibromonaphthalene-2,3-diol

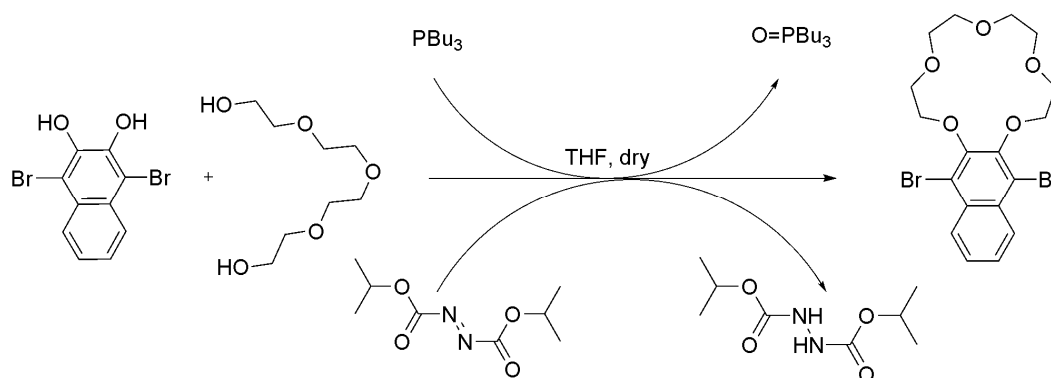
Traditionally, crown ethers are synthesized via reaction of a diol with a terminated dihalo or disulfonyl groups under Williamson condition. The disadvantage of this method is low yield together with the formation of several by-products. Mitsunobu reaction, which is widely used to convert primary and secondary alcohols to esters or ethers, can also be used to synthesize crown ethers with advantages over Williamson method, such as no use of halo-compound, very mild reaction condition and short reaction time [118]. Therefore, synthesis of crown ether moiety was performed by Mitsunobu reaction. General route for Mitsunobu reaction was illustrated in Scheme 3.13.



**Scheme 3.13** General mechanism of Mitsunobu reaction

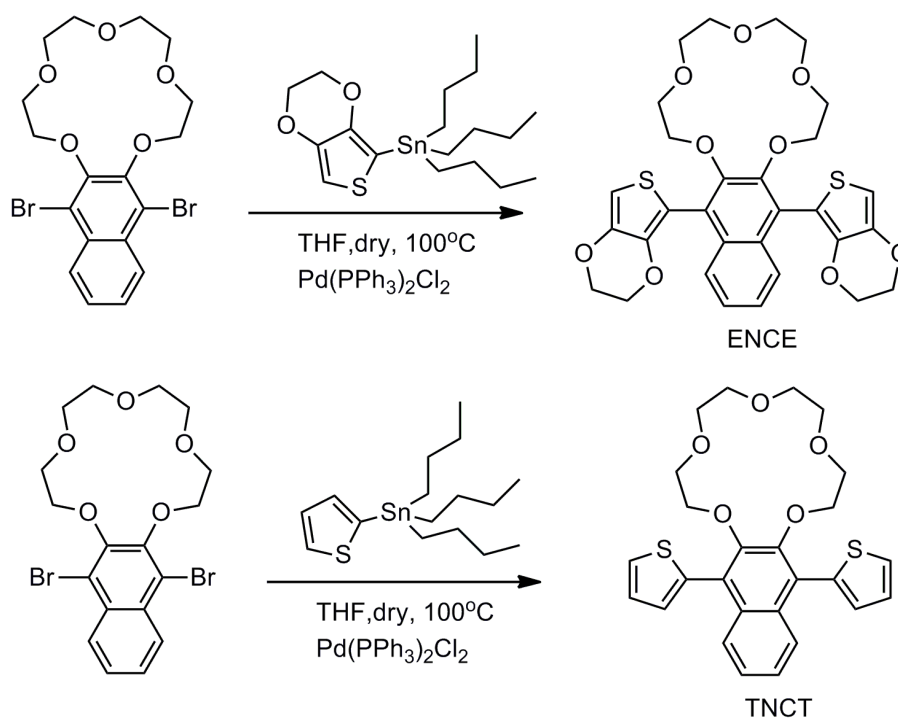
Crown ether moiety was formed with reaction of tetraethylene glycol and BrNPOH in the presence of diisopropylazodicarboxylate (DIAD) and tributyl phosphine (PBU<sub>3</sub>). PBU<sub>3</sub> is very sensitive to air and humidity, thus these reactions performed with dry THF under argon atmosphere. Tetraethylene glycol, BrNPOH and tributyl phosphine were mixed and this mixture was cooled down to 0 °C due to exothermic reaction of PBU<sub>3</sub> with DIAD. Therefore, DIAD was added dropwise to control released heat. One of the by-products, tributyl phosphine oxide was removed from the reaction mixture by dissolving the reaction mixture with diethyl ether and removing the precipitate. Diethyl ether was selected as solvent since desired product BrNPCr was soluble in diethyl ether whereas tributyl phosphine oxide was not soluble.

The reaction mechanism for the synthesis of BrNPCr was given in Scheme 3.14. The tributylphosphine combined with DIAD to create a phosphonium intermediate that binds to the oxygens of BrNPOH group, activating it as a leaving group. Substitution by nucleophile tetraethylene glycol completed the process.



**Scheme 3.14** Synthetic route for 1,4-Dibromonaphthalene-2,3-diol

The Stille coupling of the purified BrNPOH with stannylated EDOT and thiophene in the presence of  $\text{Pd}(\text{PPh}_3)_2\text{Cl}_2$  yielded the monomers 14,19-bis(2,3-dihydrothieno[3,4-b][1,4]dioxin-5-yl)-2,3,5,6,8,9,11,12-octahydronaphtho[2,3-b][1,4,7,10,13]pentaoxacyclopentadecane (ENCE) and 14,19-di(thiophen-2-yl)-2,3,5,6,8,9,11,12,13a,19a-decahydronaphtho[2,3-b][1,4,7,10,13]pentaoxacyclopentadecane (TNCT), respectively (Scheme 3.15). Monomers were obtained by the purification of the reaction products by column chromatography product in order to get rid of residual tin residues and by products. The final monomer product was abbreviated as ENCE that represent EDOT-Naptho-Crown-EDOT configuration and TNCT which represent Thiophene-Naptho-Crown-Thiophene.



**Scheme 3.15** Synthetic routes for ENCE and TNCT

The structural elucidations of the monomers were done with NMR techniques. Resonance of aromatic protons on the naphthalene was observed at 7.80-7.77 and 7.33-7.36 as doublet of doublet. Chemical shifts of the protons on thiophene appeared at 7.51 ppm and 7.15 ppm as doublet for a and b protons, 7.20 ppm as triplet for b. Protons on the crown ether resonated at 4.1 and 3.7 as multiplets.  $^{13}\text{C}$ -NMR of TNCT also shows resonance of 13 different carbon atoms which is equal to the different number of carbon atoms present in TNCT structure (Figure 3.5).

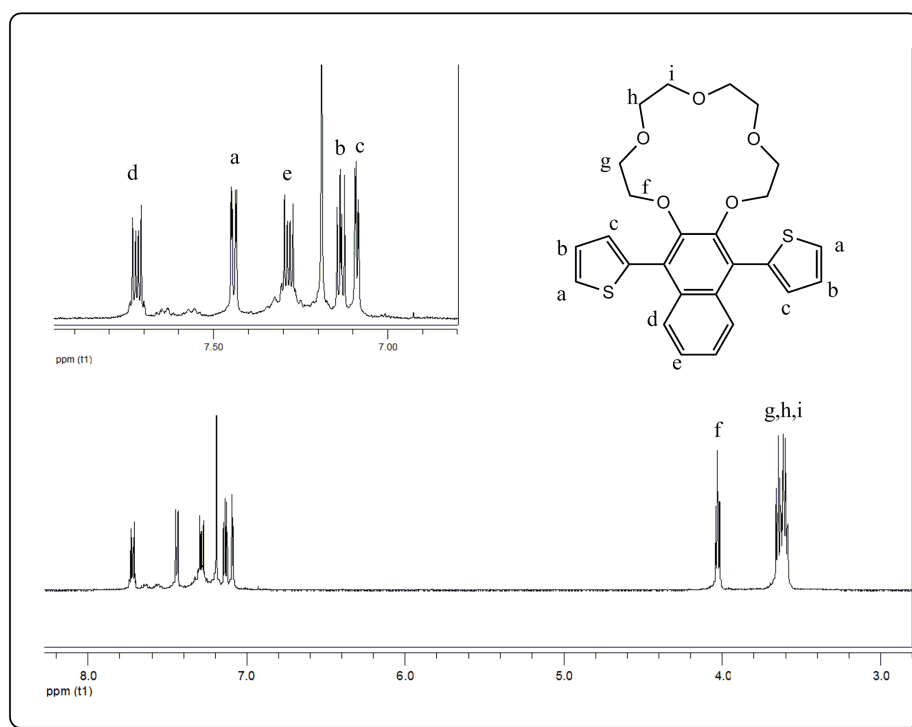


**Figure 3.5**  $^1\text{H}$ -NMR spectrum of TNCT

ENCE was also characterized by NMR technique. Resonance of aromatic protons on the naphthalene was observed at 8.22-8.25 and 7.57-7.53 as doublet of doublet. Chemical shifts of the proton on the EDOT appeared at 6.55 ppm as singlet. Protons

on the ethylenedioxy group of EDOT resonated at 4.15 and 4.15 as triplets. <sup>13</sup>C-NMR of TNCT also showed resonance of 15 different carbon atoms which is equal to the different number of carbon atoms present in ENCE structure.

### 3.3 Electrochemical Characterization of Benzotriazole Containing Polymers

BBTES, BBTEA, BBTS and BBTA monomers, containing benzylated benzotriazole as central unit, were terminated with thiophene or EDOT which has 2- or 5- positions available for the polymerization. Therefore, these monomers were all oxidatively polymerized to yield redox active polymers on ITO working electrode.

#### 3.3.1 Cyclic Voltammetry

The redox behaviors of BBTES, BBTEA, BBTS and BBTA were examined using the repeated potential scan voltammetry on indium tin oxide (ITO) coated glass electrode in the same electrolytic medium containing 0.1 M tetrabutylammonium hexafluorophosphate (TBAPF<sub>6</sub>)/ ACN:DCM acetonitrile:dichloromethane (95:5) solution. The ACN and DCM solvent mixture was used due to poor solubility of monomers in ACN.

Figure 3.6 and Figure 3.7 show the cyclic voltammograms (CV) of BBTES and BBTEA which were scanned between -0.5 V and 1.0 V and between -0.2 V and 1.4 V respectively at a scan rate of 100 mV/s.

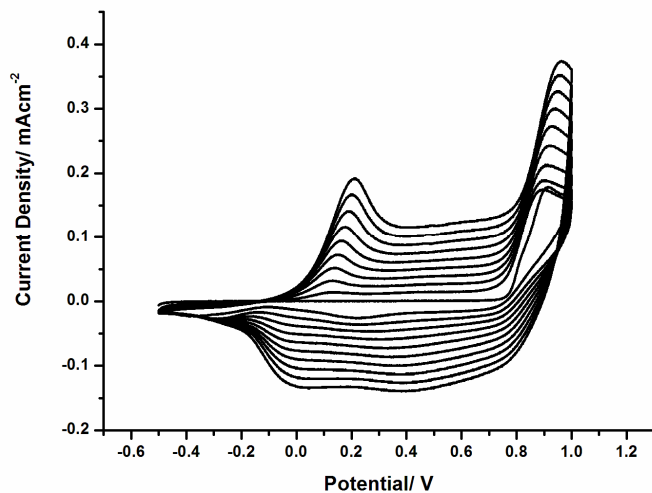


**Figure 3.6** The cyclic voltammogram of the BBTES between -0.5 to +1.0 V at 100 mVs<sup>-1</sup> in 0.1 M TBAPF<sub>6</sub>/CH<sub>2</sub>Cl<sub>2</sub> /ACN on an ITO electrode

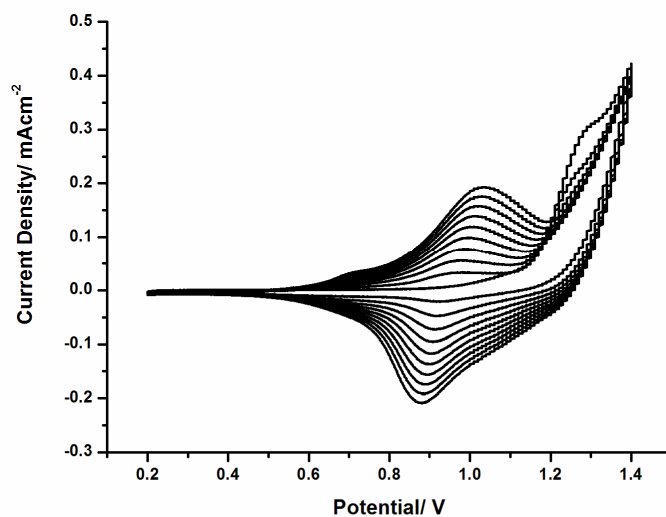
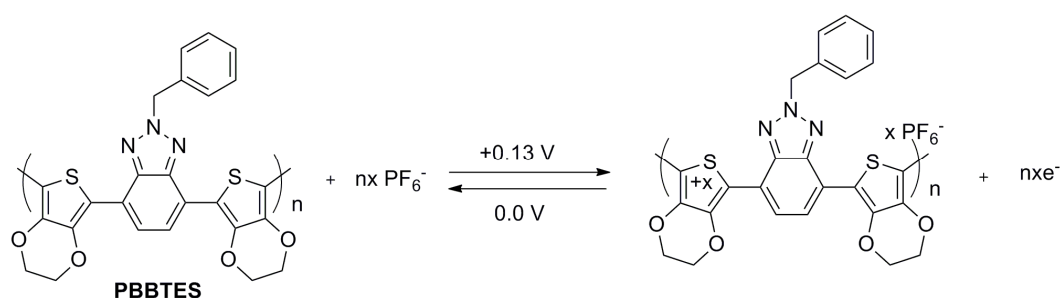


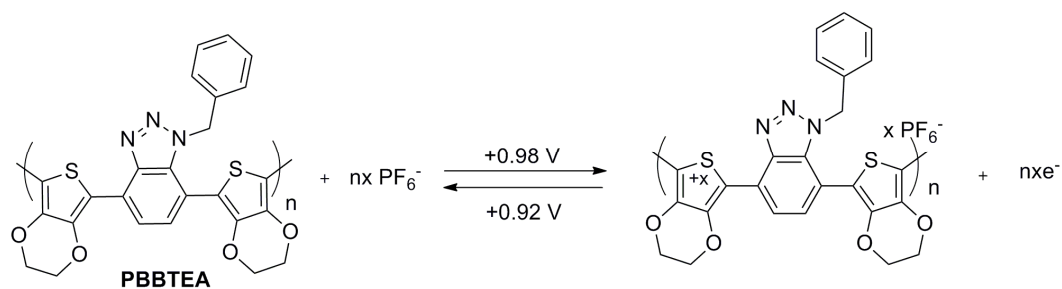
**Figure 3.7** The cyclic voltammogram of the BBTEA between 0.2 to +1.4 V at 100 mVs<sup>-1</sup> in 0.1 M TBAPF<sub>6</sub>/CH<sub>2</sub>Cl<sub>2</sub> /ACN on an ITO electrode.

BBTES exhibited a broad oxidation peak at 0.92 V indicating the irreversible oxidation of the monomer. Upon repeated scanning, formation of a new redox couple associated with the oxidation and reduction of the polymer growth onto the electrode surface was observed. Oxidation peak at 0.13 V and a reversible reduction peak at around 0.0 V were developed for the polymer (Scheme 3.16).



**Scheme 3.16** p-doping of PBBTES

In the cyclic voltammetry studies of BBTEA, monomer oxidation peak was observed at 1.25 V during the first anodic sweep indicating the radical cation formation. After the monomer oxidation, oligomers were formed and finally the polymer film was deposited on the ITO electrode. The reversible redox couple observed in the second cycle proves the formation of oligomers. Moreover, the increase in the current density of oxidation/ reduction peaks exhibits the generation of the electroactive conducting polymer on the ITO electrode surface. The broad oxidation and reduction peaks were observed at 0.98 V and 0.92 V versus Ag wire pseudo-reference electrode, respectively (Scheme 3.17). The potential difference between the polymer oxidation and reduction values was determined as 0.06 V which reveals that the redox couple corresponds to reversible one-electron transfer during redox process for PBBTEA.



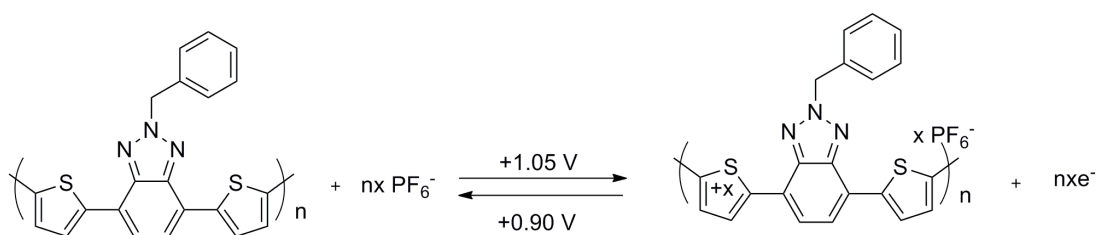
**Scheme 3.17** p-doping of PBBTEA

The shape of cyclic voltammogram of BBTEA was drastically different from the curve obtained for BBTES since change of benzylation position on benzotriazole ring alters the electronic structures of the resultant monomers and polymers. The oxidation potential of BBTES was lower than that of BBTEA measured under the described conditions indicating that the HOMO level of BBTES is higher than that of BBTEA. This hypothesis was also supported by the band gap values obtained from spectroelectrochemical data of PBBTES and PBBTEA (Section 3.3.2).

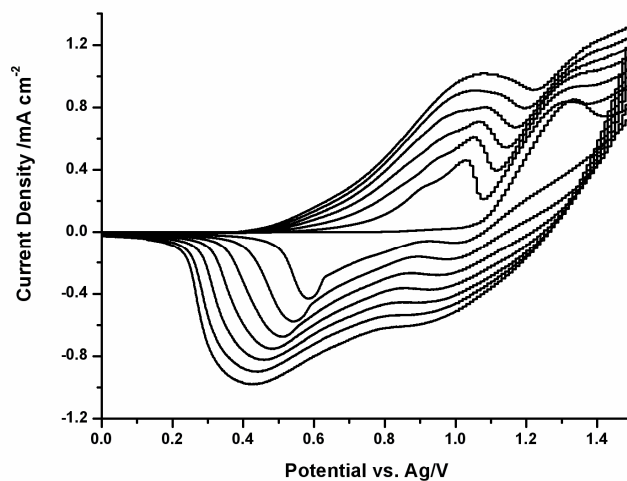
In order to determine redox reactions during electrochemical polymerization and film deposition, monomers; BBTS and BBTA were initially subjected to cyclic voltammetry in the same electrolytic medium described for BBTES and BBTEA.

Figure 3.8 shows typical cyclic voltammogram recorded during continuously applied cyclic scans for BBTS. In the first cycle, BBTS exhibited an irreversible monomer oxidation at 1.33 V versus Ag wire pseudo-reference electrode. After the first run, reversible redox peaks were evolved at 1.0 V and 0.6 V and the anodic and cathodic currents were increased as a result of regular growth of PBBTS on ITO electrode.

The resulting polymer PBBTS was oxidized and reduced reversibly at 1.05 V and 0.9 V, respectively in a monomer free solution (Scheme 3.18). Single scan cyclic voltammetry of PBBTS in monomer free 0.1 M TBAPF<sub>6</sub>/ACN solution showed that PBBTS was also n-type dopable (Figure 3.9) when the polymer was cycled between negative potentials. The n-type doping property was determined for PBBTS with a reversible couple at -2.02 V and -1.21 V versus Ag wire reference electrode.



**Scheme 3.18** p-doping of PBBTS



**Figure 3.8** The cyclic voltammogram of the BBTS between 0.0 to +1.5 V at 100 mVs<sup>-1</sup> in 0.1 M TBAPF<sub>6</sub>/CH<sub>2</sub>Cl<sub>2</sub> /ACN on an ITO electrode

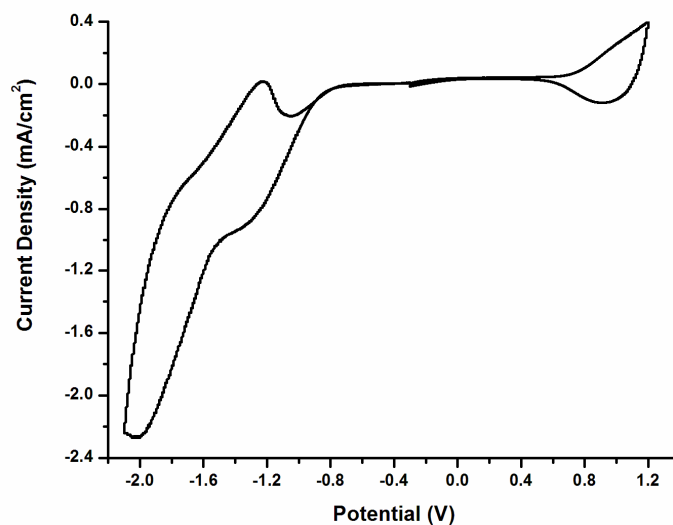
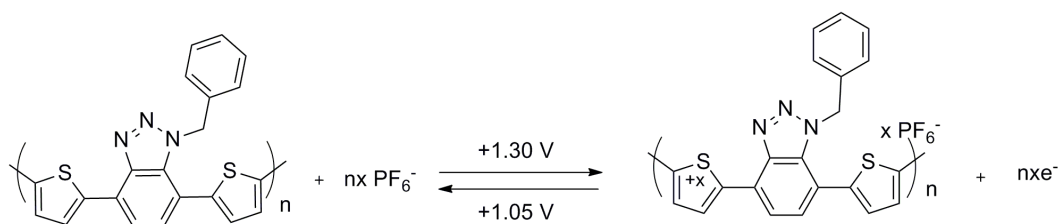


**Figure 3.9** Single scan cyclic voltammogram of PBBTS films between 1.2 V and -2.1 V using ACN as the solvent and TBAPF<sub>6</sub> as supporting electrolyte at a scan rate of 100 mV/s.

Cyclic voltammetry of BBTS led to the formation of the corresponding polymer PBBTS, whereas BBTA did not form well adhered film on ITO even continuous scans were applied (Figure 3.10a). Only the monomer oxidation peak was observed at 1.5 V and the formed oligomers dissolved in the electrolytic medium, thus the current measured during consecutive cycles did not increase. Therefore, BBTA was polymerized at 1.5 V constant potential vs. the same reference electrode where the homogenous film formation took place on ITO.

After synthesis of PBBTA, the p-doping electrochemistry was probed by oxidative cycling of the polymer film between +0.5 V and +1.65 V in a monomer free environment (Figure 3.10b). PBBTA has a broad oxidation peak at 1.30 V and a clear reduction peak at 1.05 V (Scheme 3.19).



**Scheme 3.19** p-doping of PBBTA

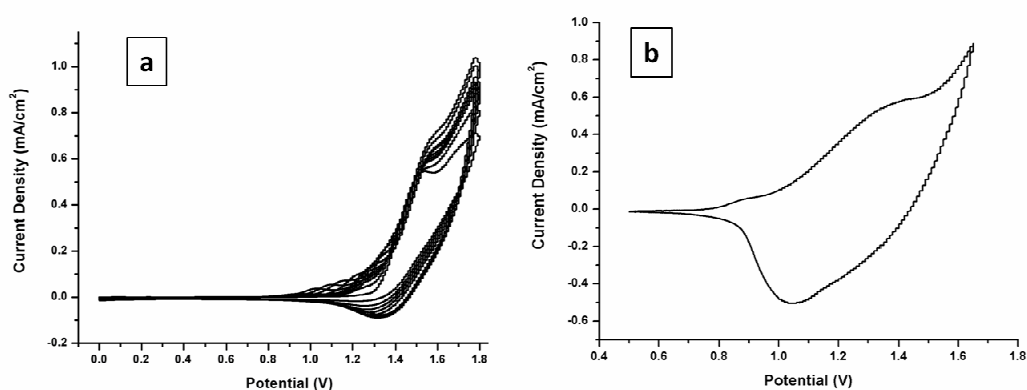


**Figure 3.10** a) The cyclic voltammogram of the BBTA between -0.3 to +1.7 V at 100  $\text{mVs}^{-1}$  in 0.1 M TBAPF<sub>6</sub>/CH<sub>2</sub>Cl<sub>2</sub> /ACN on an ITO electrode b) Single scan cyclic voltammogram of PBBTA film between 0.5 V and 1.65 V at 100  $\text{mVs}^{-1}$  in 0.1 M TBAPF<sub>6</sub>/ACN on an ITO electrode

PBBTS and PBBTES have lower oxidation potentials compared to PBBTA and PBBTEA. From these electrochemical data, it was interpreted that the nature of the central unit has major effect on the oxidation and reduction potentials of the resultant polymers. Changing the benzylation position from 1- to 2- position significantly lowers the oxidation potential. Moreover, the electron-rich character for the donor groups follows the trend EDOT > thiophene as evidenced by the oxidation potentials of the monomer and polymers.

The benzotriazole group in PBBTS was substituted from the 2- position and in literature, 2-substituted triazole ring is known as an electron-accepting unit. Therefore, electron density on PBBTS chain is lower compared to PBBTA and it is eager to take an electron, in other words to get reduced and n-type doped. When PBBTES and PBBTEA were concerned, electron donor ethylene dioxy groups increased the electron density on the polymer chains and PBBTES and PBBTEA become electron compared thiophene containing polymer PBBTA and PBBTS. These differences explain why PBBTS is an n-type dopable polymer while others not.

According to modified Randles-Sevcik equation, there exists a linear relationship between the peak current and the scan rate when the redox process is a non-diffusion controlled redox process. Therefore, polymers PBBTES, PBBTEA, PBBTS and PBBTA were cycled between their redox potential ranges in the monomer free electrolytic medium containing 0.1 M TBAPF<sub>6</sub>.

The scan rate dependence of the polymer films were shown in Figure 3.11 and Figure 3.12. A linear relationship between the peak current and the scan rate designates that the electroactive polymer films were well adhered on ITO electrode and the redox processes were non-diffusion controlled [119].

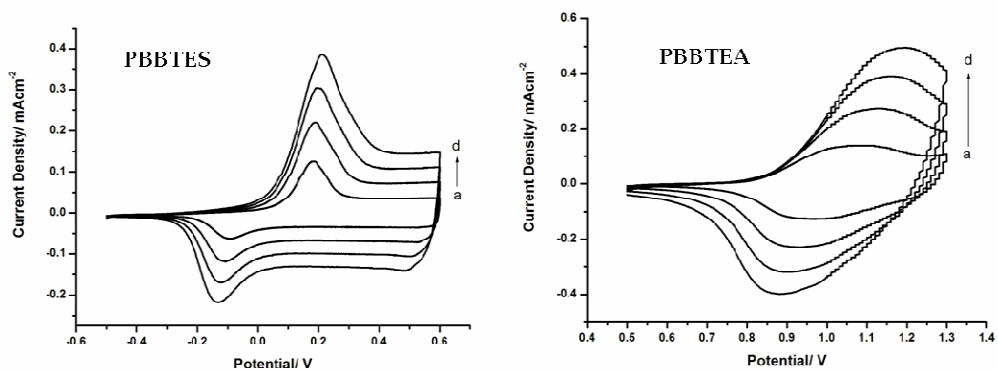


**Figure 3.11** Scan rate dependencies of BBTES and BBTEA at a)50 b) 100 c) 150 d) 200 mV/s in 0.1 M TBAPF<sub>6</sub>/CH<sub>2</sub>Cl<sub>2</sub> /ACN on an ITO electrode.

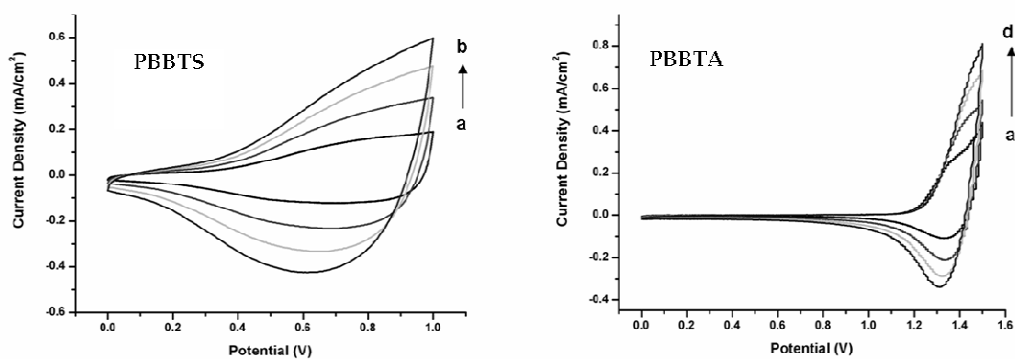


**Figure 3.12** Scan rate dependencies of BBTA and BBTS at a)50 b) 100 c) 150 d) 200 mV/s in 0.1 M TBAPF<sub>6</sub>/CH<sub>2</sub>Cl<sub>2</sub> /ACN on an ITO electrode.

### 3.3.2 Spectroelectrochemistry of Benzotriazole Containing Polymers

Spectroelectrochemical studies of the PBBTES and PBBTEA polymers were carried out by sweeping the potentials from -0.5 V to 0.8 V and 0.0 V to 1.2 V in a monomer free 0.1 M TBAPF<sub>6</sub> / ACN solution. The wavelength, at which a polymer shows  $\pi$ - $\pi^*$  transition, is defined as the maximum wavelength ( $\lambda_{\text{max}}$ ) which was at 625 nm for the PBBTES and 477 nm for the BBTEA. The band gap ( $E_g$ ) values for PBBTES and PBBTEA were calculated as 1.48 and 1.57 eV from the onset of their lowest energy transition, respectively.

Upon p-type doping, the absorption in the visible region at 625 nm started to decrease for PBBTES and new bands were intensified at around 900 nm and 1800 nm due to the formation of charge carriers on the polymer backbone (Figure 3.13) . When 0.3 V was applied to PBBTES, a sharp absorption increase in the near-IR region was observed due to the oxidation of the polymer film. It is common in literature that DAD type polymers usually reveal two  $\pi$ - $\pi^*$  transitions in the visible region. However, PPBTES showed only one transition in this region which is similar to its benzotriazole containing counterparts owing to dominant donor characteristic of the EDOT moiety. [115]

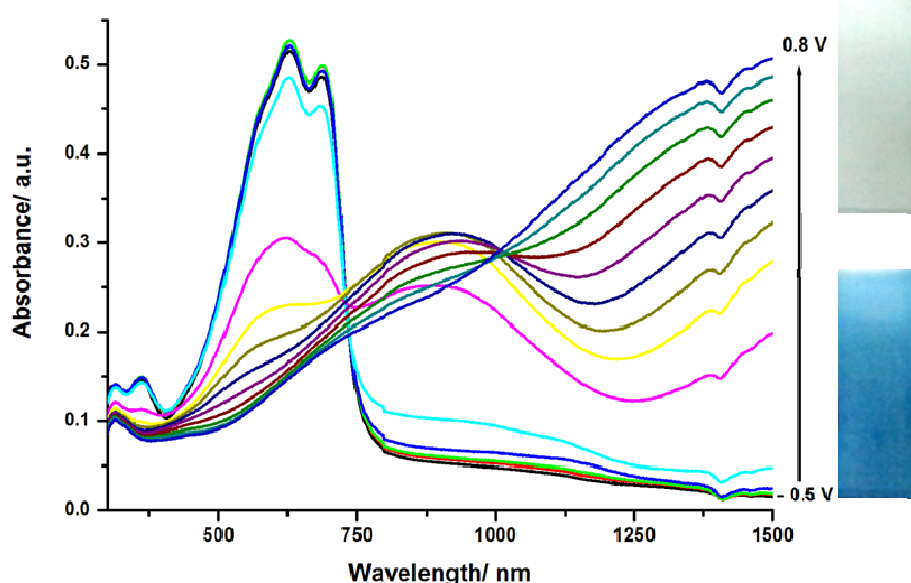


**Figure 3.13** Spectroelectrochemistry of PBBTES film on an ITO coated glass slide in monomer-free, 0.1 M TBAPF<sub>6</sub>/ACN electrolyte-solvent couple at applied potentials (V) a) -0.5 b) -0.4 c) -0.3 d) -0.2 e) -0.1 f) 0.0 g) 0.1 h) 0.2 i) 0.3 j) 0.4 k) 0.5 l) 0.6 m) 0.7 n) 0.8.

At 0.0 V, PBBTEA was in its neutral form and exhibited an absorption peak at 477 nm due to  $\pi$ - $\pi^*$  transition. As the applied potential increased, polaron charge carriers were formed with similar absorption value at 540 nm and a broad absorption at about 1200 nm, corresponding to formation bipolaron charges, was generated (Figure 3.14). The brown color of the film at the neutral state, turned into the gray at highly oxidized state. The absorption wavelength of polaron charge carriers were observed to be very close to neutral state absorption wavelength. The benzyl substitution at 1-position of benzotriazole unit induced a strong interaction between the benzyl substituent and the polymer chain. The enhanced possibility of  $\pi$  interaction between the 1-positioned benzyl unit and the polymer backbone resulted in the steric hinderance and restricted the rotation of benzyl substituent.

Thus, the injection and ejection of the counter ions upon oxidation became less favorable and the charges were trapped in the PBBTEA film.

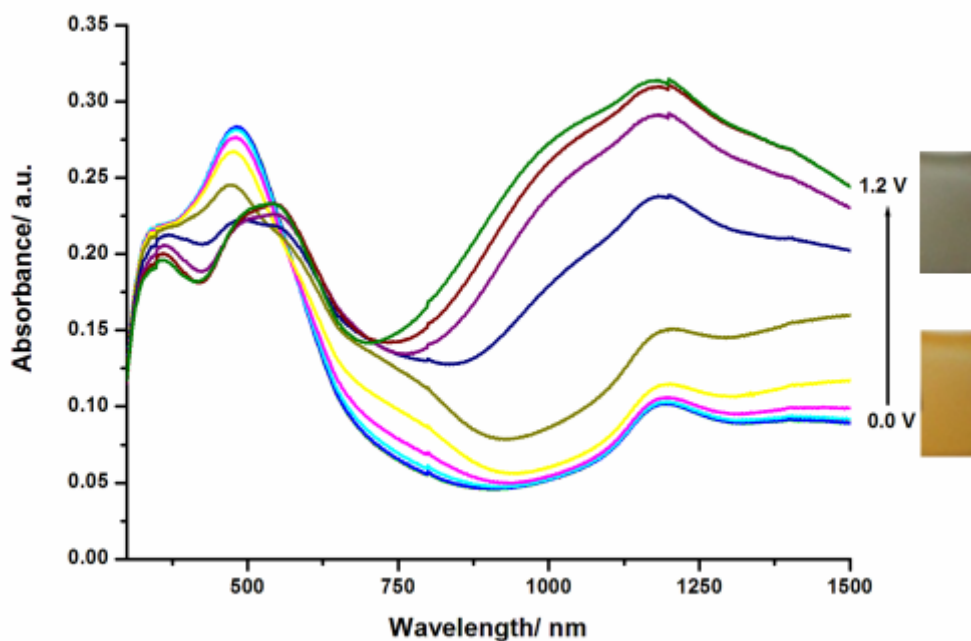


**Figure 3.14** Spectroelectrochemistry of PBBTEA film on an ITO coated glass slide in monomer-free, 0.1 M TBAPF<sub>6</sub>/ACN electrolyte-solvent couple at applied potentials (V) a) 0.0 b)0.1 c)0.2 d)0.3 e)0.4 f)0.5 g)0.6 h)0.7 i)0.8 j)0.9 k)1.0 l)1.1 m)1.2.

In order to observe the polymer characteristics upon applied external bias, spectroelectrochemistry studies of PBBTS and PBBTA were performed in a monomer free 0.1 M TBAPF<sub>6</sub> solution.

Spectroelectrochemistry of PBBTS showed  $\lambda_{\text{max}}$  at 504 nm which corresponds to red color for the neutral polymer. As the potential was increased gradually, new

electronic transitions progressively intensified at 685 nm owing to the formation of charge carriers such as polarons. Since these transitions was lying in the visible region of the electromagnetic spectrum, PBBTS showed multicolored states in its intermediate doping levels. Red color of the polymer film turned into purple and than gray upon oxidation. Moreover, further oxidation of PBBTS resulted in blue color due to increased absorption at 685 nm together with a diminished neutral state absorption. Compared to previously reported polymer PTBT [115], green color was not detected for PBBTS in its partially oxidized forms since the absorptions were not distinct at around 500 and 680 nm, which is essential for a green color. Band gap of PBBTS was determined as 1.55 eV from the onset value of lowest energy transition (Figure 3.15).

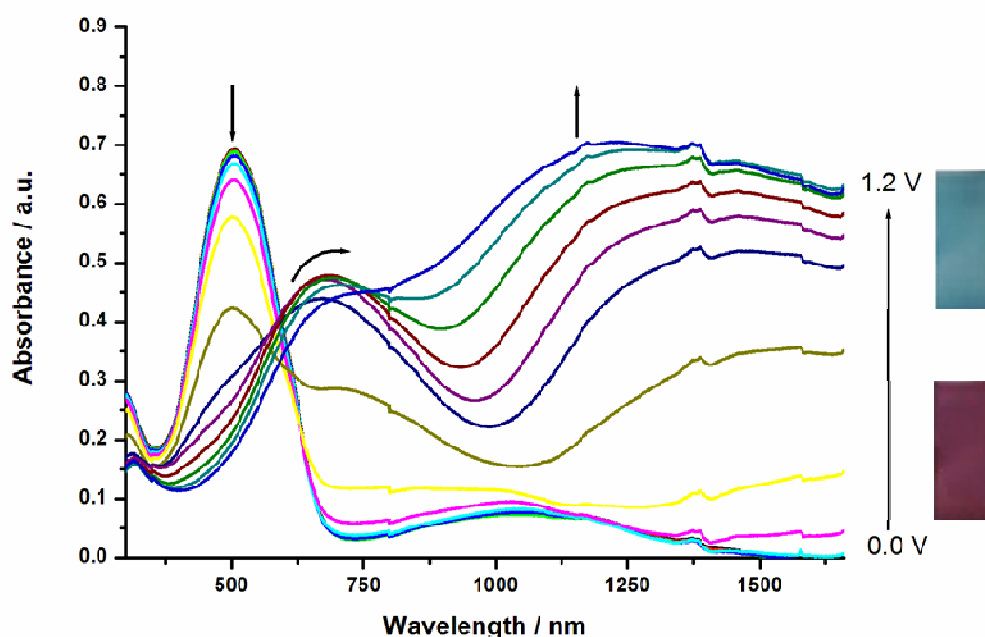


**Figure 3.15** Spectroelectrochemistry of PBBTS film on an ITO coated glass slide in monomer-free, 0.1 M TBAPF<sub>6</sub>/ACN electrolyte-solvent couple at applied potentials (V) a) 0.0 b) 0.1 c) 0.2 d) 0.3 e) 0.4 f) 0.5 g) 0.6 h) 0.7 i) 0.8 j) 0.9 k) 1.0 l) 1.1 m) 1.2.

The optical change that occurs during the n-doping of the polymer was examined to prove formation of charge carries on conjugated polymer chain (Figure 3.16). The reductive absorption spectrum of PBBTS was recorded between 0.0 V and at -2.05 V, which is the cathodic potential of the redox couple observed in the reduced state. The red colored neutral polymer turned in to brown upon reduction. Blue and gray colors were observed consecutively upon further reduction. PBBTS showed three different reduced state colors and turned back to its original neutral state color when compensated. This clearly confirms that the negative charge formation is taking place on the polymer backbone and n-doping process is reversible.

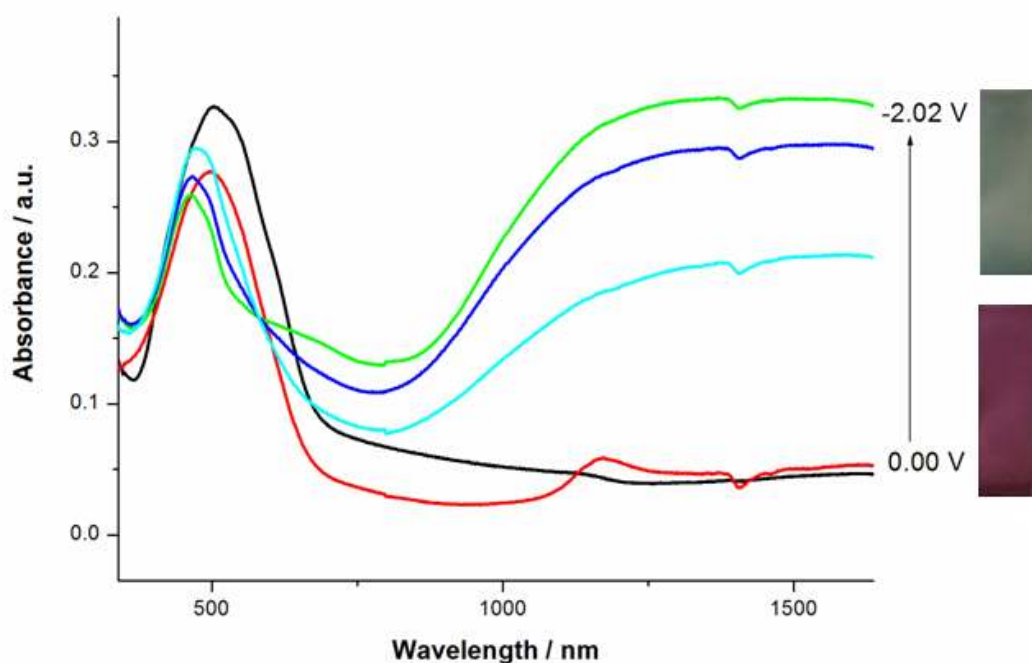


**Figure 3.16** n-Doping spectroelectrochemistry of PBBTS at applied potentials (V) a) 0.0 b) -1.65 c) -1.7 d) -1.8 e) -2.02.

The in-situ spectroelectrochemistry of PBBTA was performed between +0.5 V and +1.45 V in a monomer free ACN/0.1 M TBAPF<sub>6</sub> solution. The  $\lambda_{\max}$  for the  $\pi$ - $\pi^*$  transition in neutral state was found to be 390 nm and the electronic band gap ( $E_g$ ) was calculated as 2.25 eV from the onset potential for the neutral film at 551 nm. Although the maximum absorption was not totally in the visible region, since absorbance tails into 450 nm, PBBTA revealed yellow color in its neutral state. Upon step-wise oxidation, the intensity of absorptions corresponding to charge carriers simultaneously increased and observed at around 640 nm and 1230 nm for polarons and bipolarons, respectively (Figure 3.17). Formation of new electronic states on PBBTA altered its color from yellow to gray. For this polymer, the increase in the NIR region was not as high as the symmetric PBBTS. Since benzyl unit was placed to 1-position of benzotriazole unit, there exists a steric hindrance for counter-ion injection and increased the possibility of  $\pi$  interaction between pendant groups and the polymer backbone. Thus, the insertion of dopant ions to the polymer structure upon oxidation became less preferred.

Higher band gap and blue shifted absorptions of PBBTA compared to PBBTS suggested that the effective conjugation length is shorter in PBBTA than that of PBBTS [120]. Same trend was observed when PBBTES and PBBTEA were concerned; the lower band gap and absorption at higher wavelength indicated the higher conjugation length of PBBTES with respect to PBBTEA.

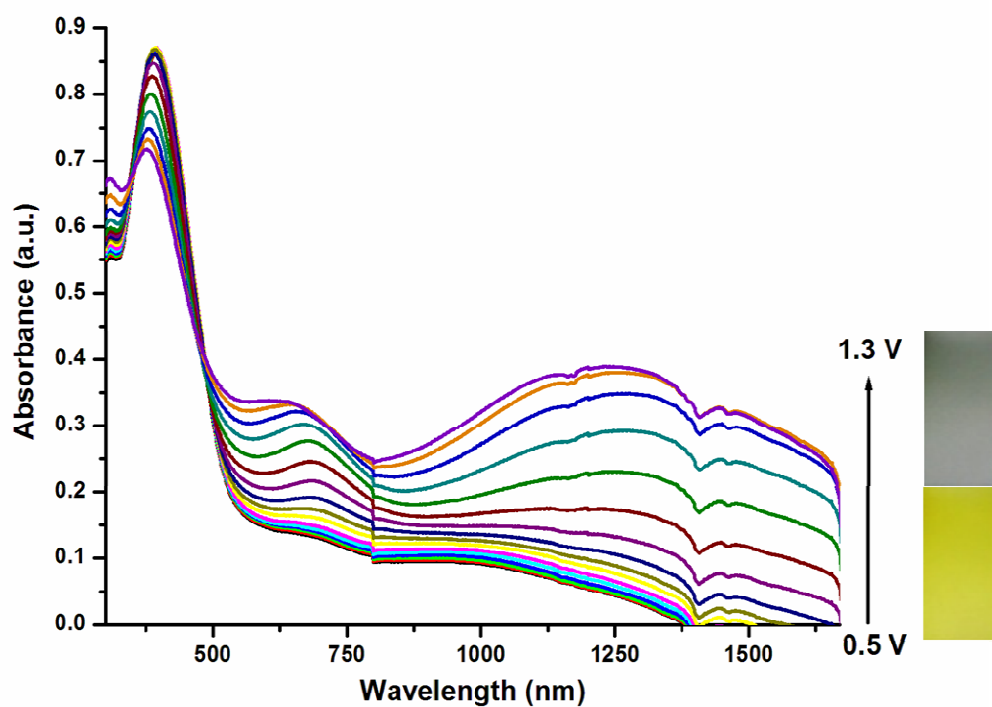


**Figure 3.17** Spectroelectrochemistry of PBBTA film on an ITO coated glass slide in monomer-free, 0.1 M TBAPF<sub>6</sub>/ACN electrolyte-solvent couple at applied potentials and corresponding colors observed at neutral and doped states.

Furthermore, keeping the central benzotiazole unit constant, change of the donor unit from thiophene to EDOT decreases the band gap due to higher donor capability of EDOT compared to thiophene. Hence, the electronic band gap energy of PBBTEA and PBBTES are lower compared to the PBBTA and PBBTS.

### 3.3.3 Kinetic Studies

Electrochromic switching studies were carried out in order to monitor the percent transmittance changes as a function of time and to calculate the switching times of the polymers at their maximum absorptions ( $\lambda_{\text{max}}$ ) by stepping potentials repeatedly between their fully neutral and oxidized states within 5 s time intervals. The switching time is calculated from the kinetic studies to determine the time required for switching between oxidized and neutral states.

PBBTES was stepped between its neutral (-0.5 V) and oxidized (+0.8 V) states to reveal a percent transmittance of 32 % at 625 nm and 56% at 1800 nm, with 0.4 s and 1 s switching times, respectively. (Figure 3.18, Table 3.1). The kinetic studies for PBBTEA cannot be performed since the stable reversible oxidation/reduction of the polymer film could not be achieved due to the difficulty of charge injection/ejection processes. Moreover, as it also shown in spectroelectrochemistry study of BBTES; the absorption wavelength of neutral and oxidized forms of PBBTEA overlap, therefore no change in percent transmittance of polymer was expected during kinetic studies.

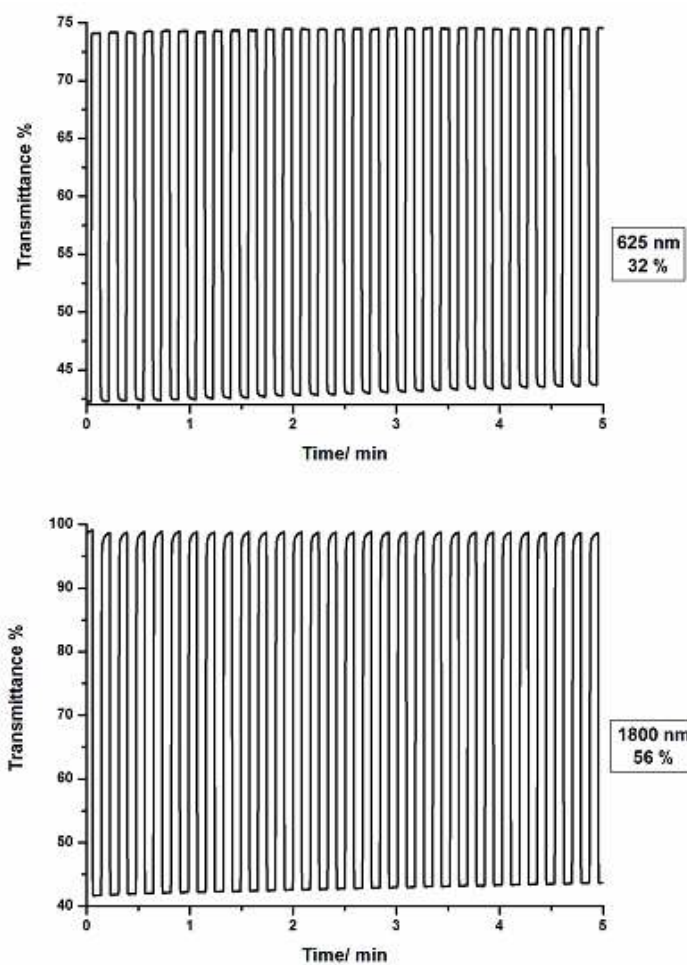


**Figure 3.18** Switching time and  $\Delta T\%$  change monitored at 625 and 1800 nm for PBBTES in 0.1 M TBAPF<sub>6</sub>/ACN.

Table 3.1 Optical contrast and switching times for PBBTES<sup>a</sup>

$\lambda$	625 nm	1800 nm
Optical contrast	32%	56%
Switching Time	0.4 sec	1.0 sec

<sup>a</sup> Switched between -0.5 and 0.8V

At its dominant wavelength in the visible region (504 nm), PBBTS showed 44% percent transmittance change (Table 3.2, Figure 3.19). Contrary to PBBTS, PBBTA had no worthy difference in percent transmittances since the PBBTA film could not be reduced and oxidized successively due to the difficulty in charge injection/ejection processes similar to PBBTEA. In NIR region PBBTS and PBBTA revealed 73 % (1225 nm) and 38 % (1300 nm) transmittance which are significant for electrochromic materials to be used for NIR applications (Table 3.3, Figure 3.20) [121,122]. Optical stabilities of the polymers were reasonable since PBBTS loses 5 % of its original contrast whereas PBBTA loses ca. 8 % of the initial contrast upon consecutive 30 full switches taking into account that the experiment was performed at atmospheric conditions.

In addition to percent transmittance changes of electrochromic materials upon doping/dedoping processes, how quickly these materials change their colors and achieve full contrast is also important issue. Considering that the PBBTS is a multicolored electrochromic material, PBBTS showed notable switching properties in visible region. The switching times at 504 nm and 1225 nm were calculated as 0.6 s and 1.2 s for PBBTS which refer to four different color transitions within that period. For PBBTA, the switching time was recorded as 0.9 s at 1300 nm.

**Table 3.2** Optical contrast and switching times for PBBTS<sup>a</sup>

$\lambda$	504 nm	1225 nm
Optical contrast	44%	73%
Switching Time	0.6 sec	1.2 sec

<sup>a</sup> Switched between 0.0 and 1.2 V

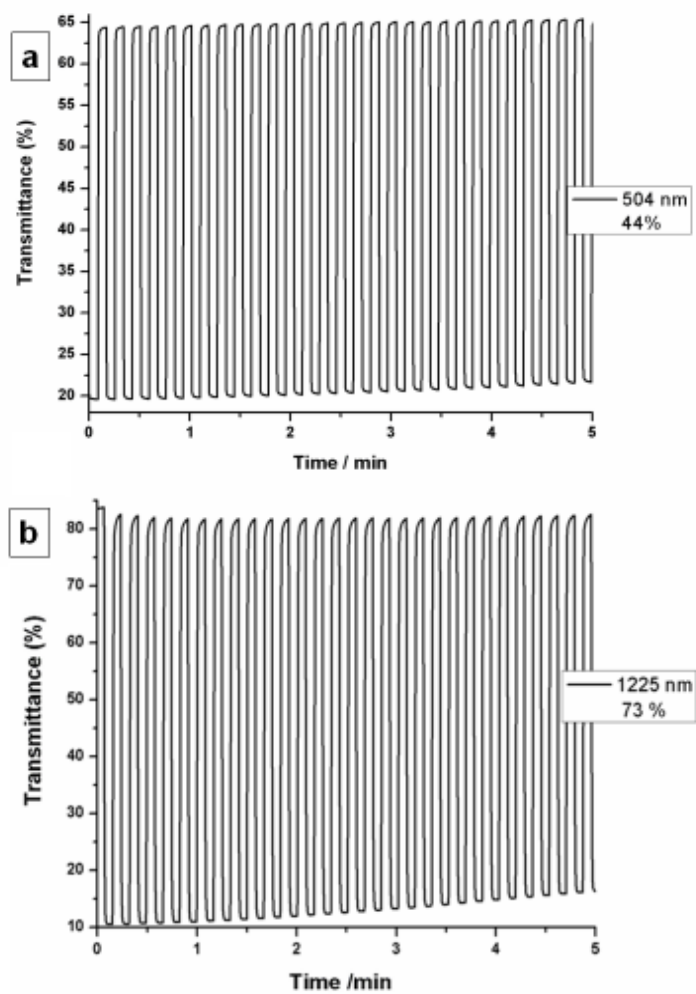


**Figure 3.19**  $\Delta T\%$  change monitored at a) 504 nm and b) 1225 nm for PBBTS in 0.1 M TBAPF<sub>6</sub>/ACN.

**Table 3.3** Optical contrast and switching times for PBBTA

$\lambda$	1300 nm
Optical contrast	38%
Switching Time	0.9 sec

<sup>a</sup> Switched between 0.5 and 1.45 V

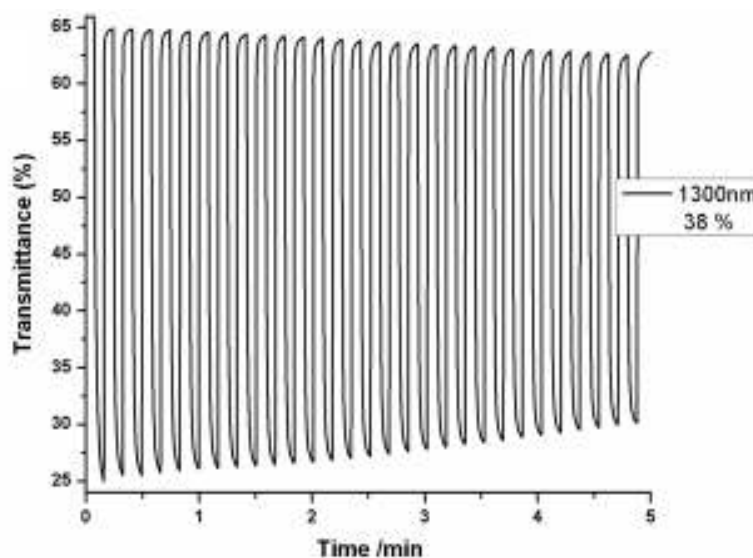


**Figure 3.20**  $\Delta T\%$  change monitored at 1225 nm and 1300 nm for PBBTS and PBBTA in 0.1 M TBAPF<sub>6</sub>/ACN, respectively.

### 3.3.4 Colorimetry Studies

Colorimetry studies were performed to identify the L,a,b coordinates for the PBBTES and PBBTEA polymers at different electrochemical states. The PBBTES was blue at highly reduced (-0.5 V) and light blue at highly oxidized states (+0.8 V). The PBBTEA was orange in its neutral form while the color turned into gray when oxidized. The colors and L, a, b values of the polymers were given in Table 3.4 for PBBTES and PBBTES.

Colorimetry analysis of p-doped PBBTS was performed to identify the color changes observed upon oxidation; the polymer is red at the reduced state (0.0 V), blue at the oxidized state (+1.2 V) with two intermediate states; gray (+0.4 V) and purple (+0.90 V). When the PBBTS was n-type doped, the polymer switches between brown (-1.7 V), blue (-1.8 V) and gray (-2.0 V) colors. The L, a and b values of colors were given

Table 3.5 together with the observed colors. The most important property of PBBTS is that it shows multicolored charged states during n-doping process. Normally both p and n type dopable polymers tend to have multicolored states however, these kind of polymers are rather rare.

The absorption of neutral PBBTA at 390 nm reveals yellow color in its neutral state, and with the application of +1.05 V, PBBTA was partially oxidized and at this voltage color of polymer was green. PBBTS exhibited gray color at highly oxidized state at 1.30 V. Table 3.6 shows L, a, b values of the PBBTS film in neutral, intermediate and oxidized states.

**Table 3.4** Colors of the PBBTES and PBBTEA at their neutral and oxidized states

<i>P(BBTES)</i>		<i>P(BBTEA)</i>	
Blue (-0.5 V)	Light Blue (+0.8 V)	Orange (0.0 V)	Gray (+1.2 V)
			
L= 50.1 a= 0.98 b= -42.3	L= 80.4 a= 0.48 b= 12.6	L= 80.6 a= 11.6 b= 80.4	L= 42.3 a= -1.95 b= 13.5

**Table 3.5** Colors of p-type and n-type doped PBBTS

<i>P(BBTS)</i>						
n-type doped			Neutral	p-type doped		
Gray (-2.0 V)	Blue (-1.8 V)	Brown (-1.7 V)	Red (0.0 V)	Purple (0.4 V)	Gray (0.9 V)	Blue (1.2 V)
						
L= 45.8 a= 4.78 b= 2.49	L= 51 a= -14.35 b= 1.20	L= 45.8 a= 5.66 b= 11.77	L= 26.62 a= 32.04 b= -4.79	L= 40 a= 17.50 b= -5.63	L= 40 a= -2.137 b= 1.45	L= 50.95 a= -13.61 b= -12.2

**Table 3.6** Colors of the PBBTA at their neutral and oxidized states

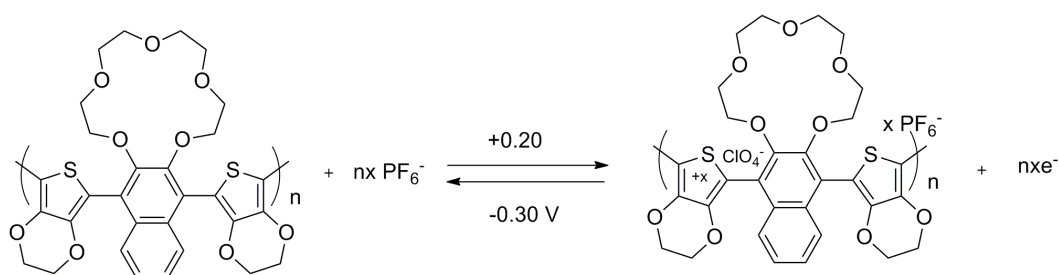
<i>P(BBTA)</i>		
Yellow (0.0 V)	Green (1.05 V)	Gray (1.30 V)
		
L= 80.04 a= -17.08 b= 44.88	L= 63.84 a= -12.76 b= 21.0	L= 50.95 a= -8.29 b= 7.20

### 3.4 Electrochemical Characterization of Naphthelene-2,3-Crown Ether Functionalized Monomers and Polymers

#### 3.4.1 Cyclic Voltammetry

Homopolymer of ENCE which is abbreviated as PENCE was achieved by electrochemical techniques. The monomer was polymerized by potentiodynamic method in the presence of 0.1 M TBAPF<sub>6</sub> as the supporting electrolyte in acetonitrile-dichloromethane (CH<sub>2</sub>Cl<sub>2</sub> :CH<sub>3</sub>CN) solvent couple in 5:95 volume % ratios with 100 mVs<sup>-1</sup> scan rate between -0.5 V and +1.0 V.

The first run of the experiment revealed the oxidation of monomer at 0.9 V in reference to Ag wire electrode. Upon sequential scanning cycles between -0.5 V and +1.0 V, the oxidation and reduction peaks belong to oligomers were observed. The decrease in the peak current at 0.9 V which indicates consumption of the monomer and the increase in the peak currents at +0.18 V and -0.3 V, which are the oxidation and reduction potentials respectively, exhibited the formation of polymer film on ITO electrode (Scheme 3.20).



Scheme 3.20 p-doping of PENCE

Although EDOT terminated crown ether derivative ENCE was polymerized by CV (potentiodynamic) method, thiophene terminated monomer TNCT could not be polymerized with the same method. As reflected in the CV (Figure 3.21), voltammogram of the monomer exhibited an irreversible electroactivity at 1.15 V.

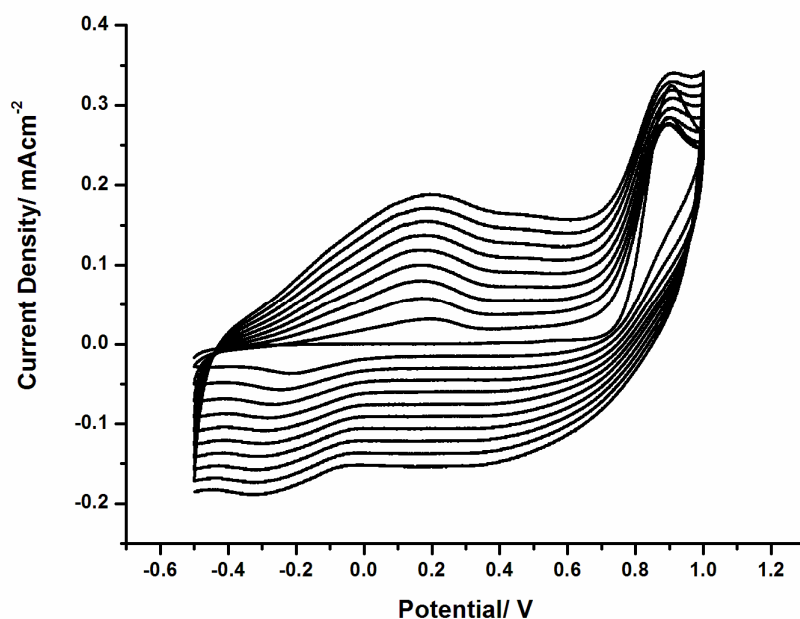


**Figure 3.21** Cyclic Voltammogram of PENCE in the presence of 0.1 M tetrabutyl ammonium hexafluorophosphate (TBAPF<sub>6</sub>) as the supporting electrolyte in acetonitrile-dichloromethane (CH<sub>2</sub>Cl<sub>2</sub> :CH<sub>3</sub>CN) solvent couple in 5:95 volume % ratios with 100 mVs<sup>-1</sup> scan rate between -0.5 V and +1.0 V.

Highly colored bluish oligomeric products were formed after the first cycle which did not adhere to the ITO electrode surface and leaked into the solution even at high monomer concentrations (Figure 3.22). In the case of the ENCE almost no coloring of the electrolyte was observed. These observations for electrochemical behaviors of

ENCE and TNCT were ascribed to the steric influence of the ether moieties which hinder formation of radical cations due to repulsion. The steric interaction of the crown ether moiety with the neighboring thiophene rings led to a decreased electronic coupling, which was caused by a simultaneously reduced conjugation of the lone pairs of the oxygens with the adjacent thiophene ring and their twisting relative to each other. Similarly, in literature, there are some other examples of crown ether functionalized monomers which can not be polymerized, and this is attributed to the conformational flexibility of crown ether substituent's to prevent polymerization. [106,123].

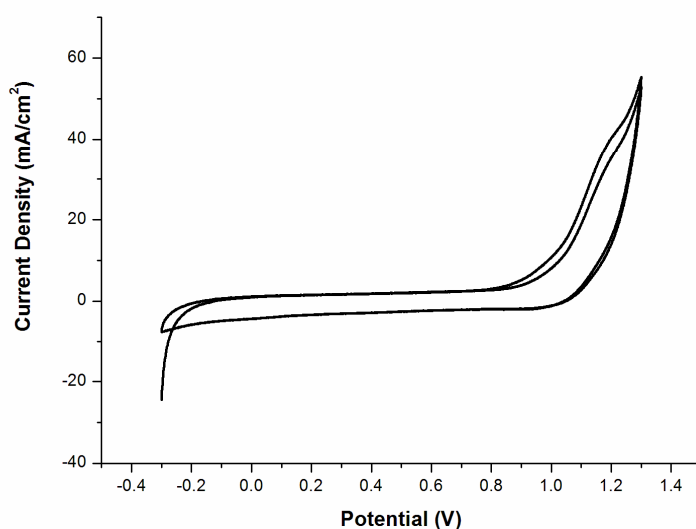


**Figure 3.22** Cyclic Voltammogram of TNCT in the presence of 0.1 M tetrabutyl ammonium hexafluorophosphate (TBAPF<sub>6</sub>) as the supporting electrolyte in acetonitrile-dichloromethane (CH<sub>2</sub>Cl<sub>2</sub> :CH<sub>3</sub>CN) solvent couple in 5:95 volume % ratios with 100 mVs<sup>-1</sup> scan rate between -0.3 V and +1.3 V.

Only electrochemical behavior of PENCE was investigated since PTNCT could not be electrochemically polymerized for further experiments. Cyclic voltammetry experiments of PENCE were performed in the presence of different supporting electrolytes such as NaClO<sub>4</sub> and LiClO<sub>4</sub> by keeping the solvent fixed in order to observe the effect of Na<sup>+</sup> and Li<sup>+</sup> cations on the electrochemical behavior crown ether functionalized polymer PENCE.

The polymer synthesized in the presence of TBAPF<sub>6</sub> supporting electrolyte was first taken into monomer free ACN solution containing 0.1 M NaClO<sub>4</sub> supporting electrolyte and the polymer was cycled between -0.8 V and +0.6 V vs Ag wire. It was observed that PENCE exhibited similar oxidation-reduction behavior to one in TPAPF<sub>6</sub> medium when NaClO<sub>4</sub> exist in electrolytic medium. This result indicates PENCE was insensitive to Na<sup>+</sup> cation.

Whereas PENCE was practically insensitive to presence of Na<sup>+</sup> cations, the CV of PENCE showed a large positive shift of oxidation potential when the experiment was repeated in the presence of LiClO<sub>4</sub>.

Moreover, as it was shown in the CV (Figure 3.23), the current density continuously increased when polymer was reduced. This behavior indicated that the polymer could not be reduced easily because the diffusion layer on electrode still contain high concentration of dopant ions and the process shown below could not be achieved reversibly by cyclic voltammetry. In order to fully reduce and regenerate the neutral state of the polymer, PENCE needs to be reduced by applying constant potential at -0.8 V.

The general trend for sensing of various 15-crown-5 containing monomers were reported as Na<sup>+</sup> > Li<sup>+</sup> in solution. However, the smaller size of Li<sup>+</sup> ion enabled it to

penetrate easily to polymer film and therefore induced a more pronounced change in the electrochemical behavior [106].

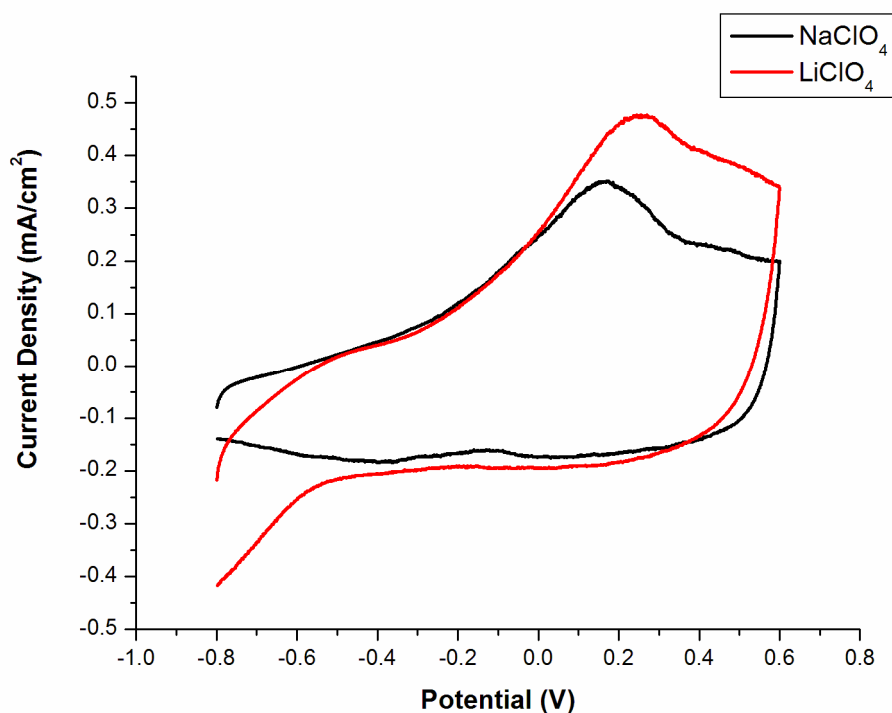
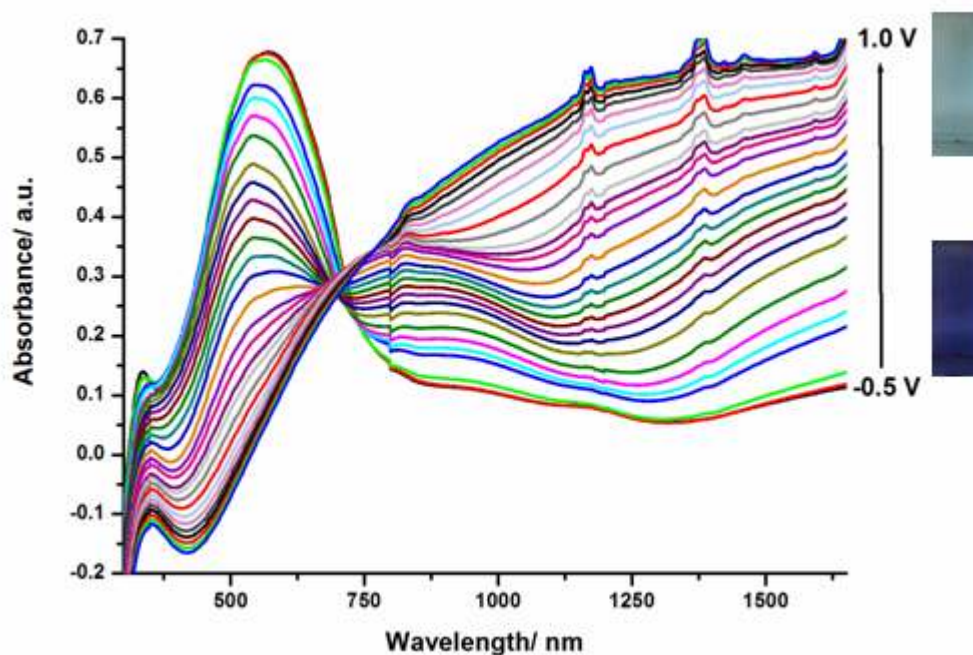


**Figure 3.23** Comparison of PENCE cyclic voltammogram in the presence of  $\text{LiClO}_4$  and  $\text{NaClO}_4$

### 3.4.2 Spectroelectrochemical Properties of PENCE

In order to examine the alteration in optical properties of PENCE, spectroelectrochemical studies were performed by UV-Vis-NIR Spectrophotometer. This experiment provided information on intergap states that appear upon doping and the band gap energy ( $E_g$ ).

PENCE coated on ITO electrode were swept between -0.5 V and +1.0 V in a monomer free 0.1 M TBAPF<sub>6</sub>/ACN electrolyte-solvent couple. The maximum wavelength ( $\lambda_{\text{max}}$ ) for the  $\pi$ - $\pi^*$  transition in neutral state at -0.5 V was found to be 567 nm and the electronic band gap ( $E_g$ ) was calculated as 1.42 eV by inserting the onset wavelength in de-Broglie equation. (Figure 3.24). The intensity of absorbance at the  $\pi$ - $\pi^*$  transition decreased as the polymer gets oxidized, and polaron and bipolaron charge carrier bands at 840 nm and 1390 nm longer wavelengths increased in intensity, respectively. The spectroelectrochemical studies revealed the presence of isosbestic point which indicates the conversion of neutral state to polaronic state is reversible and there is a charge equilibrium rearrangements taking place within the polaronic state.



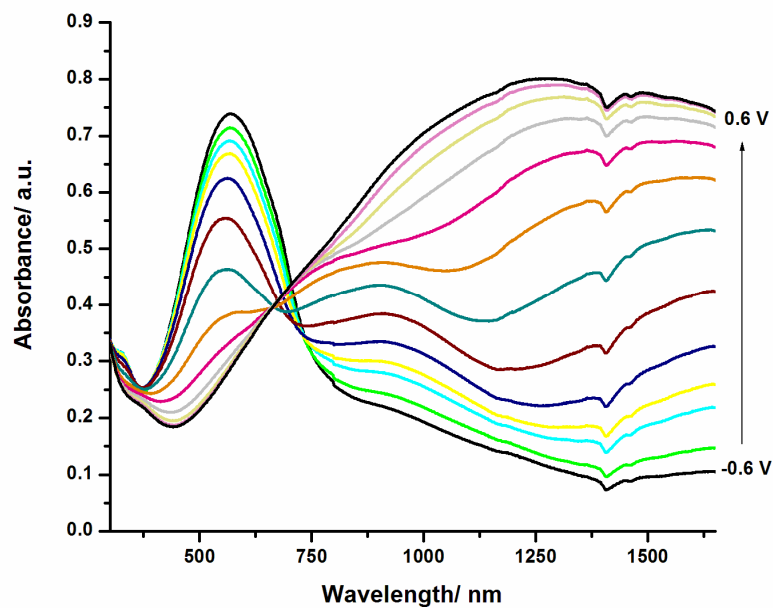
**Figure 3.24** Spectroelectrochemical spectrum of PENCE at 0.1 M TBAPF<sub>6</sub>/ACN electrolyte-solvent couple with applied potentials between -0.5 V and +1.0 V

Figure 3.25 and Figure 3.26 represent the spectroelectrochemical studies of PENCE in the presence of 0.1 M NaClO<sub>4</sub>/ACN and 0.1 M LiClO<sub>4</sub>/ACN supporting electrolyte-solvent systems. The  $\lambda_{\max}$  value of the polymer, when NaClO<sub>4</sub> was used as the supporting electrolyte, was found as 567 nm which is almost the same wavelength measured for TBAPF<sub>6</sub>. Use of LiClO<sub>4</sub> as the supporting electrolyte shifted  $\lambda_{\max}$  value to 563 nm indicating the interaction of Li<sup>+</sup> ions with the oxygen of crown ethers. This interaction diminished the electron donating effect of these oxygens, thus blue shift in  $\lambda_{\max}$  was observed together with an increase in the band gap. Spectroelectrochemical data also support the cyclic voltammetry data where anodic potential shifted to higher potentials due to decrease in electron donating effect.

The band gaps of PENCE in the presence of NaClO<sub>4</sub> and LiClO<sub>4</sub> were calculated as 1.45 eV and 1.48 eV, respectively. Higher band gap energy was due to blue shift in the  $\lambda_{\max}$  value and the  $E_g$  was calculated as 1.45 eV. The values obtained from the spectroelectrochemical experiments are given in Table 3.7.

**Table 3.7** Spectroelectrochemical properties of PENCE.

Supporting Electrolyte	$E_g$ (eV)	$\lambda_{\max}$
TBAPF <sub>6</sub>	1.42	567 nm
NaClO <sub>4</sub>	1.45	567 nm
LiClO <sub>4</sub>	1.48	563 nm



**Figure 3.25** Spectroelectrochemical spectrum of PENCE at 0.1 M NaClO<sub>4</sub>/ACN electrolyte-solvent couple with applied potentials between -0.5 V and +0.6 V

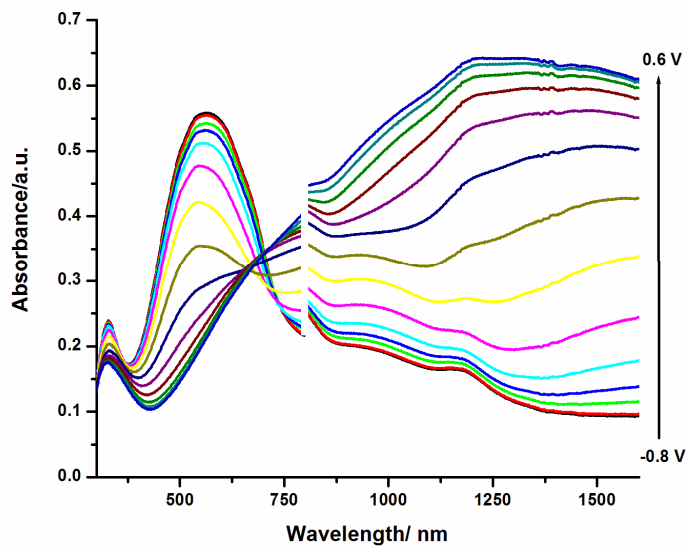


**Figure 3.26** Spectroelectrochemical spectrum of PENCE at 0.1 M LiClO<sub>4</sub> /ACN electrolyte-solvent couple with applied potentials between -0.8 V and +0.6 V

### 3.4.3 Kinetic Studies

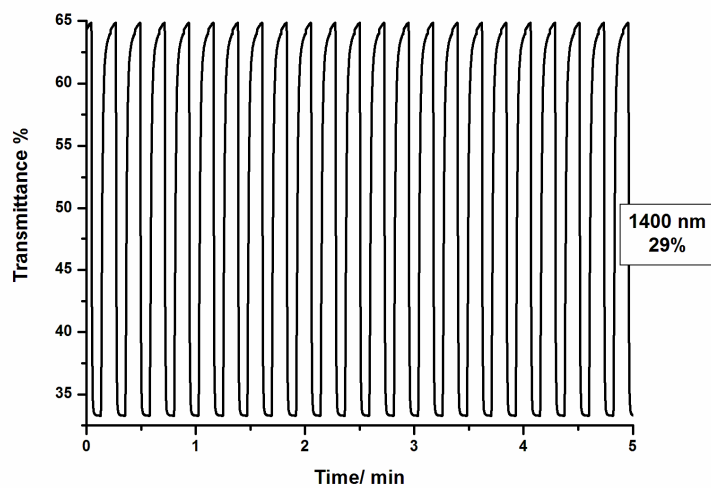
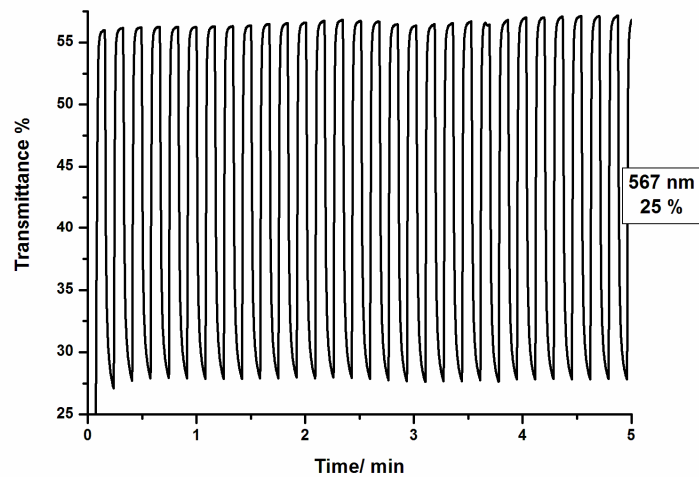
In order to investigate electrochromic switching time and percent transmittance of polymers, PENCE was coated on ITO electrode in the presence of TBAPF<sub>6</sub> electrolyte and switched between its neutral and doped states at a fixed wavelength. Experiments were carried out at 567 nm and 1400 nm via switching the potential between -0.5 V and +0.7 V with a residence time of 5 seconds. 567 nm was selected since it is the  $\lambda_{\text{max}}$  value where the PENCE is in neutral form and 1400 nm was selected owing to its high intensity at near-IR region. Optical contrasts at 565 nm and 1400 nm were found to be 25 % and 29 % respectively. The switching times, the time elapsed between the highest and lowest transmittance values, were calculated as 1.3 and 2.3 seconds at 565 nm and 1400 nm (Figure 3.27, Table 3.8).

Since the lithium ion interacts with oxygen in the crown ether moiety, consecutive oxidation and reduction of polymer therefore kinetic studies could not be achieved successfully for PENCE in LiClO<sub>4</sub>.

**Table 3.8** Optical contrast and switching times for PENCE<sup>a</sup>

$\lambda$	567 nm	1400 nm
Optical contrast	25%	29%
Switching Time	1.3 sec	2.3 sec

<sup>a</sup> Switched between -0.5 V and +0.7 V

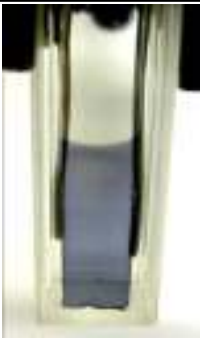


**Figure 3.27** Electrochromic switching, optical absorbance change monitored at 567 nm and 1400 nm for PENCE between -0.5 V and +0.7 V.

### 3.4.4 Colorimetry Studies

The colors observed in neutral, partially and fully doped states of P(ENCE) were determined by the colorimetry studies and they were defined in terms of luminance (L), hue (a) and saturation (b) values. P(ENCE) has indigo color at highly reduced - 0.5 V, gray at partially doped intermediate state at -0.1 V and light blue at 0.2 V. The L, a ,b values of the P(ENCE) is given in Table 3.9.

**Table 3.9** Colors of PENCE at neutral, partially and fully doped states.

<i>P(ENCE)</i>		
<b>Indigo (-0.50 V)</b>	<b>Gray (-0.10 V)</b>	<b>Blue (0.20 V)</b>
		
L= 43.6 a= 41.0 b= -65.0	L= 68.9 a= 6.1 b= -24.5	L = 77.9 a= 3.4 b= -28.4

## CHAPTER 4

### CONCLUSION

Electron deficient benzotriazole group benzylated from either 1- or 2- position was terminated with electron rich thiophene or EDOT groups by Stille coupling method to obtain four different monomers (BBTS, BBTA, BBTES, BBTEA). Experiments on their corresponding polymers (PBBTES, PBBTEA, PBBTS, PBBTA) showed that the functionalization provided different electrochemical and optoelectronic properties. PBBTS was distinguished from other polymers since it was found as multichromic at both p- and n-type doped states which is a rare property for electrochromics.

All studies confirmed that substitution of benzyl pendant group from 2- position of benzotriazole resulted in better properties such as lower oxidation potentials, higher percent transmittance changes, faster switching times and repetitive doping/dedoping processes for polymers. Changing the acceptor group from 2-benzylbenzotriazole to 1-benzylbenzotriazole central unit significantly raised the oxidation potential and optical band gap of polymers which indicates the shortening of conjugation length on polymer chains. Furthermore, keeping the central unit constant, while changing electron donation group from thiophene to EDOT also affected the oxidation potentials and band gap values. When EDOT was used as the donor unit, oxidation potential and band gap values of resultant polymer PBBTES and PBBTS were found as lower than those of PBBTEA and PBBTA. This result was in accordance with the expected trend since presence

electron rich ethylene dioxy bridges on EDOT lowers band gap and provides ease of oxidation compared to thiophene.

EDOT and thiophene terminated naphthalene-2,3-crown ether containing monomers, ENCE and TNCT, were synthesized with Stille coupling to observe the effect of crown ether moiety on the final electrochemical and optoelectronic properties of resultant polymers. Homopolymerization of TNCT could not be achieved by potentiodynamic methods due to conformational flexibility of crown ether substituent's to prevent polymerization. On the other hand, ENCE was polymerized by potentiodynamic method and the electrochemical and optoelectronic properties of its polymer PENCE coated on ITO electrode were investigated via cyclic voltammetry and spectroelectrochemistry techniques. PENCE was synthesized electrochemically in the presence of 0.1 M tetrabutyl ammonium hexafluorophosphate (TBAPF<sub>6</sub>) as the supporting electrolyte in acetonitrile. Further cyclic voltammetry experiments were performed in the presence of same solvent system but different supporting electrolytes such as NaClO<sub>4</sub> and LiClO<sub>4</sub> in order to observe the effect of Na<sup>+</sup> and Li<sup>+</sup> cations on the electrochemical behavior of PENCE. The polymer in the presence of TBAPF<sub>6</sub> and NaClO<sub>4</sub> exhibited similar oxidation-reduction behavior whereas shift to higher oxidation potential and increase on current density during polymer reduction was associated with interaction of crown ether with Li<sup>+</sup> ions.

Cyclic voltammetry revealed that the change in electrochemical properties of PENCE was due to a hindered diffusion of the Li<sup>+</sup> anions into the polymer film which is necessary for charge compensation when the PENCE is oxidized. Spectroelectrochemical studies also supported the Li<sup>+</sup> ion sensitivity with blue shift in maximum absorption wavelength. Blue shift was observed due to loss of electron donating effect of crown ether oxygens when they were in interaction with Li<sup>+</sup> ions.

In conclusion, electrochemical and optoelectronic properties of low band gap polymers can be altered by the change of donor acceptor units as well as the substitution site of pendant groups on polymer backbone. Crown ether containing conjugated polymers are strong candidates to be used as metal ion sensors by transducing sensitivity data to an electrical signal.

## REFERENCES

- [1] V.V. Walatka, M.M. Labes, J.H. Perlstein, *Phys. Rev. Lett.*, 31 (1973) 1139.
- [2] G.B. Street, W.D. Gill, R.H. Geiss, R.L. Greene, J.J. Mayerle, *J. Chem. Soc. Chem. Commun.*, (1977) 407a.
- [3] C.K. Chiang, M.J. Cohen, D.L. Peebles, A.J. Heeger, M. Akhtar, J. Kleppinger, A.G. MacDiarmid, J. Milliken, M.J. Moran, *Solid State Commun.*, 23 (1977) 607.
- [4] M. Akhtar, J. Kleppinger, A.G. MacDiarmid, J. Milliken, M.J. Moran, , C.K. Chiang, M.J. Cohen, A.J. Heeger, D.L. Peebles, *J. Chem. Soc. Chem. Commun.*, (1977) 473.
- [5] H. Shirakawa, E.J. Louis, A.G. MacDiarmid, C.K. Chiang, A.J. Heeger, *J. Chem. Soc. Chem. Commun.*, (1977) 578.
- [6] T.A. Skotheim, R.L. Elsenbaumer, J.R. Reynolds, *Handbook of Conducting Polymers*, 2nd ed.; Eds.; Marcel Dekker: New York, (1998) 197.
- [7] A.G. MacDiarmid, *Angew. Chem. Int. Ed.*, 40 (2001) 2581.
- [8] A.G. MacDiarmid, J.C. Chiang, A.F. Richter, A.J. Epstein, *Synth. Met.*, 18 (1987) 285.
- [9] A.F. Diaz, K.K. Kanazawa, G.P. Gardini, *J. Chem. Soc. Chem. Commun.*, (1979) 635.
- [10] M. Sato, S. Tanaka, K. Kaeriyama, *J. Chem. Soc. Chem. Commun.*, (1986) 873.
- [11] G. Heywang, F. Jonas, *Adv. Mater.*, 4 (1992) 116.
- [12] A. Desbene-Monvernay, P.C. Lacaze, J.E. Dubois, *J. Electroanal. Chem.*, 129 (1981) 229.
- [13] P.M. Beaujuge, W. Pisula, H.N. Tsao, S. Ellinger, K. Müllen, J.R. Reynolds, *J. Am. Chem. Soc.*, 131 (2009) 7514.

- [14] C.C. Chueh, M.H. Lai, J.H. Tsai, C.F. Wang, W.C. Chen, *J. Polym. Sci. Part A: Polym. Chem.*, 48 (2010) 74.
- [15] L.S. Hwang, J.M. Ko, H.W. Rhee, C.Y. Kim, *Synth. Met.*, 55 (1993) 3671.
- [16] J. Bobacka, *Anal. Chem.*, 71 (1999) 4932.
- [17] C.J. Tonzola, M.M. Alam, B.A. Bean, S.A. Jenekhe, *Macromolecules*, 37 (2004) 3554.
- [18] B. Winkler, F. Meghdadi, S. Tasch, R. Mtilner, R. Resel, R. Saf, G. Leising, F. Stelzer, *Optical Materials*, 9 (1998) 159.
- [19] A.P. Zoombelt, M. Fonrodona, M.G.R. Turbiez, M.M. Wienkab, R.A.J. Janssen, *J. Mater. Chem.*, 19 (2009) 5336.
- [20] Q. Zhang, A. Cirpan, T.P. Russell, T. Emrick, *Macromolecules*, 42 (2009) 1079.
- [21] L.J. Maa, Y.X. Li, X.F. Yu, Q.B. Yang, C.H. Noh, *Sol. Energy Mater. Sol. Cells*, 93 (2009) 564.
- [22] I. Schwendeman, R. Hickman, G. Sonmez, P. Schottland, K. Zong, D. M. Welsh, J.R. Reynolds, *Chem. Mater.*, 14 (2002) 3118.
- [23] R. Hoffmann, *Angew. Chem. Int. Ed.*, 26 (1987) 846.
- [24] J.L. Reddinger, J.R. Reynolds, *Advances in Polymer Science*, 145 (1999) 57.
- [25] K. Shimamura, F.E. Karasz, J.A.Hirsch, J.C. Chien, *Makromol. Chem. Rapid Commun.*, 2 (1981) 443.
- [26] U.Salzner, J.B. Lagowski, P.G. Pickup, R.A. Poirier, *Synth. Met.*, 96 (1998) 177.
- [27] M.G. Kanatzidis, *Chem. Eng. News*, 68 (1990) 36.
- [28] P. Chandrasekhar, *Conducting Polymers, Fundamentals and Applications: A Practical Approach*, Kluwer, Dordrecht, The Netherlands (1999)
- [29] S.N. Hoier, S.M. Park, *J.Phys.Chem*, 96 (1992) 5188.
- [30] J.A.A. Irvin PhD, Thesis, University of Florida, (1998).
- [31] A.J. Heeger, *J. Phys. Chem. B*, 105 (2001) 8475.
- [32] A.D. Child, J.R. Reynolds, *J. Chem. Soc., Chem. Commun*, (1991) 1779.

- [33] D.M. de Leeuw, M.M. J. Simenon, A.R. Brown, R.E.F. Einerhand, *Synth. Met.*, 87 (1997) 53.
- [34] C.J. DuBois, F. Larmat, D. J. Irvin, J.R. Reynolds, *Synth. Met.*, 119 (2001) 321.
- [35] C.J. DuBois, K.A. Abboud, J.R. Reynolds, *J. Phys. Chem. B*, 108 (2004) 8550.
- [36] C. J. DuBois, J. R. Reynolds, *Adv. Mater.*, 14 (2002) 1844.
- [37] P.J. Nigrey, A.G. MacDiarmid, A.J. Heeger, *J. Chem. Soc. Chem. Commun.*, (1979) 594.
- [38] C. K. Chiang, C. R. Fincher, Jr., Y. W. Park, A. J. Heeger, H. Shirakawa, E. J. Louis, S. C. Gau, and A. G. MacDiarmid, *Phys. Rev. Letters*, 39 (1977) 1098.
- [39] K. Gurunathan, A.V. Murugan, R. Marimuthu, U.P. Mulik, D.P. Amalnerkar, *Mater. Chem. Phys.*, 61 (1999) 173.
- [40] K.E. Ziemelis, A.T. Hussain, D.D.C. Bradley, R.H. Friend, J. Ruhe, G. Wegner, *Phys. Rev. Lett.*, 66 (1991) 2231.
- [41] A. J. Heeger, *Reviews of Modern Physics.*, 73 (2001) 681.
- [42] D. Kumar, R.C. Sharma, *Eur. Poly. J.*, 34 (1998) 1053.
- [43] M. E. G. Lyons, in *Electroactive Polymer Electrochemistry: Part I, Fundamentals*, ed. M. E. G. Lyons, Plenum Press, New York, (1994)
- [44] Y. Yamamoto, K. Sanechika, A. Yamamoto, *J. Polym. Sci. Polym.*, 18 (1980) 9.
- [45] A.N. Samukhin, V.N. Prigodin, L. Jastrabik, A.J. Epstein, *Phys. Rev. B.*, 58 (1998) 11354.
- [46] K. Yoshino, S. Hayashi, R. Sugimoto *Jpn. J. Appl. Phys. Part 2*, 23 (1984) 899.
- [47] A. Malinauskas, *Polymer* 42 (2001) 3957.
- [48] R.D. McCullough, R.D. Lowe, M. Jayaraman, D.I. Anderson, *J. Org. Chem.*, 58 (1993) 904.
- [49] G. Schopf, G. Koßmehl, *Adv. Polym. Sci.*, 129 (1997) 3.
- [50] J. Roncali, *Chem. Rev.*, 92 (1992) 711.
- [51] G. Zotti, *Handbook of Organic Conductive Molecules and Polymers*, ed. H. S. Nalwa, Wiley, Chichester, 1997, Vol. 2, Ch. 4.

- [52] J.R.Reynolds, S.G. Hsu, H.J. Arnott, *J. Polym. Sci. Pol.*, 27 (1989) 2081 4.
- [53] J.D. Strenger-Smith, *Prog. Polym. Sci.*, 23 (1998) 57.
- [54] C.A. Thomas, PhD Thesis, University of Florida, (2002).
- [55] R.M. Walczak, PhD Thesis, University of Florida, (2006).
- [56] J.P. Lowe, S.A. Kafafi, *J. Am. Chem. Soc.* 106 (1984) 5837.
- [57] F. Wudl, M. Kobayashi, A.J. Heeger, *J. Org. Chem.*, 49 (1984) 3381.
- [58] F. Wudl, M. Kobayashi, N. Colaneri, N. Boysel, A.J. Heeger, *J of Mol. Cry. Liq. Cry.*, 118 (1985) 195.
- [59] , M. Kobayashi, N. Colaneri, M. Boysel, F. Wudl, A.J. Heeger, *J. Chem Phys*, 82 (1985) 5717.
- [60] N. Colaneri, M. Kobayashi, A.J. Heeger, F. Wudl, *Synth. Met.*,14 (1986) 45.
- [61] H. Yashima, M. Kobayashi, K.B. Lee, D. Chung, A.J. Heeger, F. Wudl, *J. of Electrochem. Soc.*,134 (1987) 46.
- [62] S.M. Dale, A. Glide, A.R. Hillman, *J. Mater. Chem*, 2 (1992) 99.
- [63] J.L. Bredas, A.J. Heeger, F.Wudl, *J. Chem. Phys.*, 85 (1986) 4673.
- [64] M. Pomerantz, B. Chaloner-Gill, L.O. Harding, J.J. Tseng, W.J. Pomerantz, *Synth. Met.*,55 (1993) 960 .
- [65] K. Nayak, D.S. Marynick, *Macromolecules*, 23 (1990) 2237.
- [66] G. King, S.J. Higgins, *J. Chem. Commun.*, (1994) 825.
- [67] L. Goris, M.A. Loi, A. Cravino, H. Neugebauer, N.S. Sariciftci, I. Polec, L. Lutsen, E. Andries, J. Manca, L. De Schepper, D. Vanderzande, *Synth. Met.*,138 (2003) 249.
- [68] B. Liu, W.L. Yu, Y.H. Lai, W. Huang, *Chem. Mater.*, 13 (2001) 1984.
- [69] G. Tourillon, F. Garnier, *J. Electroanal. Chem.* ,135 (1982) 173.
- [70] C.A. Thomas, K. Zong, K. A. Abboud, P.J. Steel, J.R. Reynolds, *J. Am. Chem. Soc.*, 126 (2004) 16440.
- [71] G.G. Wallace, G.M. Spinks, L.A.P. Kane-Maguire, P.R. Teasdale, *Conductive Electroactive Polymers*, CRC Press, New York, (2003), Ch.2, 51.

- [72] G. Horowitz, *Adv. Mater*, 10 (1998) 365.
- [73] G. Inzelt, M. Pineri, J.W. Schultze, M.A. Vorotyntsev, *Electrochim. Acta*, 45 (2000) 2403.
- [74] J.W. Schultze, H. Karabulut, *Electrochim. Acta*, 50 (2005) 1739.
- [75] C.G. Granqvist, *Electrochim. Acta*, 44 (1999) 3005.
- [76] Q.T. Zhang, J.M. Tour, *J. Am Chem. Soc.*, 119 (1997) 5065.
- [77] N.R. de Tacconi, K. Rajeshwar, R.O. Lezna, *Chem. Mater.*, 15 (2003) 3046.
- [78] L.D. Burke, T.A.M. Twomey, D.P. Whelan, *J. Electroanal. Chem.*, 107 (1980) 201.
- [79] D.N. Buckley, L.D. Burke, *J. Chem. Soc. Farad. T. 1*, 71 (1975) 1447.
- [80] D.N. Buckley, L.D. Burke, J.K. Mulcahy, *J. Chem. Soc. Farad. T. 1*, 72 (1976) 1896.
- [81] L.D. Burke, E.J.M. Osullivan, *J. Electroanal. Chem.*, 93 (1978) 11.
- [82] L.D. Burke, D.P. Whelan, *J. Electroanal. Chem.*, 103 (1979) 179.
- [83] Ilsup Jin, University of California Los Angeles, (2005).
- [84] G. Sönmez, *Chem Commun.*, 42 (2005) 5251.
- [85] A.A. Argun, P.H. Aubert, B.C. Thompson, I. Schwendeman, C.L. Gaupp, J. Hwang, N.J. Pinto, D.B. Tanner, A.G. MacDiarmid, J.R. Reynolds, *Chem. Mater.*, 16 (2004) 4401.
- [86] G.A. Sotzing, J.L. Reddinger, A.R. Katritzky, J. Soloducho, R. Musgrave, J.R. Reynolds, *Chem. Mater.*, 9 (1997) 1578.
- [87] F. Wang, M.S. Wilson, R.D. Rauh, P. Schottland, B.C. Thompson, J.R. Reynolds, *Macromolecules*, 33 (2000) 2083.
- [88] G.A. Sotzing, J.R. Reynolds, P.J. Steel, *Chem. Mater.*, 8 (1996) 882.
- [89] C.J. DuBois, K.A. Abboud, J.R. Reynolds, *J. Phys. Chem. B.*, 108 (2004) 8550.
- [90] B. Reeves, PhD Thesis, University of Florida, (2005).
- [91] A.G. Jones, PhD Thesis, University of Florida, (2007).
- [92] R.J. Mortimer, A.L. Dyer, J.R. Reynolds, *Displays*, 27 (2006) 2.

- [93] R. Walker, *Corrosion*, 29 (1973) 290.
- [94] G.K. Gomma, *Mater. Chem. Phys.*, 56 (1998) 27.
- [95] R. Ravichandran, S. Nanjundan, N. Rajendran, *Appl. Surf. Sci.*, 236 (2004) 241.
- [96] A. Tanimoto, T. Yamamoto, *Macromolecules*, 39 (10) (2006) 3546.
- [97] A. Tanimoto, T. Yamamoto, *Adv. Synth. Catal.*, 346 (2004) 1818.
- [98] A. Durmus, G.E. Gunbas, P. Camurlu, L. Toppare., *Chem Commun.*, (2007) 3246.
- [99] A. Cihaner, F. Algi, *Adv. Funct. Mater.*, 18 (2008) 3583.
- [100] A. Balan, G. Gunbas, A. Durmus, L. Toppare, *Chem. Mater.*, 20 (2008) 7510.
- [101] A. Balan, D. Baran, G. Gunbas, A. Durmus, F. Ozyurt, L. Toppare, *Chem. Commun.*, (2009) 6768.
- [102] M.A. Rahman, P. Kumar, D.S. Park, Y.B. Shim, *Sensors*, 8 (2008) 118.
- [103] C.J. Pedersen, *J. Am. Chem. Soc.*, 89 (1967) 7017.
- [104] M.J. Marsella, T. M. Swager, *J. Am. Chem. Soc.*, 115 (1993) 12214.
- [105] K. Sugiyasu, T.M. Swager *Bull. Chem. Soc. Jpn.*, 80 (2007) 2074.
- [106] P. Bauerle, S. Scheib, *Acta. Polym.*, 46 (1995) 124.
- [107] S.S. Zhu, T.M. Swager., *J. Am. Chem. Soc.*, 119 (1997) 12568.
- [108] S. Ellinger, U. Ziener, U. Thewalt, K. Landfester, M. Moller *Chem. Mater.*, 19 (2007) 1070.
- [109] B.A. Da Silveria Neto, A.L. Sant'Ana, G. Ebeling, S.R. Goncalves, E.V.U. Costa, H.F. Quina, J. Dupont, *Tetrahedron*, 61 (2005) 10975.
- [110] Y. Tsubata, T. Suzuki, T. Miyashi, Y. Yamashita, *J. Org. Chem.*, 57 (1992) 6749.
- [111] P.D. Ahn, R. Bishop, D.C. Craig, M.L. Scudder, *J. Incl. Phenom. Mol.*, 20 (1995) 267.
- [112] P. Camurlu, PhD Thesis, Middle East Technical University, (2006).
- [113] I. Schwendeman, PhD. Thesis, University of Florida, (2002).
- [114] R.F. Lane, A.T. Hubbard, *J. Phys. Chem.*, 77 (1973) 1401.
- [115] Abidin Balan, MSc. Thesis, Middle East Technical University, 2009.

- [116] M. H. Palmer, L. Simpson, and J. R. Wheeler, *Z. Naturforsch.*, 36A, (1981) 1246.
- [117] Stille J. K. *Angew. Chem., Int. Ed. Engl.* 25, (1986) 508.
- [118] J. Kim, D. Yoon, S. H. Lee, S. Ko, Y.S. Lee, K. Zong *Bull. Korean Chem. Soc.* 27 (2006) 1910
- [119] A. Kumar , D. M. Welsh, M.C. Morvant, F. Piroux, K. A. Abboud, J. R. Reynolds, *Chem. Mater.* 10 (1998) 896
- [120] S.D.D. V. Rughooputh, S. Hotta, A.J. Heeger, F. Wudl, *J. Polym. Sci., Part B, Polym. Phys.* 25 (1987) 1071.
- [121] A. M. McDonagh, S. R. Bayly, D. J. Riley, M. D. Ward, J. A. McCleverty, M. A. Cowin, C. N. Morgan, R. Varrazza, R. V. Penty and I. H. White, *Chem. Mater.* 12 (2000) 2523.
- [122] H. Meng, D. Tucker, S. Chaffins, Y. Chen, R. Helgeson, B. Dunn and F. Wudl, *Adv. Mater.* 15 (2003) 146.
- [123] S. Scheib, P. Bauerle *J. Mater. Chem.*, 9 (1999) 2139.

## APPENDIX A

### SELECTED NMR DATA

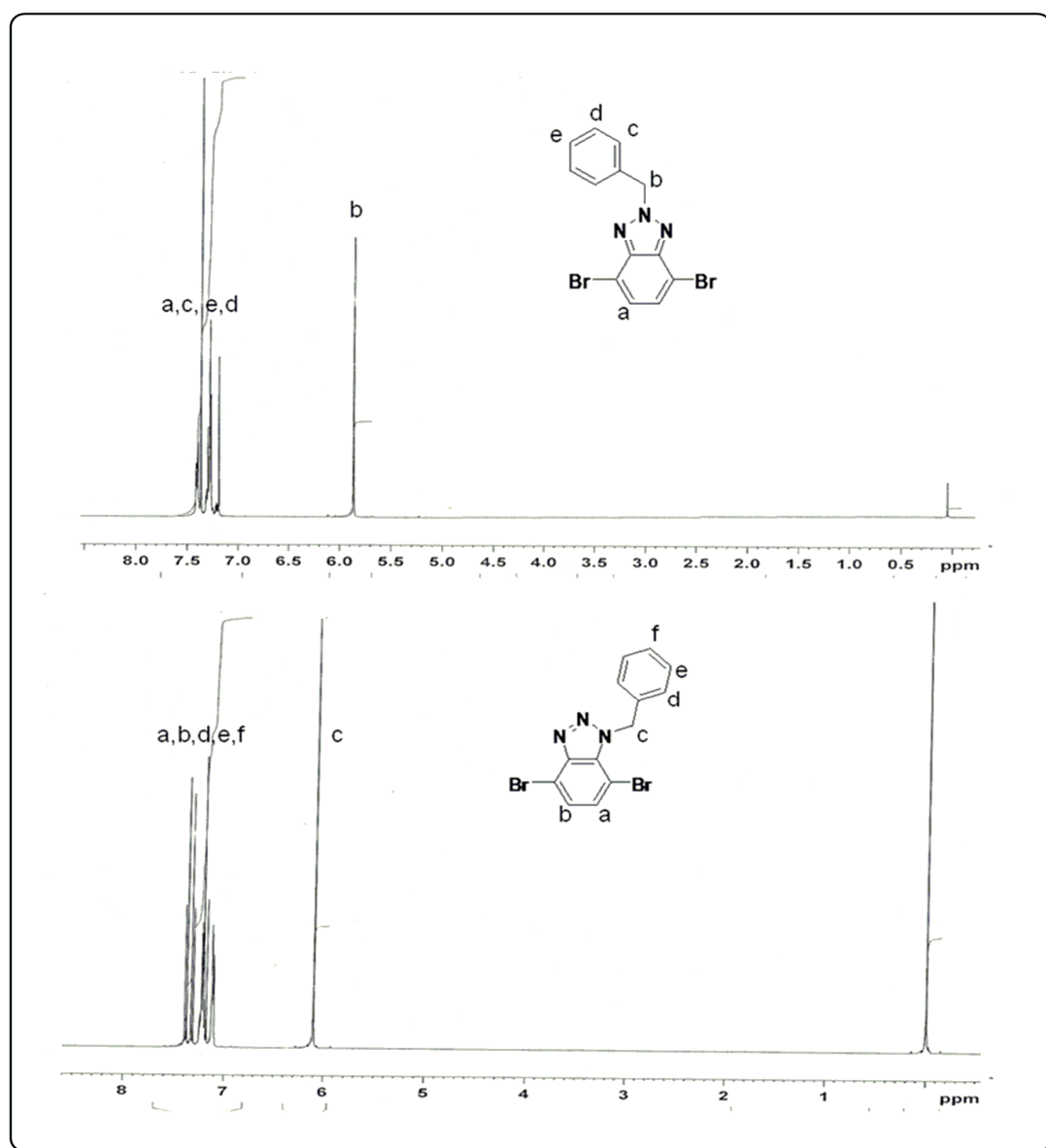


**Figure A.1.**  $^1\text{H-NMR}$  spectra of 2-Benzyl-BTBr and 1-Benzyl-BTBr

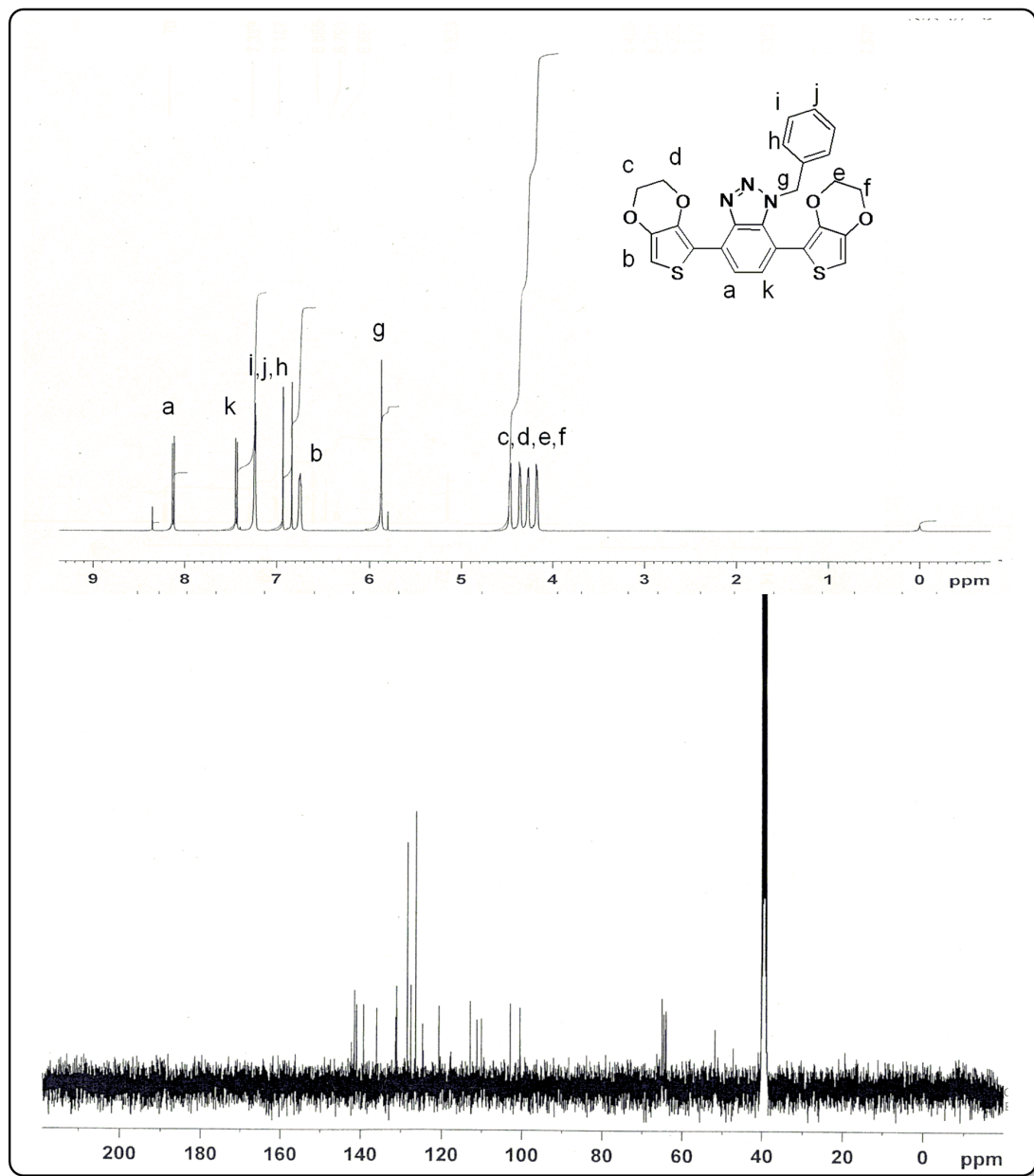
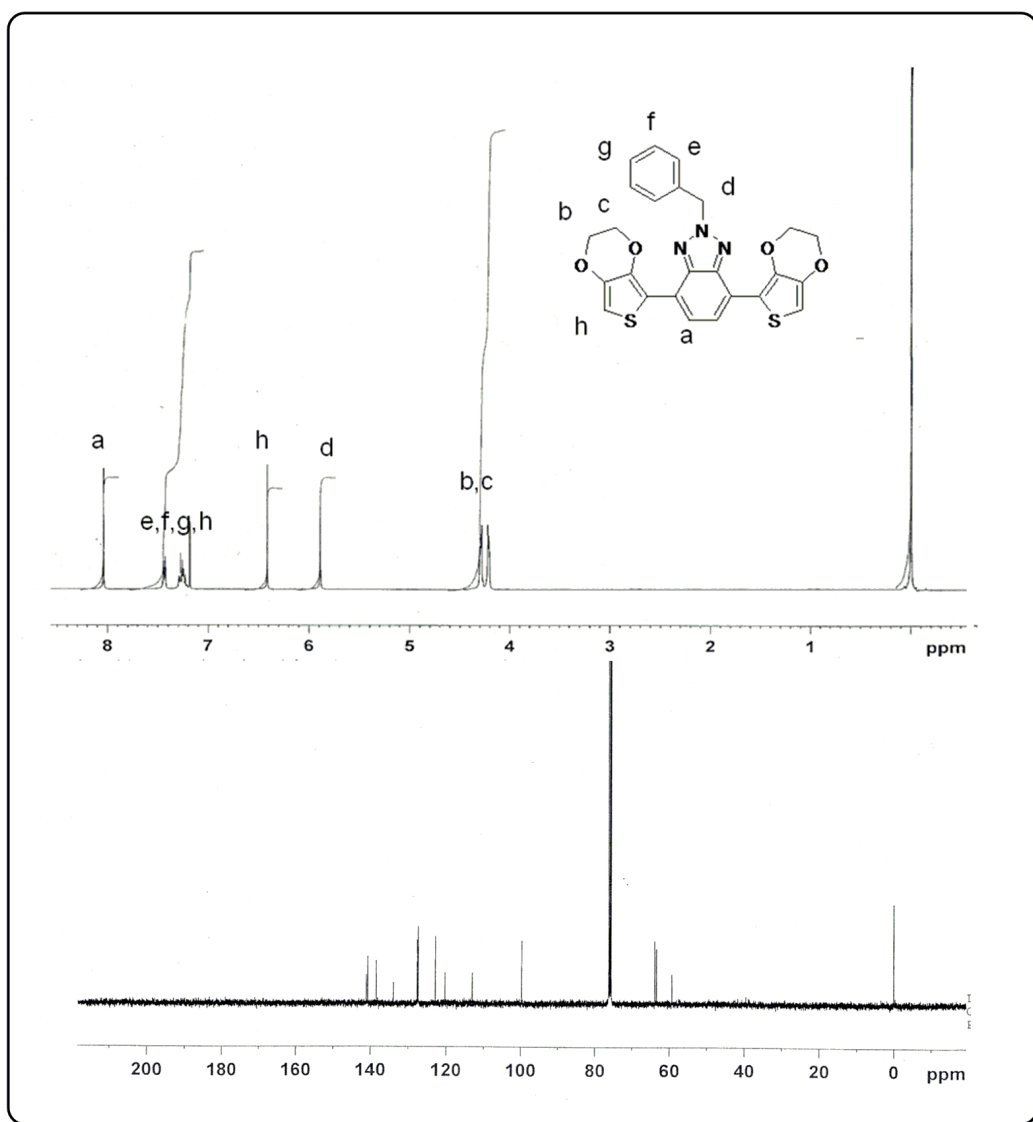
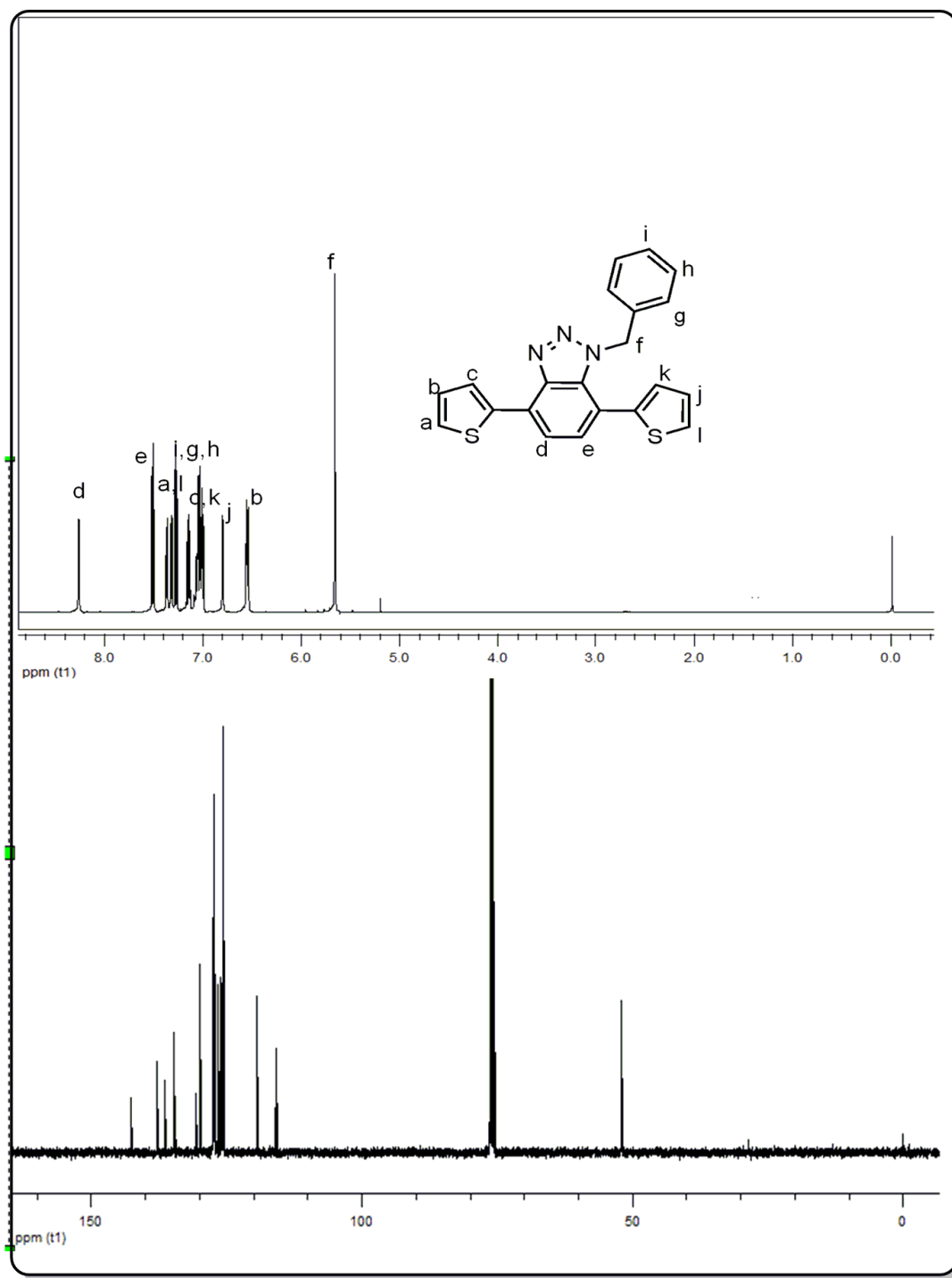


Figure A.2  $^1\text{H}$  and  $^{13}\text{C}$  NMR Spectra of BBTEA



**Figure A.3**  $^1\text{H}$ - and  $^{13}\text{C}$  NMR Spectra of BBTES



**Figure A.4**  $^1\text{H}$ - and  $^{13}\text{C}$  NMR Spectra of BBTA

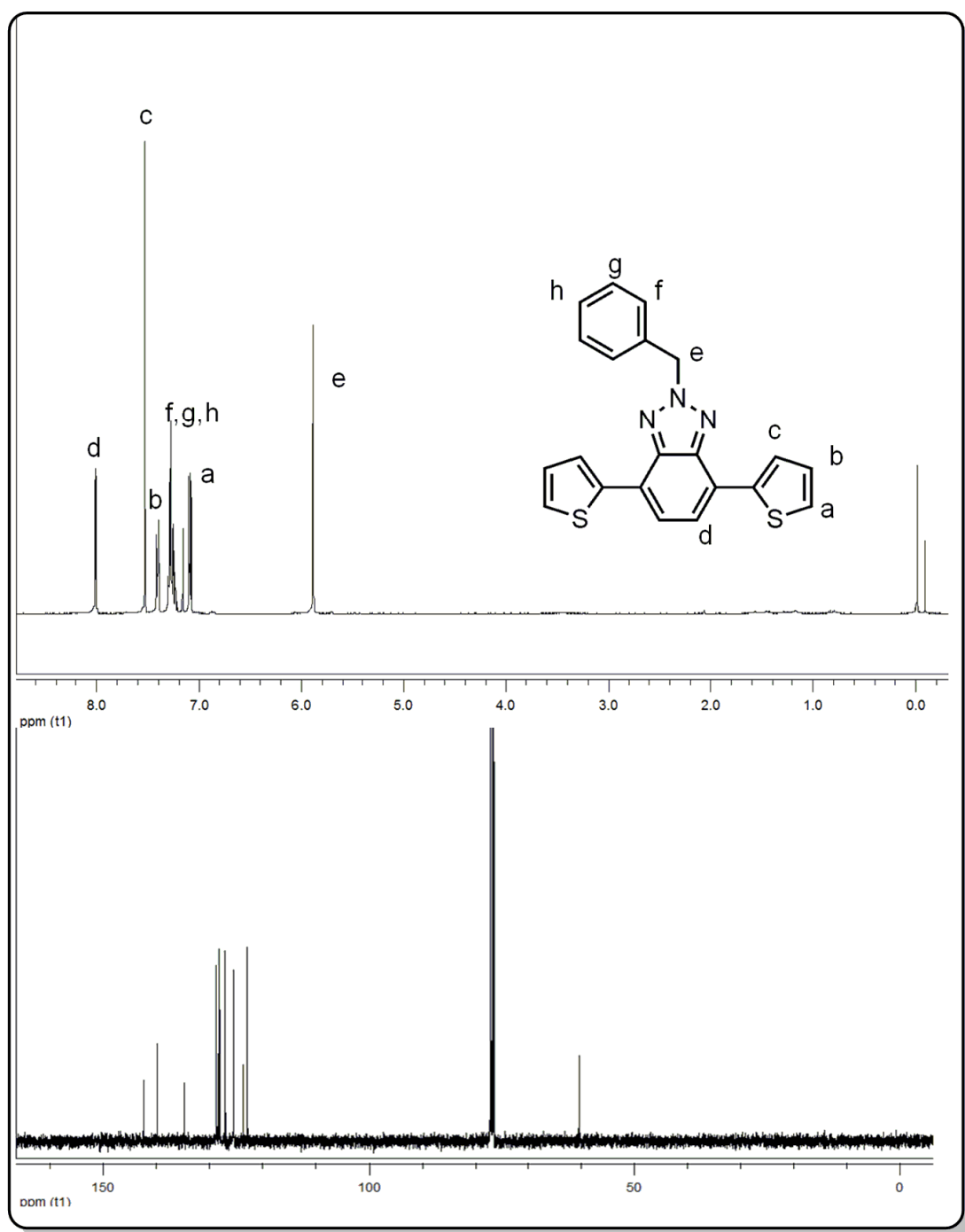


Figure A. 5  $^1\text{H}$ - and  $^{13}\text{C}$ -NMR Spectra of BBTS

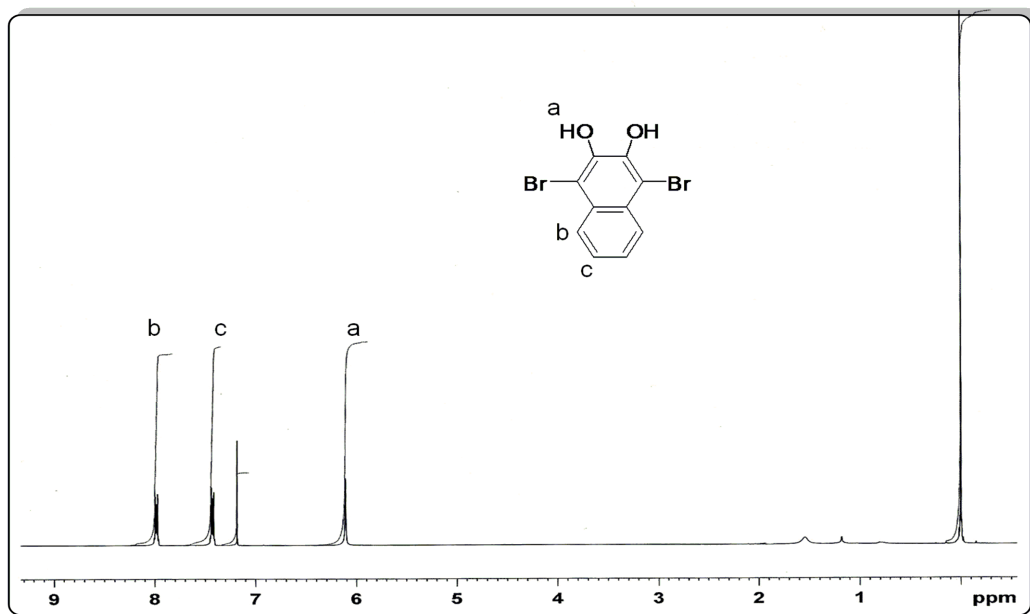


Figure A.6 <sup>1</sup>H-NMR Spectrum of NPBrOH

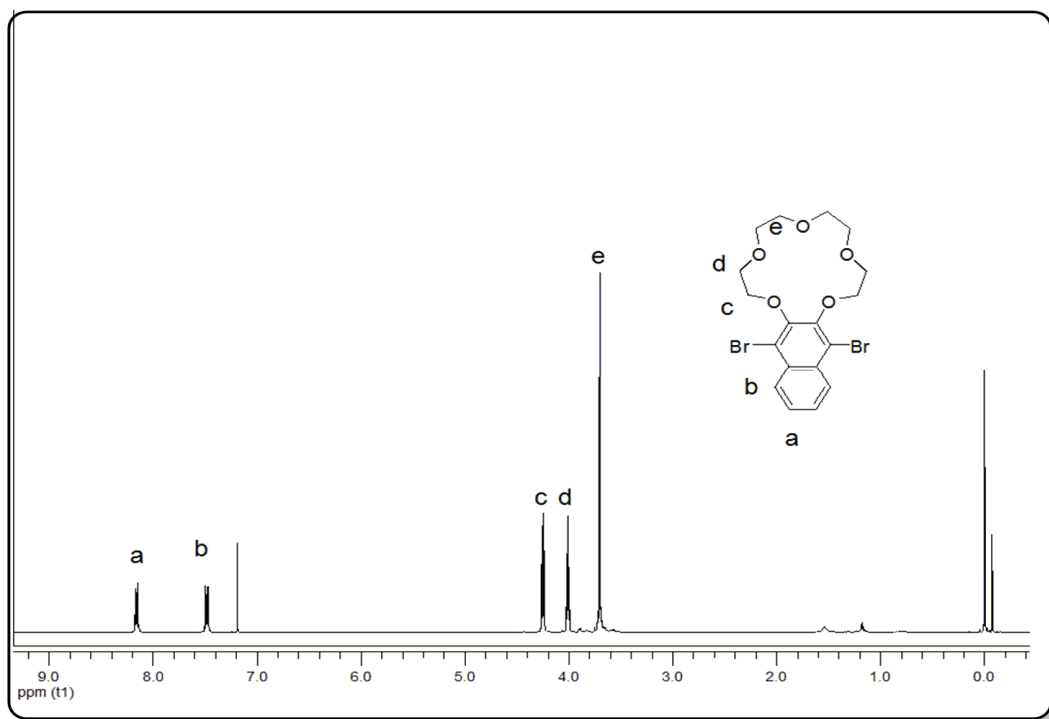


Figure A.7 <sup>1</sup>H-NMR spectrum of NPBrCr

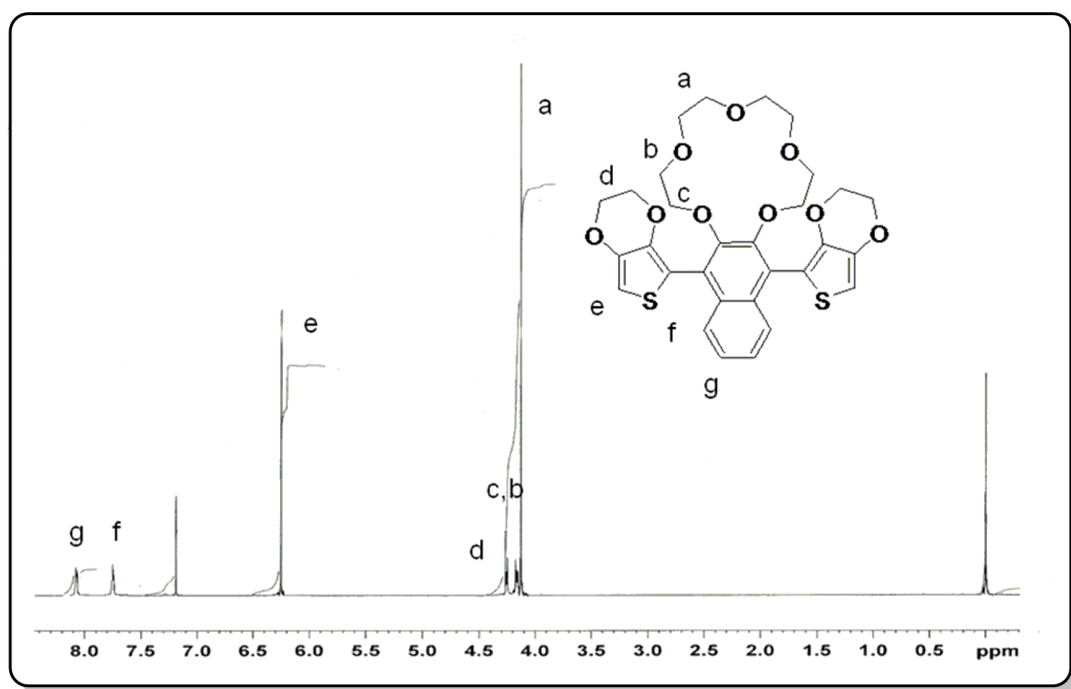


Figure A. 8  $^1\text{H-NMR}$  spectrum of ENCE

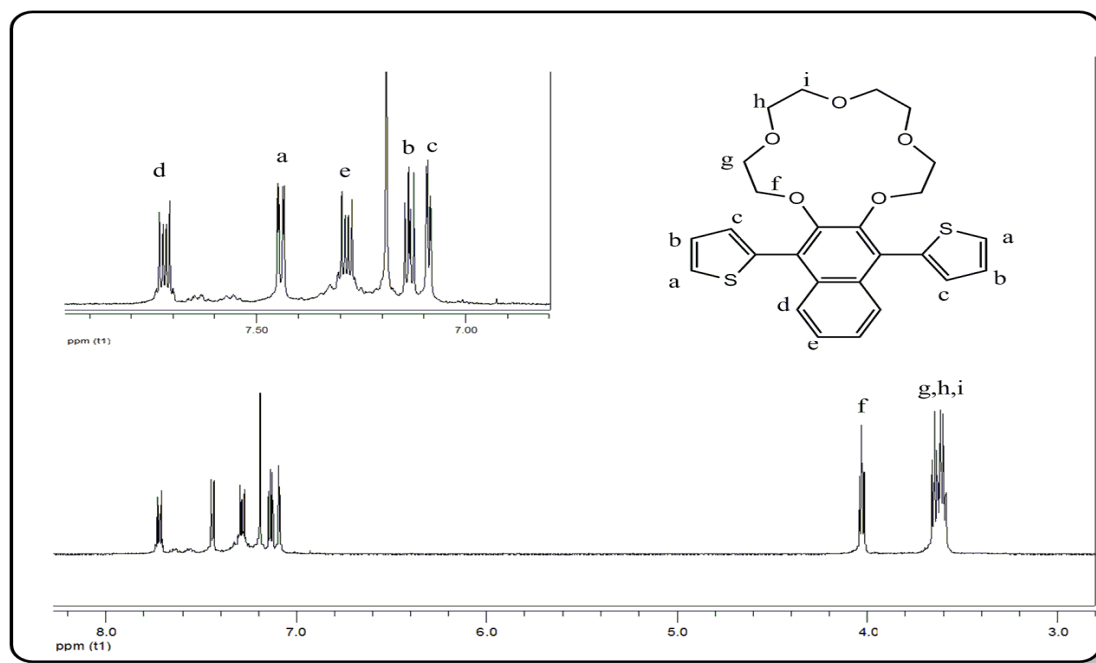


Figure A.9  $^1\text{H-NMR}$  spectrum of TNCT

## CURRICULUM VITAE

### PERSONAL INFORMATION

Surname, Name: Yiğitsoy, Başak

Nationality: Turkey

Date and Place of Birth: January 13<sup>th</sup>, 1983 , Ankara

Phone: +90 312 2415272

email: basakyigitsoy@gmail.com

### EDUCATION

Degree	Institution	Year of Graduation
MS	METU Chemistry Department	2006
BS	METU Chemistry	2005
High School	Anittepe High School, Ankara	2000

### WORK EXPERIENCE

Year	Place	Enrollment
2007-Present	Roketsan Missiles Industries	Engineer
2006-2007	METU Department of Chemistry	Research Assistant

### FOREIGN LANGUAGES

Advanced English.

## PUBLICATIONS

1. B. Yigitsoy, S. Varış , İ. Mecidoğlu, C. Tanyeli, L. Toppare "Electrochromic Properties of a Novel Low Band Gap Conductive Polymer" *Electrochimica Acta*, 52 (2007) 6561.
2. M. Ak, B. Yiğitsoy, L. Toppare, Y. Yağcı "Gas Sensing Property of A Conducting Polymer" *e-polymers*, 42 (2007) 1.
3. B.Yiğitsoy, S. Varış, C. Tanyeli, I. Akhmedov, L. Toppare "Soluble Conducting Polymer of 2,5- di(thiophen-2-yl)-1-p-tolyl-1H-pyrrole and its Electrochromic Device" *Thin Solid Films*, 515 (2007) 3898.
4. S. Çelebi, E. İbibikcan, S. Kıralp, B. Yiğitsoy, L. Toppare "Immobilization of Invertase in Copolymer of 2,5-Di(thiophen-2-yl)-1p-tolyl-1H-pyrrole with Pyrrole" *J. Macr. Sci. Pure Appl. Chem.*, 46(8) (2009) 739 .
5. M.W. Pitcher, Y. Arslan, P. Edinc, M. Kartal, M. Masjedi, Ö. Metin; F. Şen; Ö. Türkarslan; B. Yiğitsoy "Recent Advances in The Synthesis and Applications Of Inorganic Polymer" *Phosphorus Sulfur And Silicon And The Related Elements*, 182(12) (2007) 2861.
6. B .Yigitsoy, S.M. Abdul Karim, A. Balan, D. Baran, L. Toppare "Benzyl substituted benzotriazole containing conjugated polymers: Effect of position of the substituent on electrochromic properties *Synthetic Metals*, 160 (2010) 2534.
7. B .Yigitsoy, S.M. Abdul Karim, A. Balan, D. Baran, L. Toppare "Multichromic Polymers of Benzotriazole Derivatives: Effect of Benzyl Substitution" *Electrochimica Acta*, 56 (2011) 2263.